CHARACTERIZATION OF SMALL MOLECULES THAT ENHANCE MACROPHAGE ACTIVATION FOR HOST-DIRECTED THERAPY OF TUBERCULOSIS

A Dissertation

Presented to the Faculty of the Weill Cornell Graduate School

Of Medical Sciences

In Partial Fulfillment of the Requirements for the Degree of

Doctor of Philosophy

by

Shashirekha Mundhra

August, 2017

Characterization of small molecules that enhance macrophage activation for host-directed therapy of tuberculosis

Shashirekha Mundhra, Ph.D.
Cornell University 2017

Tuberculosis (TB) is a disease of global concern. *Mycobacterium tuberculosis* (Mtb), the causative agent of TB, has evolved to survive in its human host, and it frequently develops resistance to current antibiotics targeted against it with the emergence of multi drug-resistant and extensively drug-resistant strains on the rise. Furthermore, current therapeutic interventions for treatment of TB are limited in efficacy due to lengthy duration of therapy and severe lung damage. Hence, efforts are required to improve TB treatment. Host-directed therapy (HDT) might be used as an adjunctive treatment for TB along with anti-mycobacterials. Here, we characterize small molecules as potential candidates for HDT that boost immune response by enhancing macrophage activation in the presence of interferon gamma (IFNγ) *in vitro* and *in vivo*. For the purpose of our study, we define macrophage activation as an increase in production of pro-inflammatory mediators such as tumor necrosis factor alpha (TNFα) and reactive nitrogen intermediates (RNI) and a decrease in the production of the anti-inflammatory cytokine – Interleukin 10 (IL-10). We also report that protein kinase R (PKR) does not mediate the IFNγ–dependent production of IL-10 and does not restrain the IFNγ–dependent production of RNI and TNFα. PKR is dispensable for host

control of TB in mice. We show that a small molecule C2062 that enhances macrophage activation *in vitro*, also does so in a mouse model of Mtb infection. The phenotype of increased TNFα and RNI directly correlates with reduction in bacterial burden, suggesting that enhancement of macrophage activation can lead to improved control of TB. In addition, C2062 did not exacerbate immunopathology in the lung. We further show in Mtb-infected macrophages and a mouse model of Mtb infection, that C2062 modestly augments the impact of rifampicin, an antibiotic active against Mtb. Thus, targeting the pathways leading to enhancement of macrophage activation can be used to identify new HDTs that can help the immune system control TB in conjunction with anti-mycobacterial drugs.

BIOGRAPHICAL SKETCH

Shashirekha Mundhra grew up in Kolkata, India. She received her Bachelor of Science degree in microbiology from St. Xavier's College, University of Calcutta, India in 2009. She completed her Master of Science degree in virology from National Institute of Virology, University of Pune, in 2011 where she was a gold medalist. She came to USA in 2011 to pursue her PhD in the Immunology and Microbial Pathogenesis (IMP) program at Weill Cornell Graduate School of Medical Sciences, New York City, USA.

Shashirekha joined the lab of Dr. Carl Nathan in April, 2014 to perform her dissertation research.

I dedicate my PhD to Radha and Krishna, Divine Mother, Radha Baba, my Guru – Paramahansa Yogananda and to my family – Daddu, Ma, Mummy and Papa. I love you all and you made this possible.

ACKNOWLEDGMENTS

I am indebted to my mentor, Dr. Carl Nathan for his unflinching support, motivation and enthusiasm. He interviewed me for admission to Weill Cornell Graduate School and has trusted in my abilities throughout. He has given me freedom to explore my ideas and hypotheses. I will always be grateful to him for his contributions to my scientific development and his support for my future aspirations. Above all, he has taught me how to truly enjoy learning science and changed my mindset from 'failure' to 'experiential thinking'.

I would like to thank the members of my thesis committee, Dr. Michael Glickman, Dr. Lionel Ivashkiv and Dr. Hugh Hemmings for their input and suggestions over the years.

I would like to thank my friends in the Nathan, Ehrt, Rhee, and Schnappinger Labs, especially, Thulasi Warrier, Li Zhang, Landys Lopez Quezada, Tania Lupoli, Kristin Burns-Huang, Christina Maksymiuk, Elaine Ballinger, Julia Roberts, Xiuju Jiang, Yan Ling, Kan Lin, Meredith Wright, Uday Ganapathy, Susan Puckett, Weizhen Xu, Ruojun Wang, Carolina Trujillo, Julien Vaubourgeix, Selin Somersan Karakaya, Madhu Nandakumar, Ben Gold, Ruslana Bryk, Anand Balakrishnan, Kohta Saito, Gang Lin, Michele Fuortes, Kyu Rhee, Aihao Ding, Suna Park, Jianjie Mi, Elaina Weber, Madeleine Wood, Wasima Shinwari and Tierra Oulette. I am thankful for your friendship, encouragement, fascinating scientific discussions,

technical advice and assistance, and very especially, in BSL3 and for fun conversations that got me through hours of CFU assays. I am very fortunate to have worked with all of you. I specially thank Xiuju Jiang, without whom the mouse work would have been impossible. I thank Julia Roberts for assistance with macrophage infections. I thank Ruslana Bryk and Kristin Burns-Huang for their helpful advice over the years.

I thank my friends Sarah Qamar, Radhika Jalan, Bharat Vaidyanathan, Dane Samilo, Ritama Gupta, Kihyun Lee, Jennifer Oyler-Yaniv, Clarissa Campbell, Maria Sacta and Helen Kang for their help and support over the years. I specially thank Ashutosh Chaudhry and Elvira Mass for their invaluable advice on my project. I also thank every single member of my SRF family for their tremendous love and support specially Jyoti Gupte, Ashish Myles, Hemal Gala, and Varun Tamminedi.

Finally, and most importantly, I want to thank my parents, grandparents and my brothers Anil Bagri and Abhishek Bagri for their sacrifices, blessings, love and prayers, the sole reason for me being able to pursue a PhD here at Weill Cornell Graduate School.

TABLE OF CONTENTS

LIST OF FIGURES

CHAPTER 1

CHAPTER 2

CHAPTER 3

LIST OF TABLES

CHAPTER 1

CHAPTER 2

CHAPTER 3

APPENDICES

APPENDIX 1

APPENDIX 2

LIST OF ABBREVIATIONS

AMPK: 5' adenosine monophosphate-activated protein kinase.

APC: antigen-presenting cells

BCR-ABL: breakpoint cluster-Abelson tyrosine kinase

BM-MSCs: bone marrow-derived mesenchymal stromal cells

BMMs: Bone marrow-derived macrophages

CFU: Colony forming units

CTLA-4: cytotoxic-T-lymphocyte-associated antigen 4

DCs: Dendritic cells

GABA: γ-aminobutyric acid

Gal9: galectin 9

GM-CSF: granulocyte-macrophage colony-stimulating factor

HDAC: Histone deacetylase

HDT: Host-directed therapy

IFN: Interferon

IL: Interleukin

iNOS: inducible nitric oxide synthase

LAG3: lymphocyte-activation gene 3

MHC: Major Histocompatibility Complex

Mtb: *Mycobacterium tuberculosis*

NK cell: Natural Killer cell

NSAID: Non steroidal anti inflammatory drug

PARP: poly (ADP-ribose) polymerase

PKR: Protein kinase R

PD-1: programmed cell death 1

PD-L1: programmed cell death ligand 1

RNI: Reactive Nitrogen Intermediates

ROS: Reactive oxygen species

T cell: T – lymphocyte

TB: Tuberculosis

Tim3: T-cell immunoglobulin and mucin-domain containing-3

TLRs: Toll-like Receptors

TNFα: Tumor Necrosis Factor alpha

Treg: Regulatory T cell

VEGF: Vascular endothelial growth factor

CHAPTER 1

INTRODUCTION

CHAPTER 1

INTRODUCTION

Tuberculosis - Pathogen, disease, epidemiology and treatment:

Tuberculosis (TB) is an ancient infectious disease of humans caused by the bacterium *Mycobacterium tuberculosis* (Mtb). Mtb was proven to be the definitive causative agent of tuberculosis by Robert Koch in 1882 (Koch 1882). The only natural host of Mtb is *H. sapiens* humans and approximately one-third of the world's population is known to be latently infected with the bacterium (Nathan, 2009). *Mtb* is one of the most successful pathogens in terms of the proportion of the population infected (about one-third), the duration of infection (usually lifelong), and the number of resulting deaths (2–3 million a year, among the most for any single infectious agent) (Nathan and Shiloh, 2000).

In 2015, there were an estimated 1.4 million deaths from TB (Figure 1), and an additional 0.4 million deaths among people living with HIV (PLHIV) resulted from TB (WHO, 2016). TB is the most prevalent disease amongst PLHIV and the most common illness in newly HIV-diagnosed patients (Tiberi et al., 2017). Even though global TB incidence has declined slightly in the last decade, TB remained one of the top 10 causes of death worldwide in 2015 (WHO, 2016).

The advances in TB control are threatened by emergence of Mtb strains that are resistant to anti-tuberculosis drugs. The WHO has defined multi-drug resistant (MDR) strains as resistant to the two frontline drugs isoniazid and rifampicin. Extensively drug-resistant

(XDR) strains are MDR strains that are also resistant to the fluoroquinolones and second-line injectable drugs, suggesting the failure of standardized second line treatment regimens. Patients can contract drug-resistant TB by two ways: primary resistance by infection with a drug-resistant strain and secondary resistance that can arise during therapy and is also referred to as acquired resistance (Dheda et al., 2017).

TB is primarily a disease of the lung and is commonly characterized by coughing and weight loss. Mainly, new infections occur by inhalation of a droplet containing Mtb expelled from an individual suffering from active TB. After exposure, the infection can be cleared by one's immune system; progress to active infection; or be contained as a latent disease which is asymptomatic, noncontagious and characterized by slowly or non-replicating Mtb (Flynn et al., 2011; Russell, 2001). Prevalence and incidence of TB usually varies with geographic location. Highest TB burden usually correlates with compromised socio-economic status (Dye and Williams, 2010).

In the early days, once the etiology of the disease was known and primary mode of transmission identified, simple interventions such as isolation of patients and improvement of ventilation in buildings were used. In 1921, the only licensed vaccine for the prevention of TB was developed by the French scientists Albert Calmette and Camille Guérin and was accordingly named bacille Calmette–Guérin (BCG). Presently, it is the most widely used vaccine in the world. It is extensively used to prevent severe forms of extra pulmonary TB in infants, but it fails to prevent pulmonary TB (the

most common form of the disease)- at any age (Colditz et al., 1994, 1995). Because of the limitations of BCG, novel vaccine candidates have been developed and reached clinical trial pipelines (Kaufmann et al., 2017).

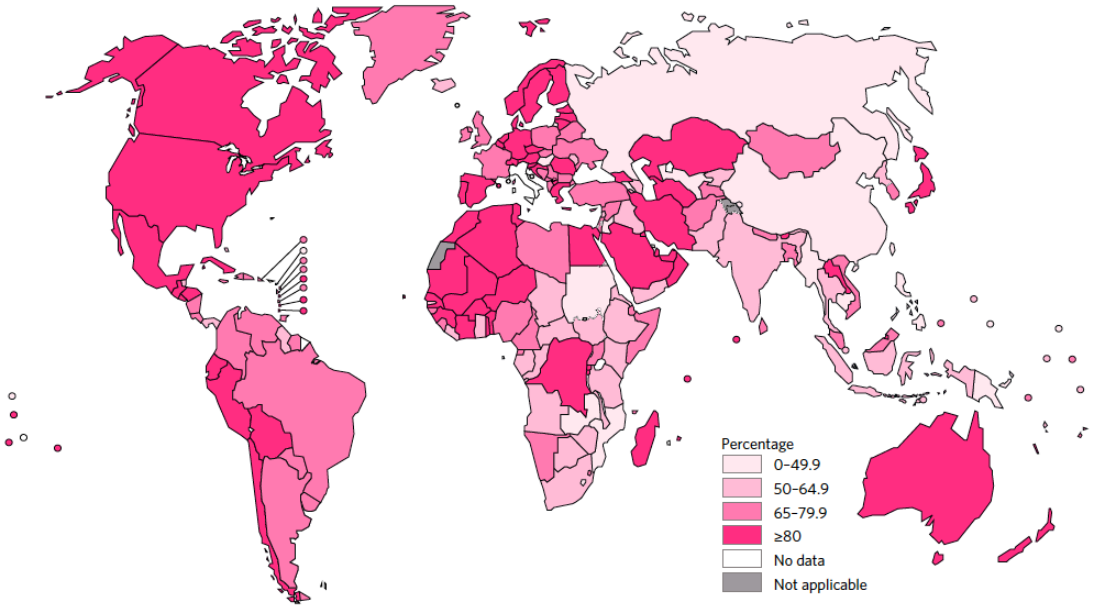

Fig.1 Percentage of present and relapse pulmonary TB cases with bacteriological confirmation in 2014-2015 (Adapted from WHO)

It is evident that the current strategy to control TB is failing and the WHO post-2015 goal of a 90% reduction in the incidence of TB by 2035 will not be met without the introduction of new and efficacious therapeutic strategies for TB.

Challenges of TB treatment and the need for an alternative approach:

Despite the availability of antibiotics, TB is a leading cause of morbidity and mortality. Improving treatment for drug sensitive and

drug-resistant (MDR, XDR) TB is a high priority in the present scenario. There are very few antimicrobials targeting Mtb currently in clinical trials and some have safety concerns. In addition, Mtb is most likely to develop resistance against the new antimicrobials that are discovered. In Mtb, drug resistance is associated entirely with chromosomal rearrangements and point mutations. Non-adherence by patients to the long-term therapy or poor availability of therapy is often regarded as a major explanation of drug resistance (Koch and Wilkinson, 2014) .

The current duration of TB therapy is 6 months in patients with drug-sensitive TB and 18-24 months in patients with MDR/XDR TB. The patients are also often left with serious permanent lung injury following the TB treatment after infection despite the infection being cured.

The widespread emergence of antimicrobial drug resistant strains enhances the need for novel interventions in addition to new antimicrobial discovery that could:

- ✓ Reduce the length of TB therapy thereby improving patient adherence and ameliorating long-term toxicity.
- ✓ Augment immune responses to eliminate or contain Mtb.
- ✓ Reduce excessive inflammation and / or repair the pulmonary damage caused by the infection and functional disability.
- ✓ Reduce morbidity and mortality caused by MDR/XDR TB.
- ✓ Prevent antimicrobial resistance.

(Wallis and Hafner, 2015; Zumla et al., 2016)

Host directed therapy

In the past few years, scientific research has been directed towards targeting host biological pathways – rather than pathogen components directly - leading towards development of a range of host-directed therapies (HDTs) to achieve an improved clinical outcome. An HDT is any substance that can enhance host defense mechanisms or regulate excessive inflammation, or both (Wallis and Hafner, 2015). HDT should improve clinical treatment outcomes as demonstrated by reduced morbidity, mortality, immunopathology and long-term recovery. Several HDT agents are currently used (Figure 2). An ideal agent for HDT can

- ✓ Augment host cellular responses to pathogens without exacerbating immunopathology
- ✓ Target virulence factors that cause disease
- ✓ Activate innate and adaptive immune responses and immunological memory.

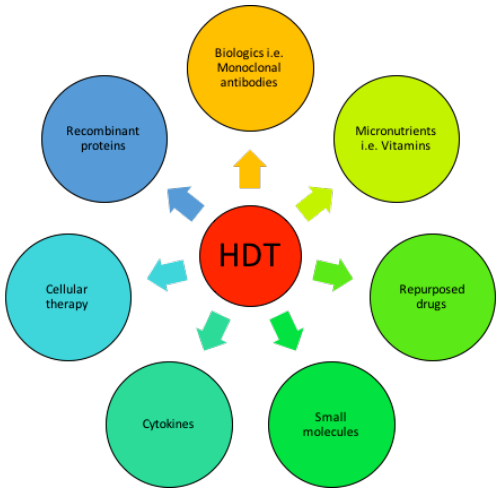

Fig. 2 Main types of host-directed therapies currently in use

Host directed therapy for TB:

A lot of research has been conducted in the last few years on HDT for TB. Some of the key drugs that are currently in clinical trials have been summarized in Table 1.

Table 1. Pipeline of host-directed therapies as adjunctive treatment of drug-sensitive and drug-resistant TB by modulating host pathways. Adapted from (Zumla et al., 2016)

Drug	Mechanism of action	Stage of development
Fatty acid oxidation and mitochondrial respiration		
Metformin (Biguanide)	Induces ROS production and interrupts the mitochondrial chain: increases mitochondrial biogenesis and respiration	Preclinical
Niraparib (PARP inhibitor)	Inhibits PARP-1 and PARP-2 activity; impairs repair of DNA single strand breaks	Preclinical
IL-15 (Cytokine)	Maintains and likely induces proliferation of CD8 T cells	Preclinical
Arachidonic acid metabolism		
Aspirin (NSAID)	Reduces TNFα levels by increasing lipoxinA4 production and achieves eicosanoid balance during chronic inflammation	Preclinical
Zileuton (Leukotriene synthesis inhibitor)	Activates cyclooxygenase to promote prostaglandin production; disrupts lipoxygenase activity and blocks leukotriene production	Preclinical
Ibuprofen (NSAID)	Inhibits cyclooxygenase activity and blocks prostaglandin production	Early phase Clinical
Corticosteroid metabolism		
Prednisone (Glucocorticoid receptor antagonist)	Interacts with glucocorticosteroid receptor and triggers transcription of several host genes critical for Mtb elimination *i.e.* iNOS and cyclooxygenase-2	Mid-late phase clinical
Host cell cytotoxicity		
Cyclophosphamide (alkylating agent)	Cytochrome P450 metabolism of this drug produces a complex that can alkylate DNA guanine to reduce cell proliferation	Untested in TB
Etoposide (Topoisomerase inhibitor)	Blocks DNA Topoisomerase II to prevent re-ligation of nascent DNA strands	Preclinical
Histone acetylation		

Table 1 (Contd.)

Valproic acid and vorinostat (HDAC inhibitor)	Acetylates lysine residues on histones to promote DNA unwinding and gene transcription	Preclinical
Phenylbutarate (HDAC inhibitor)	Same as above	Early phase clinical
Inhibition of tyrosine kinases		
Imatinib mesylate	Induces death of cancerous B cells by apoptosis; induces myelopoeisis	Early phase Clinical
Ion efflux channels		
Verapamil (Calcium channel blocker)	Modulates voltage gated calcium channel activity for maintaining cellular homeostasis	Preclinical
Carbamazepine (sodium channel blocker)	Activates AMPK to induce autophagy; activates GABA receptors for reducing sensitivity to neuropathic pain	Preclinical
Statins (Inhibitors of 3-hydroxy-3-methylglutaryl coenzyme reductase	Blocks endogenous cholesterol biosynthesis	Preclinical
Immune activation		
GM-CSF. IL-2, IFNγ (Cytokine)	Acts towards proliferation and activation of macrophages, DCs, monocytes and T cells	Mid-late phase clinical
Innate immune defenses		
Vitamin D3 (Vitamin)	Improves antigen presentation, induces cathelicidin production and augments response to IFNγ signaling	Late phase clinical
Cytokine neutralization		
Adalimumab (anti-TNFα) (Monoclonal antibody)	Removes excess of TNFα from tissue and circulation	Clinical (compassionate use)
Siltuximab (anti- IL-6) (Monoclonal antibody)	Removes excess of IL-6 from tissue and circulation	Preclinical
Immune checkpoint inhibition		
Ipilimumab (anti-CTLA4) (Monoclonal antibody)	Blocks CTLA4 to undo T-cell exhaustion and restores IL-2 secretion and signaling	Preclinical
Nivolumab (anti-PD-1) (Monoclonal antibody)	Blocks PD-1 to restore lymphocyte function. Blocking of PD-L1 on surface of APCs aids in T-cell activation	Preclinical
Anti-Tim3 (Monoclonal antibody)	Induces targeted T cell responses by regulating Tim3-Gal9 interaction	Preclinical
Anti-LAG3 (Monoclonal antibody)	Blocks LAG3 to abolish Treg interaction with CD4 and CD8 T cell	Preclinical

Table 1 (Contd.)

Angiogenesis inhibition		
Bevacizumab (anti-VEGF) (monoclonal antibody)	Blocks neovascularization induced by VEGF in tissues	Preclinical
Improved tissue regeneration by reduction of inflammation		
BM-MSCs (Cell-based therapy)	BM-MSCs can reduce severe inflammation, regenerate tissues and restore positive regulation of immune responses, activation of Tregs and secretion of soluble factors	

Host directed therapy for other infectious diseases:

Studies of HDT also pave the way for new insights into underlying mechanisms of pathogenesis and the hosts' innate and adaptive immune responses. Table 2 lists clinically relevant examples in development of candidate HDTs as an adjunctive treatment option for viral, parasitic and other bacterial infectious diseases.

Table 2. Pipeline of HDTs as adjunctive treatment for other infectious diseases. Adapted from (Zumla et al., 2016)

Drug	Mechanism of action	Stage of development
Viral infections		
Human Immunodeficiency Virus		
Anti PD-1 (monoclonal antibody)	Activates antigen-specific cells via immune checkpoint blockade	Preclinical
Hepatitis C virus		
Pegylated IFNα and IFNβ (cytokine)	Initiates pro-inflammatory antiviral immune response	In clinical use
Adenovirus		
In vitro expanded adenovirus-specific CD8 CTLs. (cellular therapy)	Reduces viral reservoirs to avoid uncontrollable viremia in individuals	In clinical use
Dengue virus		
Dasatinib (repurposed drug)	Tyrosine kinase inhibitor inhibits viral replication	Preclinical

Table 2 (Contd.)

Influenza virus		
Atorvastatin (Repurposed drug)	Blocks angiotensin-converting enzyme that reduces pro-inflammatory signaling and promotes tissue repair	Mid-late phase clinical
Parasitic diseases		
Leishmaniasis		
Imiquimod, resiquimod (Repurposed drug)	Induces B-cell activation and pro-inflammatory signaling as a TLR agonist	In clinical use
Malaria		
Desferrioxamine (Repurposed drug)	Inhibits ferrochelatase and reduces *Plasmodium sp* replication in erythrocytes	Preclinical
African trypanosomiasis		
IFNγ, IL-2, TNFα (Cytokine therapy)	Induces pro-inflammatory immune responses and intracellular antimicrobial activity	Preclinical
Schistosomiasis		
Peroxiredoxin (adjuvant to vaccine) (recombinant protein)	Modulates hydrogen peroxide concentrations in host; induces antigen-specific B-cell responses	Preclinical
Bacterial infections		
Streptococcus pneumoniae		
Prednisone (repurposed drug)	Reduces inflammation by activating the glucocorticoid pathway	Clinical (current practice)
Helicobacter pylori		
Vitamin D3 (vitamin)	Activates and enhances intracellular antimicrobial defenses (via IFNγ and IL-15 signaling)	Preclinical
Bordetella pertussis		
Antipertussis toxin antibodies (monoclonal antibodies)	Diminishes the toxin load by infusing intravenous immunoglobulins	Preclinical

Overview of host defenses in TB:

Once Mtb bacilli are inhaled via aerosol, they reach the alveolar space in lungs, where they are taken up by phagocytic cells – primarily

lung-resident macrophages. The ability to survive within the macrophages is required for Mtb to maintain infection without showing any symptoms of disease, a condition termed as latent infection. This latency, or ability to persist, allows Mtb to use the human host as a reservoir. Mtb requires the ability to proliferate, both intracellularly and extracellularly, in order to cause active TB. Although TB is mainly a pulmonary disease, Mtb is capable of disseminating to most organs and tissues causing several types of TB (Lamichhane, 2011) such as miliary TB and extrapulmonary TB (spreading to kidney, bone marrow, bone, uterus, lymph nodes, etc.)

The early events in Mtb infection are driven by an innate immune response initiated by lung-resident macrophages that lead to inflammasome activation, cytokine production and initiation of several host defense mechanisms such as production of antimicrobial peptides, reactive oxygen species (ROS), reactive nitrogen intermediates (RNI), natural killer (NK) cells, dendritic cells (DCs), epithelial cells and other immune cells add towards this process. Neutrophils transfer their granules containing antimicrobial molecules that traffic to early endosomes (containing Mtb) – to macrophages and the production of S100 proteins. In certain individuals who do not develop TB, despite repeated exposure to TB, these innate immune responses are likely sufficient to prevent infection.

Granulomas are a hallmark of TB infection. A tuberculous granuloma is an organized collection of immune cells such as macrophages (usually epitheloid), multinucleated giant cells (that are formed by macrophage fusion), lymphocytes (both CD4+ and CD8+ T

cells, B cells), neutrophils and fibroblasts and is maintained by the persistent presence of Mtb (Lin et al., 2007)

Role of IFNγ in tuberculosis

Interferons (IFNs) can be divided into two major types: Type I IFNs are induced in response to viruses: IFNα is secreted by leucocytes, and IFNβ is produced by fibroblasts. Type II IFNs, known as IFNγ, is produced by T cells and NK cells upon activation with immune and inflammatory stimuli (Cavalcanti et al., 2012). It is the most important cytokine involved in the protective immune response against mycobacterial infection. It is produced primarily by CD4 and CD8 T cells and NK cells. Natural Killer (NKT) cells and γδ T cells can also produce IFNγ in response to mycobacterial stimulation, demonstrating protection against Mtb *in vitro* and *in vivo* (Cooper and Khader, 2008). The main function of IFNγ is to activate macrophages and induce their microbicidal functions. It can do so by (a) enhancing antigen presentation and promoting differentiation of CD4 T cells into Th1 subpopulations (Oberholzer et al., 2000) (b) inducing transcription of > 200 genes including those genes that are required for the production of antimicrobial molecules like oxygen free radicals and nitric oxide, which represent indispensable mechanisms for eliminating Mtb (Cooper, 2009).

IFNγ has been shown to be important in both mice and humans in the context of mycobacterial infection. Mice deficient in IFNγ are highly susceptible to Mtb infection (Cooper et al., 1993; Flynn et al., 1993). Humans that have a deficiency in the IFNγ receptor are

extremely susceptible to mycobacterial infections (Newport et al., 1996). Humans with genetic mutations in the IFNγ receptor gene show high susceptibility to atypical mycobacterial infections (Jouanguy et al., 1996). Patients with less severe forms of pulmonary TB have a predominance of IFNγ, a Th1 type cytokine, whereas, patients with severe forms of TB have an increase in IL-4, a Th2 type cytokine (D et al., 1999; Dlugovitzky et al., 1997). Furthermore, patients with active TB have a defect in IFNγ production in response to a 30kDa antigen from Mtb, compared to healthy controls, suggesting that IFNγ plays a protective role in TB (Torres et al., 1998).

Role of TNFα in tuberculosis

TNFα is a pleiotropic cytokine produced mainly by activated macrophages, activated T cells, DCs and NK cells (Ehlers, 2003). TNFα is important for activation of macrophages and immune cell recruitment to the site of infection. It is critical in granuloma formation and maintenance.

Deficiency of the TNF gene or its receptor in mice results in acute TB (Bean et al., 1999; Flynn et al., 1995). Neutralization of TNFα has been shown to cause reactivation of TB (Mohan et al., 2001). Patients suffering from rheumatoid arthritis who are undergoing treatment with TNFα antagonists, are at significantly increased risk of reactivating latent Mtb (Solovic et al., 2010). TNFα is also known to increase the capacity of macrophages to phagocytose and kill mycobacteria; to stimulate apoptosis of macrophages thereby

depriving bacilli of host cells and causing death; and presentation by dendritic cells of mycobacterial antigens (Cavalcanti et al., 2012)

Role of IL-10 in tuberculosis

IL-10 is a cytokine with pleiotropic immunoregulatory roles. It is produced by macrophages and T cells during Mtb infection. In contrast to IFNγ and TNFα, it is mainly an anti-inflammatory cytokine, critical for balance between inflammatory and immunopathological responses. IL-$10^{-/-}$ mice on C57BL/6 background had reduced BCG burden compared to controls suggesting that deficiency in IL-10 promotes anti-mycobacterial immunity (Murray and Young, 1999). In Mtb-susceptible CBA/J mice, treatment with IL-10 blocking antibodies during chronic infection, improved survival by stabilizing bacterial burden in the lung (Beamer et al., 2008). These findings suggest that IL-10 promotes TB disease progression.

Detailed studies of IL-10 gene polymorphisms associated with infectious diseases suggests that polymorphisms associated with this gene have an important role in immunity and progression of inflammation. In humans, an SNP associated with IL-10 promoter was shown to be associated with decreased risk of TB (Shin et al., 2005). The aim of Mtb is to survive in the host by lowering the protective cellular immune responses. IL-10, TGF-βRII and other inhibitory molecules of inflammatory response were detected in sputum from TB patients, and 30 days post treatment, their levels decreased considerably with a concomitant increase in Th1 cytokines (Almeida et al., 2009). However, a study did not observe increased levels of IL-10

in peripheral blood mononuclear cells (PBMCs) from MDR-TB patients in response to mycobacterial antigens (McDyer et al., 1997).

Role of RNI in tuberculosis

RNI, or reactive nitrogen intermediates, refer to oxidation states and adducts of the nitrogenous products of the enzyme - nitric oxide synthase, such as nitric oxide (NO), nitrate (NO_3), nitrite (NO_2), peroxynitrite ($OONO_2$), S-nitrosothiols and dinitrosyl iron complexes (Nathan and Shiloh, 2000). RNI are produced by several cells and can damage DNA and several enzymes that are required for the protection and replication of DNA. NO is toxic and a potent effector of macrophage bactericidal and bacteriostatic activities (Ding et al., 1988; Liew and Cox, 1991). One such enzyme, NOS2 (Nitric Oxide Synthase 2 or iNOS) is responsible for production of RNI.

Mice deficient in the gene *Nos2* are highly susceptible to Mtb infection (MacMicking et al., 1997). RNI production has been shown to be necessary for control of Mtb infection caused by both laboratory and clinical strains (Scanga et al., 2001). Treatment with NOS2 inhibitors worsen Mtb infection in mice either in chronic or acute phase of Mtb infection (Nathan and Shiloh, 2000). Macrophages isolated from the lungs of TB patients express *Nos2* in amounts that are bactericidal to Mtb (Nicholson et al., 1996; Rich et al., 1997; Wang et al., 1998).

Role of neutrophils in tuberculosis

The overall role of neutrophils during Mtb infection is not fully

understood. As mentioned above, animals lacking IFNγ or Nos2 suffer from severe TB with increased bacterial burden and granulocytic inflammation. This correlation between granulocytes such as neutrophils and polymorphonuclear cells (PMNs), bacterial load and pathology is commonly observed in both animal models and TB patients (Berry et al., 2010; Eruslanov et al., 2005; Mattila et al., 2015). It has been suggested that Mtb infection induces a proinflammatory response that leads to the recruitment of PMNs to the lung. Loss of *Atg5* expression within the responding myeloid cells has been shown to cause uncontrolled accumulation of PMNs in the lung, in turn causing increased pathology and an expanded niche for bacterial replication (Kimmey et al., 2015). Neutrophilic inflammation has been shown to generate a nutrient replete niche that promotes Mtb growth, suggesting that Mtb exploits neutrophilic inflammation to preferentially replicate in areas of tissue damage in order to promote the dissemination of infection (Mishra et al., 2017). In I/St mice (that are genetically hyper-susceptible to Mtb infection). neutrophils have been implicated as a “Trojan horse” for mycobacteria and aid in the development of severe lung inflammation instead of protection of the host (Eruslanov et al., 2005). This was not observed in A/Sn mice (that are known to be resistant to Mtb infection). Furthermore, neutrophil depletion *in vivo* in Mtb-infected I/St mice reduced lung pathology and bacterial burden, resulting in an increase in survival time (Yeremeev et al., 2015), thereby providing evidence of the deleterious instead of a protective role of neutrophils in Mtb infection.

However, neutrophils have been implicated in generation of Th1 and Th17 cells in response to tuberculosis vaccine. Depletion of neutrophils during vaccination abolished the induction the Th1-specific responses and prevented the reduction of bacterial burden in vaccinated animals (Trentini et al., 2016). Hence, neutrophils are multifunctional cells that play a dual role in Mtb infection. They can be bactericidal, participate in granuloma formation and development of adaptive immunity; at the same time, they may support Mtb growth, mediate tissue destruction, disease severity and progression. It has been suggested that TB disease alters neutrophil population leading to accumulation of heterogeneous subsets of activated dysfunctional cells and a decline in true neutrophils (Lyadova, 2017). The precise role of neutrophils in Mtb infection is yet to be determined.

Conclusions

In the context of tuberculosis, host directed therapy would be used as an adjunctive treatment for Mtb along with anti-mycobacterials. We chose to develop a candidate for HDT that boosts the immune response by enhancing macrophage activation in mice. We screened and identified small molecules that increased the production of pro-inflammatory mediators described earlier – TNFα and RNI, and reduced the production of IL-10 (Discussed in Chapter 2). We tested the lead inhibitors in the context of Mtb infection in mice and initiated steps to identify the mechanism of action (Discussed in Chapter 3). Please see Figure 3 for a schematic respresentation of our working model.

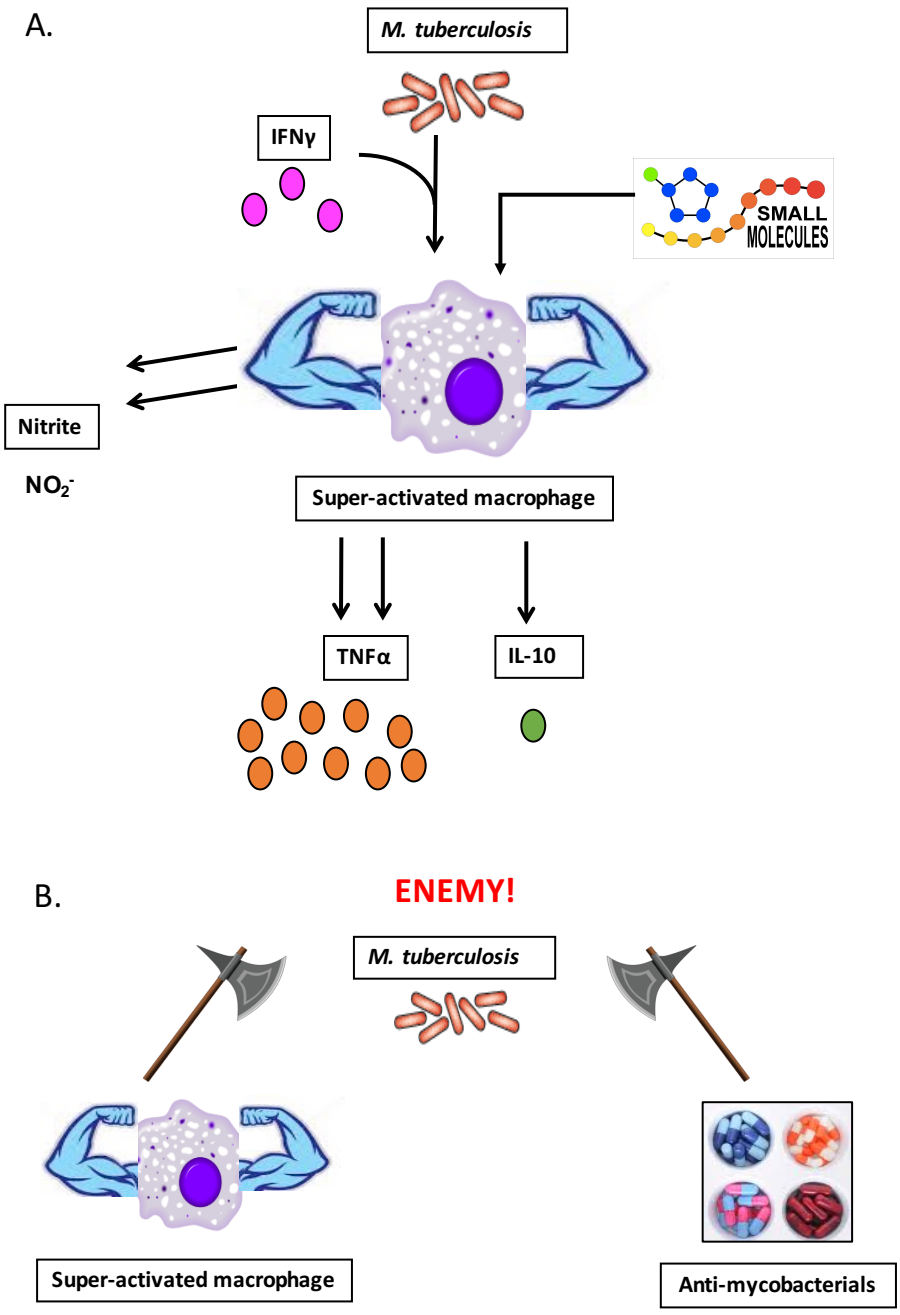

Fig. 3 Model

A. We target macrophages with small molecules in order to enhance their activation as measured by an increase in production of TNFα and nitrite and decrease in IL-10.

B. Our goal is to clear Mtb by using small molecules to enhance macrophage activation, in addition to existing anti-mycobacterials without exacerbating immunopathology.

REFERENCES

Almeida, A.S., Lago, P.M., Boechat, N., Huard, R.C., Lazzarini, L.C.O., Santos, A.R., Nociari, M., Zhu, H., Perez-Sweeney, B.M., Bang, H., et al. (2009). Tuberculosis Is Associated with a Down-Modulatory Lung Immune Response That Impairs Th1-Type Immunity. J. Immunol. *183*, 718–731.

Beamer, G.L., Flaherty, D.K., Assogba, B.D., Stromberg, P., Gonzalez-Juarrero, M., Malefyt, R. de W., Vesosky, B., and Turner, J. (2008). Interleukin-10 Promotes Mycobacterium tuberculosis Disease Progression in CBA/J Mice. J. Immunol. *181*, 5545–5550.

Bean, A.G.D., Roach, D.R., Briscoe, H., France, M.P., Korner, H., Sedgwick, J.D., and Britton, W.J. (1999). Structural Deficiencies in Granuloma Formation in TNF Gene-Targeted Mice Underlie the Heightened Susceptibility to Aerosol Mycobacterium tuberculosis Infection, Which Is Not Compensated for by Lymphotoxin. J. Immunol. *162*, 3504–3511.

Berry, M.P.R., Graham, C.M., McNab, F.W., Xu, Z., Bloch, S.A.A., Oni, T., Wilkinson, K.A., Banchereau, R., Skinner, J., Wilkinson, R.J., et al. (2010). An interferon-inducible neutrophil-driven blood transcriptional signature in human tuberculosis. Nature *466*, 973–977.

Cavalcanti, Y.V.N., Brelaz, M.C.A., Neves, J.K. de A.L., Ferraz, J., Candido, Pereira, V., R&#xea, R., and Alves, G. (2012). Role of TNF-Alpha, IFN-Gamma, and IL-10 in the Development of Pulmonary Tuberculosis. Pulm. Med. *2012*, e745483.

Colditz, G.A., Brewer, T.F., Berkey, C.S., Wilson, M.E., Burdick, E., Fineberg, H.V., and Mosteller, F. (1994). Efficacy of BCG vaccine in the prevention of tuberculosis. Meta-analysis of the published literature. JAMA *271*, 698–702.

Colditz, G.A., Berkey, C.S., Mosteller, F., Brewer, T.F., Wilson, M.E., Burdick, E., and Fineberg, H.V. (1995). The efficacy of bacillus Calmette-Guérin vaccination of newborns and infants in the prevention of tuberculosis: meta-analyses of the published literature. Pediatrics *96*, 29–35.

Cooper, A.M. (2009). Cell-Mediated Immune Responses in Tuberculosis. Annu. Rev. Immunol. *27*, 393–422.

Cooper, A.M., and Khader, S.A. (2008). The role of cytokines in the initiation, expansion, and control of cellular immunity to tuberculosis. Immunol. Rev. *226*, 191–204.

Cooper, A.M., Dalton, D.K., Stewart, T.A., Griffin, J.P., Russell, D.G., and Orme, I.M. (1993). Disseminated tuberculosis in interferon gamma gene-disrupted mice. J. Exp. Med. *178*, 2243–2247.

D, D., Ml, B., L, R., L, U., Cf, R., C, L., Ma, F., O, M., and Oa, B. (1999). In vitro synthesis of interferon-gamma, interleukin-4, transforming growth factor-beta and interleukin-1 beta by peripheral blood mononuclear cells from tuberculosis patients: relationship with the severity of pulmonary involvement. Scand. J. Immunol. *49*, 210–217.

Dheda, K., Gumbo, T., Maartens, G., Dooley, K.E., McNerney, R., Murray, M., Furin, J., Nardell, E.A., London, L., Lessem, E., et al. (2017). The epidemiology, pathogenesis, transmission, diagnosis, and management of multidrug-resistant, extensively drug-resistant, and incurable tuberculosis. Lancet Respir. Med.

Ding, A.H., Nathan, C.F., and Stuehr, D.J. (1988). Release of reactive nitrogen intermediates and reactive oxygen intermediates from mouse peritoneal macrophages. Comparison of activating cytokines and evidence for independent production. J. Immunol. Baltim. Md 1950 *141*, 2407–2412.

Dlugovitzky, D., Torres-Morales, A., Rateni, L., Farroni, M. a., Largacha, C., Molteni, O., and Bottasso, O. (1997). Circulating profile of Th1 and Th2 cytokines in tuberculosis patients with different degrees of pulmonary involvement. FEMS Immunol. Med. Microbiol. *18*, 203–207.

Dye, C., and Williams, B.G. (2010). The population dynamics and control of tuberculosis. Science *328*, 856–861.

Ehlers, S. (2003). Role of tumour necrosis factor (TNF) in host defence against tuberculosis: implications for immunotherapies targeting TNF. Ann. Rheum. Dis. *62*, ii37-ii42.

Eruslanov, E.B., Lyadova, I.V., Kondratieva, T.K., Majorov, K.B., Scheglov, I.V., Orlova, M.O., and Apt, A.S. (2005). Neutrophil responses to Mycobacterium tuberculosis infection in genetically susceptible and resistant mice. Infect. Immun. *73*, 1744–1753.

Flynn, J.L., Chan, J., Triebold, K.J., Dalton, D.K., Stewart, T.A., and Bloom, B.R. (1993). An essential role for interferon gamma in resistance to Mycobacterium tuberculosis infection. J. Exp. Med. *178*, 2249–2254.

Flynn, J.L., Goldstein, M.M., Chan, J., Triebold, K.J., Pfeffer, K., Lowenstein, C.J., Schrelber, R., Mak, T.W., and Bloom, B.R. (1995). Tumor necrosis factor-α is required in the protective immune response against mycobacterium tuberculosis in mice. Immunity *2*, 561–572.

Flynn, J.L., Chan, J., and Lin, P.L. (2011). Macrophages and control of granulomatous inflammation in tuberculosis. Mucosal Immunol. *4*, 271–278.

Jouanguy, E., Altare, F., Lamhamedi, S., Revy, P., Emile, J.-F., Newport, M., Levin, M., Blanche, S., Seboun, E., Fischer, A., et al. (1996). Interferon-γ –Receptor Deficiency in an Infant with Fatal Bacille Calmette–Guérin Infection. N. Engl. J. Med. *335*, 1956–1962.

Kaufmann, S.H.E., Weiner, J., and von Reyn, C.F. (2017). Novel approaches to tuberculosis vaccine development. Int. J. Infect. Dis. *56*, 263–267.

Kimmey, J.M., Huynh, J.P., Weiss, L.A., Park, S., Kambal, A., Debnath, J., Virgin, H.W., and Stallings, C.L. (2015). Unique role for ATG5 in neutrophil-mediated immunopathology during M. tuberculosis infection. Nature *528*, 565–569.

Koch, A., and Wilkinson, R.J. (2014). The road to drug resistance in Mycobacterium tuberculosis. Genome Biol. *15*, 520.

Lamichhane, G. (2011). Mycobacterium Tuberculosis Response to Stress from Reactive Oxygen and Nitrogen Species. Front. Microbiol. *2*.

Liew, F.Y., and Cox, F.E. (1991). Nonspecific defence mechanism: the role of nitric oxide. Immunol. Today *12*, A17-21.

Lin, P.L., Plessner, H.L., Voitenok, N.N., and Flynn, J.L. (2007). Tumor Necrosis Factor and Tuberculosis. J. Investig. Dermatol. Symp. Proc. *12*, 22–25.

Lyadova, I.V. (2017). Neutrophils in Tuberculosis: Heterogeneity Shapes the Way?

MacMicking, J.D., North, R.J., LaCourse, R., Mudgett, J.S., Shah, S.K., and Nathan, C.F. (1997). Identification of nitric oxide synthase as

a protective locus against tuberculosis. Proc. Natl. Acad. Sci. *94*, 5243–5248.

Mattila, J.T., Maiello, P., Sun, T., Via, L.E., and Flynn, J.L. (2015). Granzyme B-expressing neutrophils correlate with bacterial load in granulomas from Mycobacterium tuberculosis-infected cynomolgus macaques. Cell. Microbiol. *17*, 1085–1097.

McDyer, J.F., Hackley, M.N., Walsh, T.E., Cook, J.L., and Seder, R.A. (1997). Patients with multidrug-resistant tuberculosis with low CD4+ T cell counts have impaired Th1 responses. J. Immunol. *158*, 492–500.

Mishra, B.B., Lovewell, R.R., Olive, A.J., Zhang, G., Wang, W., Eugenin, E., Smith, C.M., Phuah, J.Y., Long, J.E., Dubuke, M.L., et al. (2017). Nitric oxide prevents a pathogen-permissive granulocytic inflammation during tuberculosis. Nat. Microbiol. *2*, 17072.

Mohan, V.P., Scanga, C.A., Yu, K., Scott, H.M., Tanaka, K.E., Tsang, E., Tsai, M.C., Flynn, J.L., and Chan, J. (2001). Effects of Tumor Necrosis Factor Alpha on Host Immune Response in Chronic Persistent Tuberculosis: Possible Role for Limiting Pathology. Infect. Immun. *69*, 1847–1855.

Murray, P.J., and Young, R.A. (1999). Increased Antimycobacterial Immunity in Interleukin-10-Deficient Mice. Infect. Immun. *67*, 3087–3095.

Nathan, C. (2009). Taming tuberculosis: a challenge for science and society. Cell Host Microbe *5*, 220–224.

Nathan, C., and Shiloh, M.U. (2000). Reactive oxygen and nitrogen intermediates in the relationship between mammalian hosts and microbial pathogens. Proc. Natl. Acad. Sci. U. S. A. *97*, 8841–8848.

Newport, M.J., Huxley, C.M., Huston, S., Hawrylowicz, C.M., Oostra, B.A., Williamson, R., and Levin, M. (1996). A Mutation in the Interferon-γ –Receptor Gene and Susceptibility to Mycobacterial Infection. N. Engl. J. Med. *335*, 1941–1949.

Nicholson, S., Bonecini-Almeida, M. da G., Silva, J.R.L. e, Nathan, C., Xie, Q.W., Mumford, R., Weidner, J.R., Calaycay, J., Geng, J., Boechat, N., et al. (1996). Inducible nitric oxide synthase in pulmonary alveolar macrophages from patients with tuberculosis. J. Exp. Med. *183*, 2293–2302.

Oberholzer, A., Oberholzer, C., and Moldawer, L.L. (2000). Cytokine signaling--regulation of the immune response in normal and critically ill states. Crit. Care Med. *28*, N3-12.

Rich, E.A., Torres, M., Sada, E., Finegan, C.K., Hamilton, B.D., and Toossi, Z. (1997). Mycobacterium tuberculosis (MTB)- stimulated production of nitric oxide by human alveolar macrophages and relationship of nitric oxide production to growth inhibition of MTB. Tuber. Lung Dis. *78*, 247–255.

Russell, D.G. (2001). Mycobacterium tuberculosis: here today, and here tomorrow. Nat. Rev. Mol. Cell Biol. *2*, 569–586.

Scanga, C.A., Mohan, V.P., Tanaka, K., Alland, D., Flynn, J.L., and Chan, J. (2001). The Inducible Nitric Oxide Synthase Locus Confers Protection against Aerogenic Challenge of Both Clinical and Laboratory Strains of Mycobacterium tuberculosis in Mice. Infect. Immun. *69*, 7711–7717.

Shin, H.D., Park, B.L., Kim, L.H., Cheong, H.S., Lee, I.H., and Park, S.K. (2005). Common interleukin 10 polymorphism associated with decreased risk of tuberculosis. Exp. Mol. Med. *37*, 128–132.

Solovic, I., Sester, M., Gomez-Reino, J.J., Rieder, H.L., Ehlers, S., Milburn, H.J., Kampmann, B., Hellmich, B., Groves, R., Schreiber, S., et al. (2010). The risk of tuberculosis related to tumour necrosis factor antagonist therapies: a TBNET consensus statement. Eur. Respir. J. *36*, 1185–1206.

Tiberi, S., Carvalho, A.C.C., Sulis, G., Vaghela, D., Rendon, A., Mello, F.C. de Q., Rahman, A., Matin, N., Zumla, A., and Pontali, E. (2017). The cursed duet today: Tuberculosis and HIV-coinfection. Presse Medicale Paris Fr. 1983 *46*, e23–e39.

Torres, M., Herrera, T., Villareal, H., Rich, E.A., and Sada, E. (1998). Cytokine profiles for peripheral blood lymphocytes from patients with active pulmonary tuberculosis and healthy household contacts in response to the 30-kilodalton antigen of Mycobacterium tuberculosis. Infect. Immun. *66*, 176–180.

Trentini, M.M., Oliveira, D., M, F., Kipnis, A., and Junqueira-Kipnis, A.P. (2016). The Role of Neutrophils in the Induction of Specific Th1 and Th17 during Vaccination against Tuberculosis. Front. Microbiol. *7*.

Wallis, R.S., and Hafner, R. (2015). Advancing host-directed therapy for tuberculosis. Nat. Rev. Immunol. *15*, 255–263.

Wang, C.H., Liu, C.Y., Lin, H.C., Yu, C.T., Chung, K.F., and Kuo, H.P. (1998). Increased exhaled nitric oxide in active pulmonary tuberculosis due to inducible NO synthase upregulation in alveolar macrophages. Eur. Respir. J. *11*, 809–815.

Yeremeev, V., Linge, I., Kondratieva, T., and Apt, A. (2015). Neutrophils exacerbate tuberculosis infection in genetically susceptible mice. Tuberc. Edinb. Scotl. *95*, 447–451.

Zumla, A., Rao, M., Wallis, R.S., Kaufmann, S.H.E., Rustomjee, R., Mwaba, P., Vilaplana, C., Yeboah-Manu, D., Chakaya, J., Ippolito, G., et al. (2016). Host-directed therapies for infectious diseases: current status, recent progress, and future prospects. Lancet Infect. Dis. *16*, e47-63.

CHAPTER 2

Protein kinase R is dispensable for host control of tuberculosis in mice

CHAPTER TWO

PROTEIN KINASE R IS DISPENSABLE FOR HOST CONTROL OF TUBERCULOSIS IN MICE[1]

SUMMARY

Genetic deletion of protein kinase R (PKR) in mice was reported (Wu et al., 2012) to enhance macrophage activation *in vitro* in response to interferon-γ (IFNγ) and to reduce the burden of *Mycobacterium tuberculosis* (Mtb) *in vivo*. Consistent with this, treatment of wild-type (WT) macrophages *in vitro* with a novel PKR inhibitor (Bryk et al., 2011) also enhanced IFNγ–dependent macrophage activation. Herein, co-treatment with IFNγ and a highly selective PKR inhibitor likewise induced macrophages to produce more reactive nitrogen intermediates (RNI) and tumor necrosis factor alpha (TNFα) and less interleukin 10 (IL-10) than IFNγ alone. Surprisingly, the PKR inhibitor had a comparable effect on PKR-deficient macrophages. The retrospective investigation revealed that PKR-deficient mice used in the original study had not been backcrossed. On comparing extensively genetically matched PKR-deficient and WT mice, we saw no impact of PKR deficiency on macrophage activation *in vitro* or during the course of infection *in vivo*. Responses of 129S1/SvImJ macrophages to IFNγ were much greater than those of C57BL/6 macrophages, but PKR was not required to mediate the IFNγ–dependent production of IL-10 and did not restrain the IFNγ–dependent production of RNI and TNFα.

[1] Shashirekha Mundhra, Ruslana Bryk, Natalie Hawryluk, Tuo Zhang, Xiuju Jiang, Carl F. Nathan. Protein kinase R is dispensable for host control of tuberculosis in mice. *(Manuscript in Submission)*.

INTRODUCTION

Tuberculosis (TB) is now the leading cause of death by a single infectious agent in humans. The World Health Organization (WHO) has estimated that 2015 witnessed 10.4 million new TB cases and 1.8 million deaths from TB. The emergence of multidrug-resistant (MDR) and extensively drug-resistant (XDR) TB in individuals in more than 100 countries increases the global threat. The effort to find new treatments has expanded to consider potential host-directed therapies (HDT) (Wallis and Hafner, 2015)(Zumla et al., 2016).

One target proposed as a candidate for HDT was protein kinase R (Wu et al., 2012). PKR is a widely expressed serine/threonine protein kinase (Fig. 1) that is activated by double-stranded RNA (dsRNA) (Proud, 1995; Robertson and Mathews, 1996; Williams, 1999). Binding of dsRNA promotes PKR's homodimerization, autophosphorylation, and activation (Dey et al., 2005). PKR function is diverse and well-characterized. PKR is induced by type I IFN, and reciprocally, enhances IFN-α/β production by stabilizing IFN-α/β mRNA in response to several RNA viruses, such as Semiliki Forest Virus (Schulz et al., 2010). PKR promotes antiviral activity by inhibiting translation through phosphorylation of eukaryotic initiation factor 2α (eIF-2α) (de Haro et al., 1996). PKR can be activated in response to lipopolysaccharide (LPS), cytokines such as IFNγ, IL-1 and TNFα, oxidative stress and polyanions such as heparin and dextran sulphate (Williams, 2001) and it can mediate an inflammatory response through

activation of NF-κB (Zamanian-Daryoush et al., 2000). PKR also has pro-apoptotic functions (Der et al., 1997).

Despite PKR's widespread actions, its genetic disruption does not produce an overt phenotype in mice unless they are infected with certain pathogens. In fact, during Mtb infection, PKR-deficient mice had a reduced mycobacterial burden and less immunopathology than PKR-sufficient mice (Wu et al., 2012). *In vivo* and *in vitro*, PKR-deficient macrophages underwent more apoptosis than WT macrophages when infected with Mtb (Wu et al., 2012). In response to IFNγ, PKR-deficient macrophages produced more inducible nitric oxide synthase (iNOS), RNI and TNFα than PKR-sufficient macrophages (Wu et al., 2012). The inference that the difference in expression of PKR was a critical factor in those experiments was reinforced by evidence that treatment of WT macrophages with a PKR inhibitor, N-(2(1H-indol-3-yl)ethyl)-4-(2-methyl-1H-indol-3-yl)-pyrimin-2-amine increased the extent of macrophage activation in response to IFNγ above that seen with IFNγ alone (Bryk et al., 2011). Treatment of macrophages with IFNγ induced the production of IL-10 (Wu et al., 2012), a cytokine that opposes many of the actions of IFNγ on macrophages (Bogdan et al., 1991). The IFNγ-dependent induction of IL-10 was markedly reduced in PKR-deficient macrophages, and reduction in IL-10 contributed to the ability of PKR-deficient macrophages to respond more robustly to IFNγ than WT macrophages (Wu et al., 2012). For all these reasons, inhibition of PKR appeared to hold promise as a candidate for HDT of TB.

The PKR inhibitor, N-(2(1H-indol-3-yl)ethyl)-4-(2-methyl-1H-indol-3-yl)-pyrimin-2-amine developed earlier (Bryk et al., 2011) was not characterized in terms of its selectivity. We set out to develop a highly selective PKR inhibitor. As part of our analysis of potential inhibitors, we compared their impact on macrophages that did or did not contain PKR. To our surprise, their effect was similar whether macrophages contained PKR or not. This prompted a re-investigation of the earlier study on responses of PKR-deficient macrophages to Mtb (Wu et al., 2012). An issue was uncovered regarding the backcrossing of those mice, so we repeated key observations of that work using macrophages from two strains of PKR knockout mice- those deficient either in the regulatory domain or in the kinase domain of PKR (Yang et al., 1995) (Abraham et al., 1999)- whose genetic background we confirmed. We also studied the course of Mtb infection in co-housed mice of the F2 generation arising from a PKR KO and background-matched WT parental strains. The results revealed that macrophages from 129S1/SvImJ mice respond much more robustly to IFNγ than those from C57BL/6J mice, but PKR plays no appreciable role in the response of mouse macrophages to IFNγ *in vitro* or in the course of Mtb infection *in vivo*. Hence, PKR can be ruled out as a target for HDT.

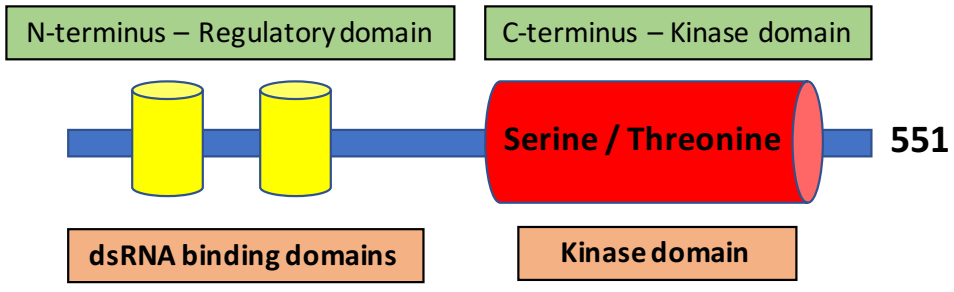

Fig. 1 Schematic representation of domains of protein kinase R.

RESULTS

Screening of kinase inhibitors for macrophage activation phenotypes in collaboration with Celgene Global Health.

Since PKR was reported to be important in the control of TB (Wu et al., 2012), we hypothesized that targeting PKR would be an effective strategy for HDT of TB. A PKR inhibitor used extensively in the literature, Imoxin (C16) (Nakamura et al., 2014) was found to inhibit 107 out of 258 kinases when tested at a concentration of 3 μM (Table 1), confirming its non-specificity. The PKR inhibitor developed earlier, N-[2-(1H-indol-3-yl)ethyl]-4-(2-methyl-1H-indol-3-yl)pyrimidin-2-amine (compound 51) (Bryk et al., 2011) was not characterized in terms of its selectivity. This necessitated a search for a selective PKR inhibitor to be used as HDT for TB. We collaborated with Celgene Global Health (CGH) to develop PKR inhibitors with better characterized selectivity than those reported to date. My colleague, Ruslana Bryk screened a small molecule kinase library from CGH against recombinant human PKR, and together we screened on bone marrow-derived macrophages (BMMs) for the three phenotypes – elevation of nitrite and TNFα and reduction of IL-10 compared to controls, in the presence of IFNγ. Fig. 2 describes a flowchart of the screening process along with the experimental design. Table 2 lists all the compounds that were tested for this thesis.

Table 1. Kinase selectivity panel of Imoxin

Imoxin was tested at 3 μM for kinase selectivity assay performed at Life Technologies' SelectScreen® Profiling Service) for Celgene Global Health. The values are mean of % activity remaining, calculated by subtracting the mean of % inhibition from 100 %. The kinases for which mean % inhibition was > 80 (% activity remaining < 20) have been highlighted in red.

Kinase	oxin @ 3.0 μM	Kinase	oxin @ 3.0 μM	Kinase	oxin @ 3.0 μM	Kinase	oxin @ 3.0 μM
ABL1	13	EGFR (ErbB1) L858R	95	LYN B	88	PLK2	7
ABL1 E255K	22	EGFR (ErbB1) L861Q	89	MAP2K1 (MEK1)	2	PLK3	45
ABL1 G250E	16	EGFR (ErbB1) T790M	46	MAP2K2 (MEK2)	113	PRKACA (PKA)	10
ABL1 T315I	76	FR (ErbB1) T790M L858R	35	MAP2K6 (MKK6)	7	PRKCA (PKC alpha)	11
ABL1 Y253F	20	EPHA1	35	MAP3K8 (COT)	1	PRKCB1 (PKC beta I)	39
ABL2 (mouse)	37	EPHA2	39	MAP3K9 (MLK1)	7	PRKCB2 (PKC beta II)	41
ACVR1B (ALK4)	60	EPHA4	36	MAP4K2 (GCK)	0	PRKCD (PKC delta)	7
ADRBK1 (GRK2)	91	EPHA5	99	MAP4K4 (HGK)	-5	PRKCE (PKC epsilon)	33
ADRBK2 (GRK3)	97	EPHA8	79	MAP4K5 (KHS1)	2	PRKCG (PKC gamma)	32
AKT1 (PKB alpha)	76	EPHB1	19	MAPK1 (ERK2)	2	PRKCH (PKC eta)	11
AKT2 (PKB beta)	72	EPHB2	38	MAPK10 (JNK3)	32	PRKCI (PKC iota)	81
AKT3 (PKB gamma)	69	EPHB3	60	MAPK11 (p38 beta)	93	PRKCN (PKD3)	39
AMPK A1/B1/G1	1	EPHB4	96	MAPK12 (p38 gamma)	15	PRKCQ (PKC theta)	39
AMPK A2/B1/G1	3	ERBB2 (HER2)	97	MAPK13 (p38 delta)	27	PRKCZ (PKC zeta)	81
AURKA (Aurora A)	2	ERBB4 (HER4)	70	MAPK14 (p38 alpha)	85, 99	PRKD1 (PKC mu)	20
AURKB (Aurora B)	9	FER	21	MAPK3 (ERK1)	-1	PRKD2 (PKD2)	14
AURKC (Aurora C)	25	FES (FPS)	21	MAPK8 (JNK1)	23	PRKG1	9
AXL	43	FGFR1	11	MAPK9 (JNK2)	13	PRKG2 (PKG2)	5
BLK	20	FGFR2	50	MAPKAPK2	84	PRKX	7
BMX	95	FGFR3	62	MAPKAPK3	80	PTK2 (FAK)	39
BRAF	104	FGFR3 K650E	4	MAPKAPK5 (PRAK)	53	PTK2B (FAK2)	91
BRAF V599E	-4	FGFR4	91	MARK1 (MARK)	6	PTK6 (Brk)	77
BRSK1 (SAD1)	0	FGR	10	MARK2	5	AF1 (cRAF) Y340D Y341D	1
BTK	91	FLT1 (VEGFR1)	88	MATK (HYL)	94	RET	3
AMK1D (CaMKI delta)	67	FLT3	-5	MELK	4	RET V804L	1
AMK2A (CaMKII alpha)	15	FLT3 D835Y	1	MERTK (cMER)	83	RET Y791F	1
AMK2B (CaMKII beta)	97	FLT4 (VEGFR3)	8	MET (cMet)	81	ROCK1	7
AMK2D (CaMKII delta)	6	FRAP1 (mTOR)	97	MET M1250T	11	ROCK2	9
CAMK4 (CaMKIV)	65	FRK (PTK5)	109	MINK1	-1	ROS1	95
CDC42 BPA (MRCKA)	78	FYN	45	MKNK1 (MNK1)	2	RPS6KA1 (RSK1)	8
CDC42 BPB (MRCKB)	78	GRK4	37	MST1R (RON)	62	RPS6KA2 (RSK3)	2
CDK1/cyclin B	0	GRK5	55	MST4	-1	RPS6KA3 (RSK2)	8
CDK2/cyclin A	2	GRK6	25	MUSK	95	RPS6KA4 (MSK2)	1
CDK5/p25	2	GRK7	20	MYLK2 (skMLCK)	-1	RPS6KA5 (MSK1)	12
CDK5/p35	1	GSG2 (Haspin)	0	NEK1	14	RPS6KA6 (RSK4)	67
CDK7/cyclin H/MNAT1	6	GSK3A (GSK3 alpha)	0	NEK2	76	RPS6KB1 (p70S6K)	18
CDK9/cyclin T1	0	GSK3B (GSK3 beta)	1	NEK4	88	SGK (SGK1)	5
CHEK1 (CHK1)	3	HCK	41	NEK6	54	SGK2	8
CHEK2 (CHK2)	17	HIPK1 (Myak)	22	NEK7	76	SGKL (SGK3)	31
CHUK (IKK alpha)	0	HIPK2	9	NEK9	25	SNF1LK2	14
CLK1	3	HIPK3 (YAK1)	24	NTRK1 (TRKA)	3	SRC	88
CLK2	1	HIPK4	24	NTRK2 (TRKB)	71	SRC N1	31
CLK3	29	IGF1R	79	NTRK3 (TRKC)	62	SRMS (Srm)	98
CSF1R (FMS)	76	IKBKB (IKK beta)	29	NUAK1 (ARK5)	2	SRPK1	88
CSK	70	IKBKE (IKK epsilon)	14	PAK1	85	SRPK2	97
SNK1A1 (CK1 alpha 1)	72	INSR	69	PAK2 (PAK65)	68	STK22B (TSSK2)	91
CSNK1D (CK1 delta)	21	INSRR (IRR)	88	PAK3	79	STK22D (TSSK1)	37
CSNK1E (CK1 epsilon)	14	IRAK1	5	PAK4	45	STK23 (MSSK1)	96
SNK1G1 (CK1 gamma 1)	68	IRAK4	21	PAK6	75	STK24 (MST3)	-5
SNK1G2 (CK1 gamma 2)	62	ITK	96	PAK7 (KIAA1264)	91	STK25 (YSK1)	2
SNK1G3 (CK1 gamma 3)	65	JAK1	90	PASK	23	STK3 (MST2)	-2
CSNK2A1 (CK2 alpha 1)	64	JAK2	15	PDGFRA (PDGFR alpha)	52	STK4 (MST1)	1
CSNK2A2 (CK2 alpha 2)	33	JAK2 JH1 JH2	26	PDGFRA D842V	5	SYK	77
DAPK1	18	JAK2 JH1 JH2 V617F	24	PDGFRA T674I	11	TAOK2 (TAO1)	33
DAPK3 (ZIPK)	24	JAK3	70	PDGFRA V561D	7	TBK1	89
DCAMKL2 (DCK2)	90	KDR (VEGFR2)	1	PDGFRB (PDGFR beta)	25	TEK (Tie2)	33
DNA-PK	23	KIT	101	PDK1	12, 4	TTK	-2
DYRK1A	5	KIT T670I	26	PHKG1	14	TXK	80
DYRK1B	4	LCK	19	PHKG2	18	TYK2	3
DYRK3	6	LRRK2	0	PIM1	19	TYRO3 (RSE)	91
DYRK4	49	LRRK2 G2019S	0	PIM2	28	YES1	90
EEF2K	90	LTK (TYK1)	55	PKN1 (PRK1)	27	ZAP70	104
EGFR (ErbB1)	83	LYN A	22	PLK1	72	**Hit_Score20**	**107 of 258**

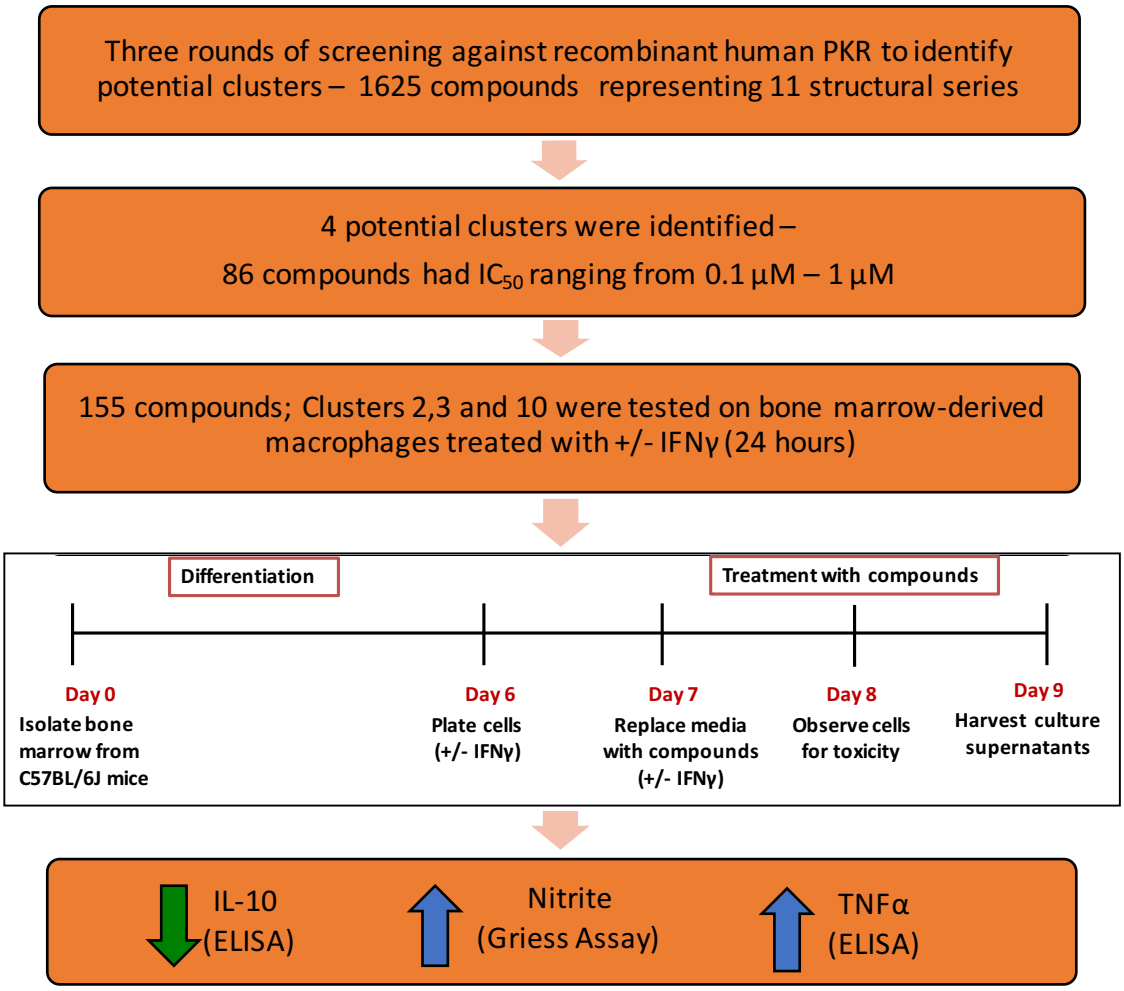

Fig. 2. Flowchart describing the progression of screening of PKR inhibitors.

R. Bryk performed all assays against human recombinant PKR. S. Mundhra screened compounds on BMMs along with R. Bryk. S.Mundhra performed all ELISAs and graphed the data. A cluster refers to a class of chemical compounds with structural and physicochemical similarities.

Table 2. Compounds tested in bone marrow-derived macrophages, with their phenotypes in presence of IFNγ.
The compounds highlighted in yellow were tested in a mouse model of Mtb infection. (Discussed in Chapter 3).

TNFα: +++ >200 pg/ml; ++ 100-200 pg/ml; + 50-100 pg/ml;

IL10: +++ 75-95% reduction; ++ 50-75%; + <50% reduction;

Nitrite: +++ > 20 μM; ++ 10-19 μM; + 5-10 μM

DNT Did not test

No.	Nitrite	TNFα	IL-10	CC#	No.	Nitrite	TNFα	IL-10	CC#	No.	Nitrite	TNFα	IL-10	CC#
C1	+	-	+	CC0223160	C51	+	-	+	CC0387223	2006	-	DNT	DNT	CC0775206
C2	-	-	-	CC0223522	C52	-	-	+	CC0386932	2007	++	+	+++	CC0775207
C3	-	-	-	CC0223643	C53	-	-	+	CC0386661	2008	-	+	-	CC0775208
C4	-	-	-	CC0224900	C54	-	-	+	CC0386662	2009	-	DNT	DNT	CC0775209
C5	-	-	-	CC0120633	C55	+++	++	+++	CC0338364	2010	++	++	+++	CC0775210
C6	++	+	+++	CC0127685	C56	++	++	+++	CC0338378	2011	++	+	++	CC0775211
C7	-	-	-	CC0313679	C57	++	+	+++	CC0327075	2013	++	+	+++	CC0776037
C8	++	+	++	CC0337140	C58	-	+	++	CC0225128	2014	-	DNT	DNT	CC0776038
C9	-	-	-	CC0342376	C59	-	-	++	CC0477489	2015	-	DNT	DNT	CC0776039
C10	-	-	-	CC0418422	C60	-	-	+	CC0191770	2016	++	+	+++	CC0776040
C11	-	-	-	CC0418340	C61	-	-	++	CC0185965	2017	++	+	++	CC0776041
C12	+	-	-	CC0741175	C62	-	-	+++	CC0225144	2018	-	DNT	DNT	CC0776042
C13	-	-	-	CC0209934	C63	++	+	+++	CC0386754	2019	-	DNT	DNT	CC0776043
C14	-	-	-	CC0223190	C64	-	-	+	CC0387222	2020	-	DNT	DNT	CC0776044
C15	-	-	-	CC0224002	C65	++	++	+++	CC0387522	2021	-	DNT	DNT	CC0776045
C16	-	-	-	CC0224004	C66	-	-	+	CC0195706	2022	-	DNT	DNT	CC0776046
C17	-	-	-	CC0223188	C67	-	-	+++	CC0327041	2031	-	-	++	CC0776118
C18	-	-	-	CC0224724	C68	-	-	++	CC0327111	2032	-	-	++	CC0776119
C19	-	-	-	CC0224830	C69	-	-	++	CC0342333	2033	+++	+	+++	CC0776120
C20	-	-	-	CC0224837	C70	-	-	+++	CC0386702	2034	+++	++	+++	CC0776121
C21	-	-	-	CC0224894	C71	+++	+	+++	CC0342393	2042	-	-	+	CC0776401
C22	-	-	-	CC0225105	C72	-	-	+++	CC0415593	2043	-	-	-	CC0776402
C23	+	+	+++	CC0225707	C73	-	-	+++	CC0415447	2044	-	++	+++	CC0776403
C24	++	-	++	CC0225137	C74	-	-	+++	CC0418912	2045	-	-	+	CC0776404
C25	-	-	+	CC0120729	C75	++	-	++	CC0338366	2046	-	DNT	DNT	CC0776876
C26	-	-	-	CC0145783	C76	-	-	++	CC0199406	2047	-	-	++	CC0776877
C27	++	+	+	CC0387097	C77	++	-	+++	CC0225146	2048	-	DNT	DNT	CC0776878
C28	-	+	-	CC0387495	C78	-	++	+++	CC0338382	2049	-	DNT	DNT	CC0776879
C29	+++	++	+++	CC0390602	C79	-	-	+++	CC0327104	2050	-	DNT	DNT	CC0777483
C30	-	-	+	CC0185921	C80	-	-	+++	CC0342369	2051	-	-	+++	CC0777484
C31	-	-	-	CC0195708	C81	-	-	++	CC0342330	2060	-	DNT	DNT	CC0777877
C32	-	-	+	CC0193701	C82	-	-	+	CC0338381	2061	-	-	-	CC0777878
C33	-	-	-	CC0195707	C83	-	+	+++	CC0338449	2062	+++	++	+++	CC0777879
C34	++	+	+++	CC0326986	C84	-	+	-	CC0387518	2063	-	DNT	DNT	CC0777880
C35	++	+	+++	CC0338377	C85	+++	++	+++	CC0387206	2064	-	DNT	DNT	CC0777881
C36	+	+	+++	CC0326965	C90	-	-	-	CC0338418	2067	-	DNT	DNT	CC0778344
C37	-	-	-	CC0342377	C91	++	+	+++	CC0327112	2068	-	-	++	CC0778345
C38	++	+	++	CC0386753	C92	-	-	-	CC0387222	2069	-	-	+++	CC0778346
C39	-	-	-	CC0418512	C93	-	-	-	CC0342396	2070	+	+	++	CC0778347
C40	-	-	-	CC0440647	C94	-	-	-	CC0225107	2071	++	+	+++	CC0778348
C41	+++	+++	++	CC0326962	C95	-	-	-	CC0417775	2072	-	DNT	DNT	CC0778349
C42	-	-	increase	CC0387762	C96	-	-	-	CC0480383	2073	-	DNT	DNT	CC0778350
C43	-	-	+++	CC0477769	C97	-	-	-	CC0224626	2074	-	DNT	DNT	CC0778351
C44	++	+++	+	CC0223159	1999	-	DNT	DNT	CC0775199	2081	-	DNT	DNT	CC0778729
C45	+	++	++	CC0195742	2000	-	DNT	DNT	CC0775200	2082	-	-	++	CC0778730
C46	-	-	-	CC0386751	2001	-	DNT	DNT	CC0775201	2083	-	DNT	DNT	CC0778731
C47	-	-	+	CC0227142	2002	++	-	+++	CC0775202	2084	-	-	++	CC0778732
C48	-	-		CC0225101	2003	+	+	+++	CC0775203	2833	-	-	-	
C49	-	-		CC0224989	2004	++	++	+++	CC0775204					
C50	-	+	+	CC0127686	2005	-	DNT	DNT	CC0775205					

Testing of a relatively selective PKR inhibitor on wild-type macrophages

A screen of over 2000 kinase inhibitors and their congeners in a CGH library against recombinant human PKR was conducted. C85 was one of 160 compounds identified as active and was tested for its ability to increase the release of nitrite and TNFα and to decrease the release of IL-10 from BMMs from WT C57BL/6J mice that had been treated with IFNγ (10 ng/mL) for 24 hours. C85 was an ATP-competitive inhibitor with an IC_{50} of 23 nM against PKR (Fig. 3A). C85 was relatively selective, in that it inhibited only 5 out of 258 kinases when tested at a concentration of 3 μM (Table 3). C85 was not toxic to BMMs (Fig. 3B). Treatment of IFNγ-primed, WT C57BL/6J BMMs with C85 led to a marked reduction in IL-10 and a marked increase in RNI and TNFα compared to exposure to IFNγ alone (Fig. 3C). These results appeared consistent with those reported using a chemically distinct inhibitor of uncharacterized specificity (Wu et al., 2012). However, the kinome includes more than 200 additional enzymes whose possible inhibition by C85 was not tested. To establish whether the effect of C85 on macrophages was due to inhibition of PKR or other targets, we next tested C85 on macrophages from WT and PKR KO mice.

Figure 1

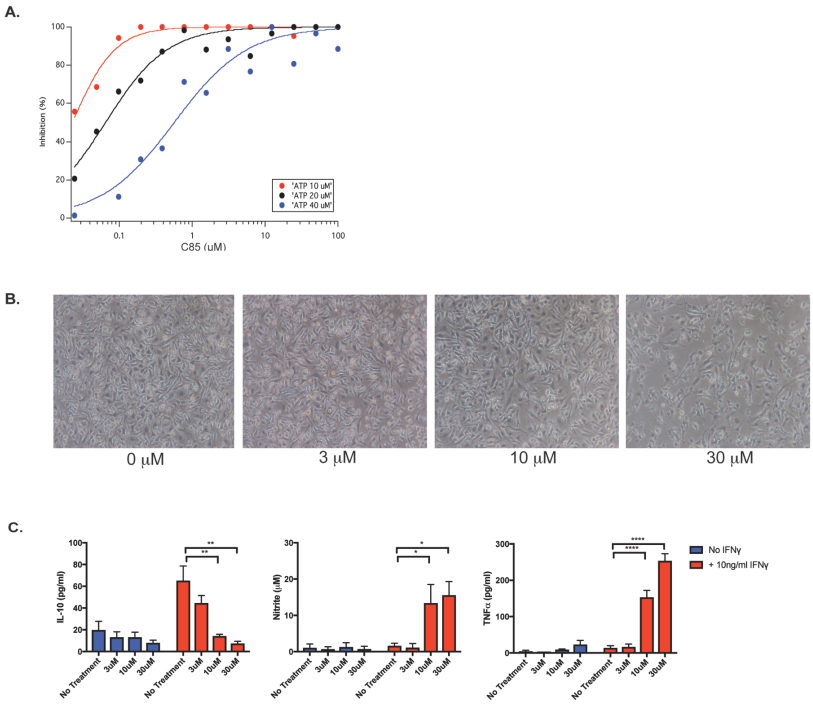

Figure 3. Compound 85 inhibits PKR *in vitro* and enhances macrophage activation with minimal toxicity.

A) Concentration-response for inhibition of human PKR by C85 at 10 μM ATP (red circles) or 20 μM ATP (black circles) or 40 μM (blue circles). *R. Bryk contributed this figure.*

B) Images of BMMs treated with indicated concentrations of C85 for 24 hr at 20X magnification.

C) Dose-response curve of C85 and its impact on IL-10 reduction, nitrite production and TNFα production on WT BMMs primed with IFNγ (10 ng/ml) for 24 hr then treated with C85 for 48 hr. Results in (C) are means ± SEM of two independent experiments each performed in triplicate. $p < 0.05$ = *; $p < 0.01$ = **; $p < 0.005$ = ***; $p < 0.001$ = ****.

Table 3. Kinase Selectivity of C85

C85 was at tested at 3 μM for kinase selectivity in an assay performed at Life Technologies' SelectScreen® Profiling Service for Celgene Global Health. The values are mean % activity remaining, calculated by subtracting mean % inhibition from 100 %. The kinases where mean % inhibition was > 80 (% activity remaining < 20) have been highlighted in red.

Kinase	85 @ 3.0 μM	Kinase	85 @ 3.0 μM	Kinase	85 @ 3.0 μM	Kinase	85 @ 3.0 μM
ABL1	80	EGFR (ErbB1) L858R	99	LYN B	91	PLK2	51
ABL1 E255K	69	EGFR (ErbB1) L861Q	98	MAP2K1 (MEK1)	94	PLK3	25
ABL1 G250E	70	EGFR (ErbB1) T790M	88	MAP2K2 (MEK2)	81	PRKACA (PKA)	99
ABL1 T315I	87	EGFR (ErbB1) T790M L858R	84	MAP2K6 (MKK6)	92	PRKCA (PKC alpha)	67
ABL1 Y253F	61	EPHA1	92	MAP3K8 (COT)	90	PRKCB1 (PKC beta I)	91
ABL2 (mouse)	71	EPHA2	96	MAP3K9 (MLK1)	76	PRKCB2 (PKC beta II)	96
ACVR1B (ALK4)	97	EPHA4	100	MAP4K2 (GCK)	7	PRKCD (PKC delta)	86
ADRBK1 (GRK2)	100	EPHA5	96	MAP4K4 (HGK)	0	PRKCE (PKC epsilon)	120
ADRBK2 (GRK3)	99	EPHA8	90	MAP4K5 (KHS1)	22	PRKCG (PKC gamma)	63
AKT1 (PKB alpha)	98	EPHB1	104	MAPK1 (ERK2)	107	PRKCH (PKC eta)	100
AKT2 (PKB beta)	99	EPHB2	97	MAPK10 (JNK3)	90	PRKCI (PKC iota)	96
AKT3 (PKB gamma)	84	EPHB3	104	MAPK11 (p38 beta)	94	PRKCN (PKD3)	118
AMPK A1/B1/G1	54	EPHB4	95	MAPK12 (p38 gamma)	90	PRKCQ (PKC theta)	87
AMPK A2/B1/G1	84	ERBB2 (HER2)	102	MAPK13 (p38 delta)	99	PRKCZ (PKC zeta)	113
AURKA (Aurora A)	88	ERBB4 (HER4)	92	MAPK14 (p38 alpha)	100, 92	PRKD1 (PKC mu)	90
AURKB (Aurora B)	83	FER	78	MAPK3 (ERK1)	96	PRKD2 (PKD2)	99
AURKC (Aurora C)	89	FES (FPS)	89	MAPK8 (JNK1)	74	PRKG1	90
AXL	85	FGFR1	90	MAPK9 (JNK2)	90	PRKG2 (PKG2)	69
BLK	41	FGFR2	100	MAPKAPK2	82	PRKX	87
BMX	183	FGFR3	97	MAPKAPK3	32	PTK2 (FAK)	93
BRAF	90	FGFR3 K650E	95	MAPKAPK5 (PRAK)	75	PTK2B (FAK2)	94
BRAF V599E	87	FGFR4	97	MARK1 (MARK)	83	PTK6 (Brk)	95
BRSK1 (SAD1)	81	FGR	78	MARK2	84	RAF1 (cRAF) Y340D Y341D	71
BTK	70	FLT1 (VEGFR1)	96	MATK (HYL)	99	RET	87
CAMK1D (CaMKI delta)	86	FLT3	49	MELK	74	RET V804L	91
CAMK2A (CaMKII alpha)	82	FLT3 D835Y	42	MERTK (cMER)	80	RET Y791F	88
CAMK2B (CaMKII beta)	84	FLT4 (VEGFR3)	78	MET (cMet)	359	ROCK1	98
CAMK2D (CaMKII delta)	74	FRAP1 (mTOR)	86	MET M1250T	97	ROCK2	95
CAMK4 (CaMKIV)	82	FRK (PTK5)	103	MINK1	6	ROS1	84
CDC42 BPA (MRCKA)	107	FYN	124	MKNK1 (MNK1)	95	RPS6KA1 (RSK1)	90
CDC42 BPB (MRCKB)	105	GRK4	57	MST1R (RON)	94	RPS6KA2 (RSK3)	82
CDK1/cyclin B	83	GRK5	93	MST4	89	RPS6KA3 (RSK2)	81
CDK2/cyclin A	83	GRK6	97	MUSK	98	RPS6KA4 (MSK2)	92
CDK5/p25	77	GRK7	60	MYLK2 (skMLCK)	63	RPS6KA5 (MSK1)	73
CDK5/p35	71	GSG2 (Haspin)	60	NEK1	44	RPS6KA6 (RSK4)	74
CDK7/cyclin H/MNAT1	148	GSK3A (GSK3 alpha)	16	NEK2	160	RPS6KB1 (p70S6K)	97
CDK9/cyclin T1	47	GSK3B (GSK3 beta)	26	NEK4	98	SGK (SGK1)	70
CHEK1 (CHK1)	92	HCK	77	NEK6	77	SGK2	65
CHEK2 (CHK2)	100	HIPK1 (Myak)	75	NEK7	95	SGKL (SGK3)	81
CHUK (IKK alpha)	43	HIPK2	63	NEK9	121	SNF1LK2	72
CLK1	84	HIPK3 (YAK1)	83	NTRK1 (TRKA)	101	SRC	101
CLK2	53	HIPK4	75	NTRK2 (TRKB)	83	SRC N1	67
CLK3	92	IGF1R	99	NTRK3 (TRKC)	70	SRMS (Srm)	86
CSF1R (FMS)	20	IKBKB (IKK beta)	62	NUAK1 (ARK5)	18	SRPK1	84
CSK	96	IKBKE (IKK epsilon)	46	PAK1	98	SRPK2	100
CSNK1A1 (CK1 alpha 1)	85	INSR	103	PAK2 (PAK65)	102	STK22B (TSSK2)	93
CSNK1D (CK1 delta)	98	INSRR (IRR)	97	PAK3	201	STK22D (TSSK1)	87
CSNK1E (CK1 epsilon)	90	IRAK1	47	PAK4	52	STK23 (MSSK1)	88
CSNK1G1 (CK1 gamma 1)	93	IRAK4	109	PAK6	155	STK24 (MST3)	92
CSNK1G2 (CK1 gamma 2)	86	ITK	100	PAK7 (KIAA1264)	60	STK25 (YSK1)	103
CSNK1G3 (CK1 gamma 3)	93	JAK1	75	PASK	96	STK3 (MST2)	63
CSNK2A1 (CK2 alpha 1)	96	JAK2	58	PDGFRA (PDGFR alpha)	93	STK4 (MST1)	75
CSNK2A2 (CK2 alpha 2)	81	JAK2 JH1 JH2	54	PDGFRA D842V	85	SYK	25
DAPK1	65	JAK2 JH1 JH2 V617F	68	PDGFRA T674I	102	TAOK2 (TAO1)	100
DAPK3 (ZIPK)	95	JAK3	69	PDGFRA V561D	66	TBK1	33
DCAMKL2 (DCK2)	96	KDR (VEGFR2)	77	PDGFRB (PDGFR beta)	88	TEK (Tie2)	87
DNA-PK	91	KIT	80	PDK1	81, 104	TTK	112
DYRK1A	82	KIT T670I	84	PHKG1	111	TXK	94
DYRK1B	75	LCK	85	PHKG2	87	TYK2	79
DYRK3	78	LRRK2	28	PIM1	91	TYRO3 (RSE)	58
DYRK4	103	LRRK2 G2019S	44	PIM2	75	YES1	94
EEF2K	98	LTK (TYK1)	84	PKN1 (PRK1)	132	ZAP70	93
EGFR (ErbB1)	101	LYN A	90	PLK1	94	Hit_Score20	5 of 258

PKR expression in the C57BL/6J background does not impact the effect of C85 on macrophage activation.

To test whether PKR was the functionally relevant target of C85 in macrophage activation, we obtained extensively backcrossed breeding pairs of a PKR knockout strain deficient in the PKR kinase domain (Abraham et al., 1999; Lu et al., 2012) and femurs from another PKR knockout strain lacking in the PKR regulatory domain (Chakrabarti et al., 2008; Yang et al., 1995). We confirmed that their genetic backgrounds were largely C57BL/6J by SNP genotyping (Table. 4). Surprisingly, IFNγ-primed macrophages from WT C57BL/6J mice and from each of the knockout strains responded similarly to C85 with a reduction in release of IL-10 (Fig. 4A, B, C left panel), increase in RNI (Fig. 4A, B, C middle panel) and increase in TNFα (Fig. 4A, B, C right panel). These results demonstrated that C85's effects were PKR-independent.

Table 4. SNP genotyping of mice used in this study.
Results are representative of two biological replicates.

Type of strain	Background
PKR-regulatory domain KO mice	94.6% C57BL/6J
PKR- kinase domain KO mice	97.3% C57BL/6J
WT mice	99.8 % C57BL/6J
PKR-regulatory domain KO mice on mixed background	98.9% 129S1/SvImJ

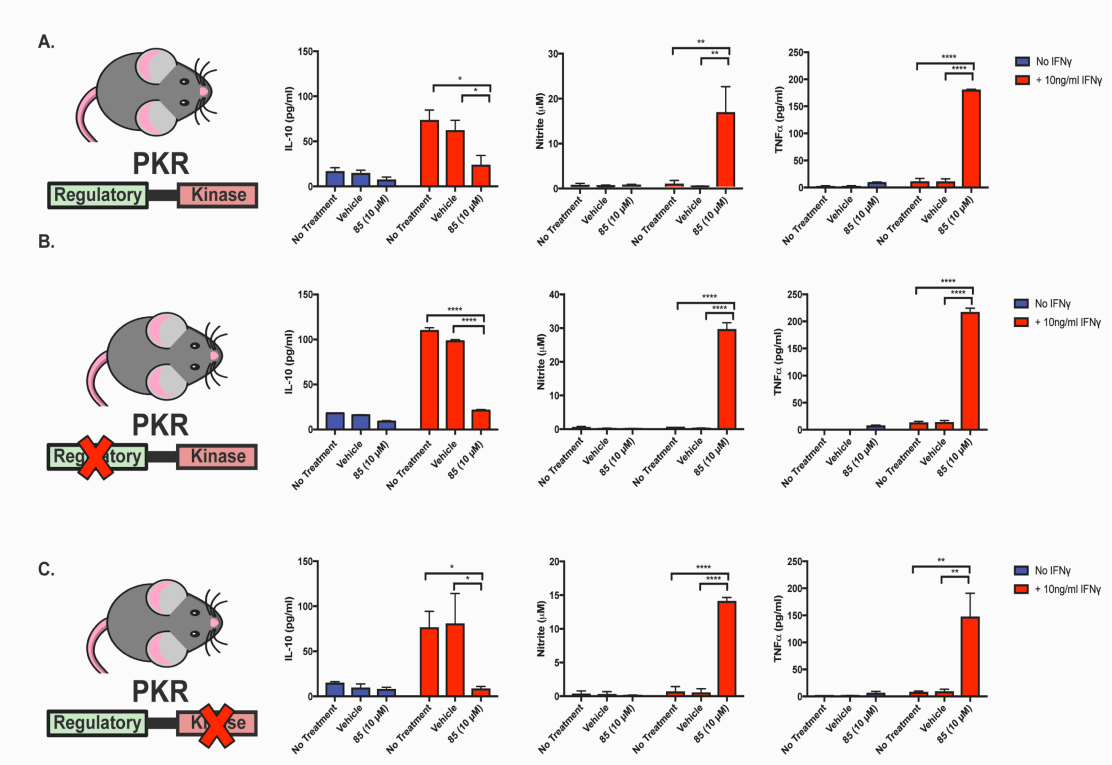

Figure 4. PKR deficiency or sufficiency on C57BL/6J background does not impact the effect of C85 on macrophage activation.

A) C85 reduces IL-10 and increases nitrite and TNFα in response to IFNγ in WT (B6) macrophages.

B) C85 reduces IL-10 and increases nitrite and TNFα in response to IFNγ in PKR-regulatory domain KO (B6) macrophages.

C) C85 reduces IL-10 and increases nitrite and TNFα in response to IFNγ in PKR-kinase domain KO (B6) macrophages.

Results in (A) - (C) are means ± SEM of two independent experiments each performed in triplicate. $p < 0.05$ = *; $p < 0.01$ = **; $p < 0.005$ = ***; $p < 0.001$ = ****

Macrophages from 129S1/SvImJ show enhanced macrophage activation in response to IFNγ.

The foregoing results conflicted with those reported earlier with another strain of PKR regulatory domain knockout mice (Wu et al., 2012). We suspected that those mice were not sufficiently

backcrossed. The investigation leading back to the original laboratory notebooks revealed that the mice had not been backcrossed in the producing lab (Yang et al., 1995). SNP genotyping revealed that our colony, derived from breeders from the original lab, was 98.9% 129S1/SvImJ. We then compared macrophages from these mice and from 129S1/SvImJ WT mice and observed that IFNγ induced little production of IL-10 in either case (Fig. 5A left panel). However, IFNγ alone induced production of RNI and TNFα in 129S1/SvImJ macrophages- whether WT or PKR-deficient— to levels as high as those produced by C57BL/6J macrophages exposed to IFNγ and C85 (Fig. B, middle panels).

Similar Mtb burden in WT and PKR-deficient mice with a shared C57BL/6 background.

Finally, we infected PKR kinase domain knockout and WT mice with Mtb by low-dose aerosol infection. In order to minimize any differences in genetic background or microbiome, we used as parental strains WT C57BL/6J mice and PKR kinase domain knockout mice that were 97.3% C57BL/6J (Table 3), mated them, interbred their F1 littermates, and genotyped the resulting F2 littermates to identify WT and homozygous PKR-deficient individuals. The latter two groups had indistinguishable pulmonary (Fig. 6A) burdens of Mtb at days 14, 29, 57 and 120 post low-dose aerosol infection and indistinguishable splenic (Fig. 6B) burdens of Mtb at days 29, 57 and 120 post low-dose aerosol infection.

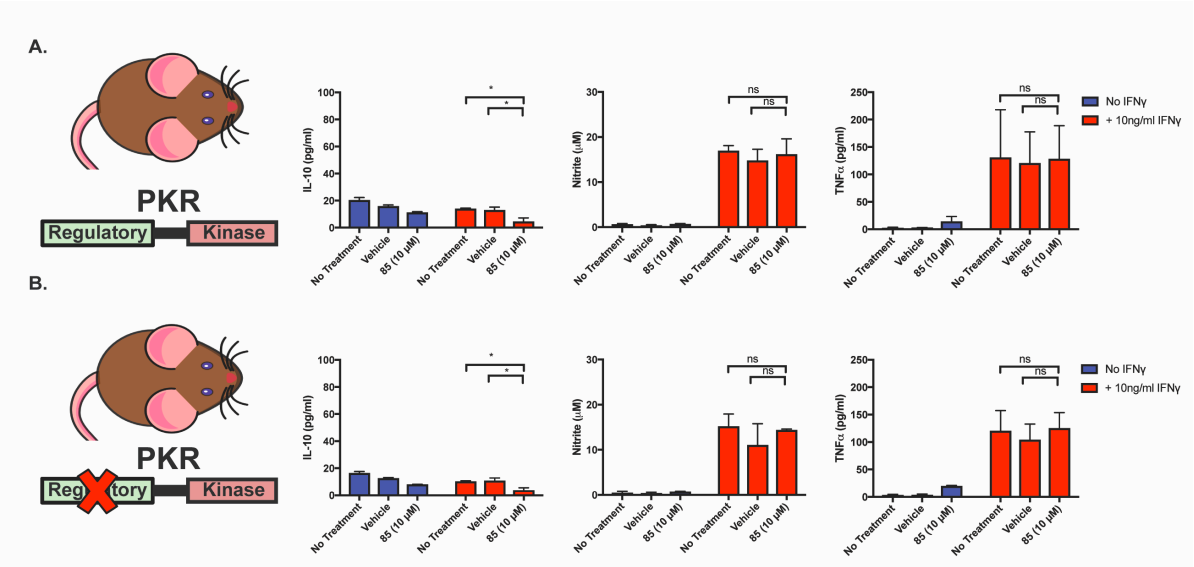

Figure 5. Macrophages from 129S1/SvImJ mice show enhanced macrophage activation in response to IFNγ.

A) IFNγ does not induce the production of IL-10 and induces the production of nitrite and TNFα in WT (129S1/SvImJ) macrophages.

B) IFNγ does not induce the production of IL-10 and induces the production of nitrite and TNFα in PKR regulatory domain (129S1/SvImJ) macrophages.

Results in (A) and (B) are means ± SEM of two independent experiments each performed in triplicate. $p < 0.05$ = *; ns = non-significant

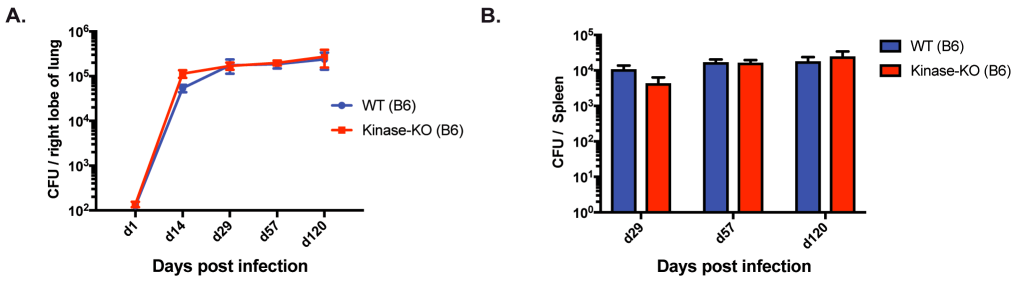

Figure 6. Similar Mtb burden in WT and PKR-deficient mice with a shared C57BL/6 background.

A) CFU (colony forming units) burden in lung; B) CFU burden in spleen. Numbers of mice (n) = 3 for day 1; n = 4 for day 14; n = 5 for days 29, 57 and 120. Data are means ± SEM

DISCUSSION

During our screen, we observed that some compounds were not active on isolated PKR but produced the desired phenotypes in BMMs (such as 2033, 2034 in Table 2), and some compounds active on isolated PKR did not produce desired phenotypes in BMMs (such as 2044, 2045 in Table 2). We hypothesized that our inhibitors could be acting upstream of PKR.

In addition, IC_{50} values were determined on human PKR, whereas we tested in mouse BMMs and a mouse model of Mtb infection. Between mouse and human PKR, there is 58% identity; the active site and ATP binding site are nearly identical. (Fig. 7)

Fig 7. The similarity in domains between mouse PKR (*Mus musculus*) and human PKR (*Homo sapiens*). Source: Uniprot. org

These inhibitors were screened against PKR before we identified that in the original study the phenotypes were due to strain dependency and not PKR.

This study rectifies a previous conclusion that was based on a misinterpretation of the strain backgrounds in knockout and control mice (Wu et al., 2012), and in so doing reinforces the importance of using mice with matched genetic backgrounds in studies based on gene disruption. The present work also illustrates that chemical

probes selected for their ability to inhibit a given kinase, even when found to be highly selective for that kinase, may nonetheless give phenotypes that are unrelated to inhibition of the kinase against which they were selected. The main conclusion of the present study is that PKR need not be considered as a target for HDT of TB.

Another observation from this work is that BMMs of the 129S1/SvImJ strain respond to IFNγ with greater production of RNI and TNFα than those of C57BL/6J origin. This observation extends earlier evidence that 129 strains and C57BL/6J strains produce different levels of IFNs and have different responses to other IFNs. For example, naïve 129Sv mice had higher levels of circulating plasmacytoid dendritic cells (DCs) than C57BL/6 mice (Asselin-Paturel et al., 2003). 129S7 mice produced higher levels of type I and type III IFNs and higher mortality when challenged with influenza virus than C57BL/6 mice (Davidson et al., 2014). Mice lacking the type I IFN receptor (IFNAR KO mice) on the C57BL/6 background fared comparably to WT C57BL/6 mice when infected with Mtb (Desvignes et al., 2012; Stanley et al., 2007), while IFNAR KO mice on the 129S2 background succumbed much more rapidly than the WT controls (Dorhoi et al., 2014). The WT strains themselves respond differently to Mtb as well: C57BL/6J mice are classified as highly resistant to Mtb and 129/SvJ mice as highly susceptible (Medina and North, 1998).

We do not know the mechanism for the strikingly different responses of 129S1/SvImJ BMMs and C57BL/6J BMMs to IFNγ. A comparison of the sequences of IFNγ receptor genes *Ifngr1* and *Ifngr2* in 17 inbred mouse strains (B et al., 2011; Keane et al., 2011) (Tables

5 and 6) mostly revealed intronic variants. These could conceivably affect alternative splicing, which in turn can impact expression level, or might impact downstream regulatory elements. We observed that in response to IFNγ alone, WT 129S1/SvImJ produced 8-fold more *Tnf* expression and 70-fold more *Nos2* expression and had reduced levels of *Il10* expression compared to WT C57BL/6J mice (Fig. 8). We performed RNA-seq on RNA extracted from BMMs of these mice in the absence and presence of IFNγ for 24 hrs.

RNA-seq analysis revealed that in the presence of IFNγ, *Ifngr1* expression was lower and *Ifngr2* expression was higher in 129S1/SvImJ compared to C57BL/6J BMMs (Figure 9), but we do not know if these differences lead to differential responsiveness to IFNγ.

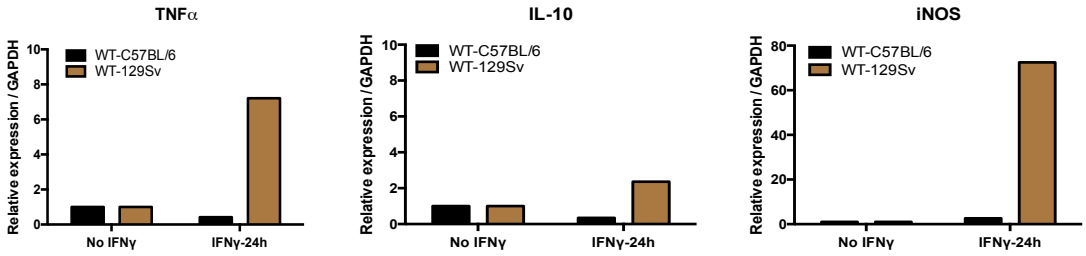

Figure 8. In response to IFNγ, WT129S1/SvImJ macrophages are more activated than WT C57BL/6J macrophages at a transcriptional level. Data representative of one experiment out of three.

Although the actions of C85 were not attributable to its inhibition of PKR, they remain of interest. Our current efforts are focused on identifying the functionally relevant targets inhibited by C85 and its congeners. We believe that we were on the right track for looking for compounds that increase nitrite and TNFα and decrease IL-

10 as those changes might lead to improved TB control by the host (Discussed in Chapter 1). It is important to be guided by BMM phenotypes for the goal of creating more stable compounds having better bioavailability *in vivo*. We have developed potentially promising agents for HDT that we tested in mouse model of Mtb infection (Chapter 3). We also developed PKR inhibitors which could find use in the context of other diseases such as insulin resistance, neurodegeneration and cancer (Mouton-Liger et al., 2015; Nakamura et al., 2014; Pataer et al., 2009).

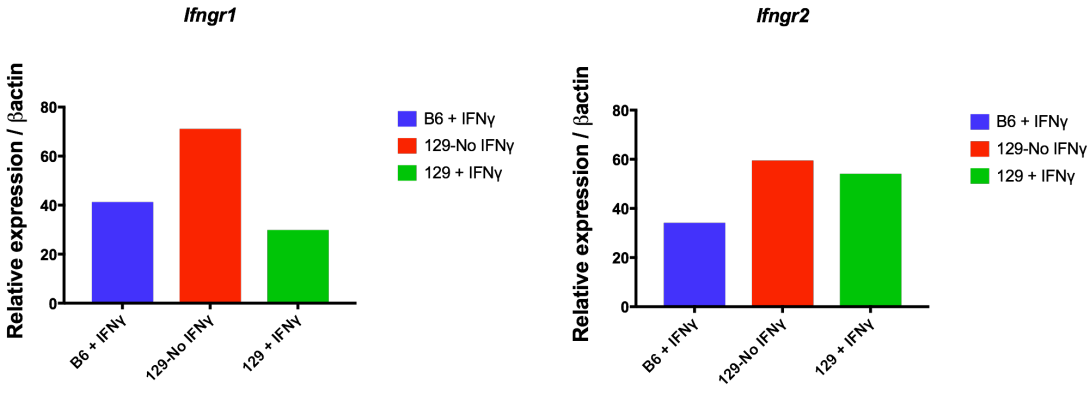

Figure. 9. *Ifngr1* and *Ifngr2* gene expression plotted from RNA-seq data (n=3) obtained from BMMs treated with or without IFNγ (10 ng/ml) for 24 hr.

METHODS

Mice

Two types of targeted mutations in PKR have been reported in mice, deletion of PKR RNA-binding domain (Yang et al., 1995) and deletion of PKR catalytic domain (Abraham et al., 1999). Femurs from PKR RNA-binding domain knockout mice were a gift from Dr. Robert Silverman (Lerner Research Institute, Cleveland, OH). Upon receipt, these mice were 94.6% C57BL/6J background, based on SNP typing by the Rockefeller University Genomics Resource Center. PKR catalytic domain knockout mice were a gift from Dr. Gokhan Hothamisligil (Harvard School of Public Health, Boston, MA). Upon receipt, these mice were 97.3% C57BL/6J background based on SNP genotyping. Experiments with BMM used femurs sent from the providing laboratories and control macrophages from C57BL/6J mice from The Jackson Laboratories, Bar Harbor, ME. For *in vivo* infection, we crossed the catalytic domain PKR knockout strain with C57BL/6J mice from The Jackson Laboratories to generate heterozygotes. The heterozygotes were interbred and the F2 littermates were genotyped. Knockout (KO) and WT mice from F2 generations were used further to expand the colony prior to use in the experiment.

For genotyping, tails of mice were digested in 500 μl Tail Lysis Buffer (50 mM Tris pH 8.0, 100 mM EDTA and 100 mM NaCl) and 10 μl of Proteinase K (20 mg/ml) overnight in a water bath at 56° C. Digested tails were spun at 13000 rpm for 10 mins to remove debris. DNA was then precipitated with equal volume of isopropanol after spinning at 13000 rpm for 5 mins. The pellets were air-dried and dissolved in TE

buffer (10 mM Tris-HCl, 1 mM EDTA, pH 8.0). Illustra PureTaq Ready-to-go beads were used for the reaction. PKR WT and KO mice were genotyped with PCR primers (KO - forward, 5′-GGAACTTTGGAGCAATGGA-3′, reverse, 5′-TGCCAATCACAAATCTAAAAC-3′; WT - forward, 5′-TGTTCTGTGGCTATCAGGG-3′, reverse, 5′-TGACGAGTTCTTCTGAGGG-3′) yielding a 240-base-pair (bp) WT DNA band and a 460-bp mutant DNA band after electrophoresis in 2% agarose gel in TAE buffer. The PCR reaction was run in a GeneAmp PCR System 9700 (Applied Biosystems) using initial denaturation at 94 °C for 3 mins, 38 cycles at 94 °C 30s, 50 °C 30s, 72 °C 30s, final extension at 72 °C for 10 mins.

Macrophages

C57BL/6J adult (> 6 weeks and < 4 months) female mice were used for the culture of BMMs. Bone marrow cells were flushed from femurs. Cells were differentiated for 6 days in Petri dishes in Dulbecco's minimal Eagle medium (DMEM) containing 1% HEPES, 0.29 g/L L-glutamine, 1 mM sodium pyruvate, 10% fetal bovine serum (FBS) and 20% L929 fibroblast-conditioned medium. Macrophages were collected on day 6 by incubation in 1 mM EDTA in PBS for 10 mins on ice, washed once with PBS and seeded into 48-well plates (Corning) overnight at density of 2.5×10^5 cells per well. Purified recombinant mouse IFNγ (Roche) was used at 10 ng/ml in all studies.

Mtb infection in mice

8 - 12-week-old WT and kinase domain KO female mice on C57BL/6J background were infected with about 100 CFU of Mtb H37Rv by using an Inhalation Exposure System (Glas-Col). Mid-log phase Mtb culture was grown in 7H9 broth (BD Biosciences) with BBL Middlebrook OADC Enrichment (Becton Dickinson) and 0.05% (vol/vol) Tween 80 (Sigma-Aldrich) and washed once in PBS + 0.05% Tween 80, centrifuged once at 120 *g* for 12 mins to prepare single cell suspension. The inoculum (5 ml, adjusted to an OD580 = 0.1-0.2 in PBS) was nebulized for 40 min. At indicated time points, mice were euthanatized and the lungs (all but not left lobe) and spleen were homogenized in 2 mls PBS (Bullet blender) and plated with and without serial dilution on 7H10-OADC agar containing 0.5 % glycerol. The plates were incubated at 37°C for 3 weeks for determination of colony-forming units (CFU).

Measurements of Cytokines and RNI

TNFα and IL-10 in culture supernatants were measured by ELISA (R&D Systems) according to manufacturer's protocols, with values in cell-free medium subtracted. Assays were performed in triplicate for each experiment. RNI were measured as nitrite by mixing 50 μL of supernatant with 50 μL of Griess reagent prepared by mixing equal volumes of Griess Reagent 1 (2% sulphanilamide in 5% H_3PO_4) and Griess Reagent 2 (0.2% naphthylethylenediamine dihydrochloride). Absorbance at 550 nm was measured with sodium nitrite as standard. Nitrite content of cell-free medium was subtracted.

PKR Assay

The assay was performed as reported (Bryk et al., 2011)

Statistical Analysis

PRISM 7.0 Graphpad software was applied for statistical analyses. Concentrations of cytokines and nitrite were statistically analyzed using two-way ANOVA comparing mean differences between groups treated ± IFNγ . p-values < 0.05 were considered statistically significant.

Contributions

All experiments on isolated human PKR were performed by R. Bryk. The project on PKR screening was started in collaboration withR. Bryk.
S. Mundhra cultured and plated all BMMs and performed all ELISAs and most of the nitrite assays.
R. Bryk and S. Mundhra jointly optimized assays. S. Mundhra identified that the discrepancy between mouse backgrounds and phenotypes were mouse background dependent.
X. Jiang and S. Mundhra jointly performed Mtb infection in mice and S. Mundhra analyzed and graphed the data.
C. Nathan helped with editing a part of this chapter that was written as a manuscript.

REFERENCES

Abraham, N., Stojdl, D.F., Duncan, P.I., Méthot, N., Ishii, T., Dubé, M., Vanderhyden, B.C., Atkins, H.L., Gray, D.A., McBurney, M.W., et al. (1999). Characterization of transgenic mice with targeted disruption of the catalytic domain of the double-stranded RNA-dependent protein kinase, PKR. J. Biol. Chem. *274*, 5953–5962.

Asselin-Paturel, C., Brizard, G., Pin, J.-J., Brière, F., and Trinchieri, G. (2003). Mouse strain differences in plasmacytoid dendritic cell frequency and function revealed by a novel monoclonal antibody. J. Immunol. Baltim. Md 1950 *171*, 6466–6477.

B, Y., K, W., A, A., M, G., Tm, K., X, G., C, N., L, G., J, N., A, B., et al. (2011). Sequence-based characterization of structural variation in the mouse genome. Nature *477*, 326–329.

Bogdan, C., Vodovotz, Y., and Nathan, C. (1991). Macrophage deactivation by interleukin 10. J. Exp. Med. *174*, 1549–1555.

Bryk, R., Wu, K., Raimundo, B.C., Boardman, P.E., Chao, P., Conn, G.L., Anderson, E., Cole, J.L., Duffy, N.P., Nathan, C., et al. (2011). Identification of new inhibitors of protein kinase R guided by statistical modeling. Bioorg. Med. Chem. Lett. *21*, 4108–4114.

Chakrabarti, A., Sadler, A.J., Kar, N., Young, H.A., Silverman, R.H., and Williams, B.R.G. (2008). Protein kinase R-dependent regulation of interleukin-10 in response to double-stranded RNA. J. Biol. Chem. *283*, 25132–25139.

Davidson, S., Crotta, S., McCabe, T.M., and Wack, A. (2014). Pathogenic potential of interferon αβ in acute influenza infection. Nat. Commun. *5*, 3864.

Der, S.D., Yang, Y.L., Weissmann, C., and Williams, B.R. (1997). A double-stranded RNA-activated protein kinase-dependent pathway mediating stress-induced apoptosis. Proc. Natl. Acad. Sci. U. S. A. *94*, 3279–3283.

Desvignes, L., Wolf, A.J., and Ernst, J.D. (2012). Dynamic roles of type I and type II interferons in early infection with Mycobacterium tuberculosis. J. Immunol. Baltim. Md 1950 *188*, 6205–6215.

Dey, M., Cao, C., Dar, A.C., Tamura, T., Ozato, K., Sicheri, F., and Dever, T.E. (2005). Mechanistic link between PKR dimerization,

autophosphorylation, and eIF2alpha substrate recognition. Cell *122*, 901–913.

Dorhoi, A., Yeremeev, V., Nouailles, G., Weiner, J., Jörg, S., Heinemann, E., Oberbeck-Müller, D., Knaul, J.K., Vogelzang, A., Reece, S.T., et al. (2014). Type I IFN signaling triggers immunopathology in tuberculosis-susceptible mice by modulating lung phagocyte dynamics. Eur. J. Immunol. *44*, 2380–2393.

de Haro, C., Méndez, R., and Santoyo, J. (1996). The eIF-2alpha kinases and the control of protein synthesis. FASEB J. Off. Publ. Fed. Am. Soc. Exp. Biol. *10*, 1378–1387.

Keane, T.M., Goodstadt, L., Danecek, P., White, M.A., Wong, K., Yalcin, B., Heger, A., Agam, A., Slater, G., Goodson, M., et al. (2011). Mouse genomic variation and its effect on phenotypes and gene regulation. Nature *477*, 289–294.

Lu, B., Nakamura, T., Inouye, K., Li, J., Tang, Y., Lundbäck, P., Valdes-Ferrer, S.I., Olofsson, P.S., Kalb, T., Roth, J., et al. (2012). Novel role of PKR in inflammasome activation and HMGB1 release. Nature *488*, 670–674.

Medina, E., and North, R.J. (1998). Resistance ranking of some common inbred mouse strains to Mycobacterium tuberculosis and relationship to major histocompatibility complex haplotype and Nramp1 genotype. Immunology *93*, 270–274.

Mouton-Liger, F., Rebillat, A.-S., Gourmaud, S., Paquet, C., Leguen, A., Dumurgier, J., Bernadelli, P., Taupin, V., Pradier, L., Rooney, T., et al. (2015). PKR downregulation prevents neurodegeneration and β-amyloid production in a thiamine-deficient model. Cell Death Dis. *6*, e1594.

Nakamura, T., Arduini, A., Baccaro, B., Furuhashi, M., and Hotamisligil, G.S. (2014). Small-molecule inhibitors of PKR improve glucose homeostasis in obese diabetic mice. Diabetes *63*, 526–534.

Pataer, A., Swisher, S.G., Roth, J.A., Logothetis, C.J., and Corn, P. (2009). Inhibition of RNA-dependent protein kinase (PKR) leads to cancer cell death and increases chemosensitivity. Cancer Biol. Ther. *8*, 245–252.

Proud, C.G. (1995). PKR: a new name and new roles. Trends Biochem. Sci. *20*, 241–246.

Robertson, H.D., and Mathews, M.B. (1996). The regulation of the protein kinase PKR by RNA. Biochimie *78*, 909–914.

Schulz, O., Pichlmair, A., Rehwinkel, J., Rogers, N.C., Scheuner, D., Kato, H., Takeuchi, O., Akira, S., Kaufman, R.J., and Reis e Sousa, C. (2010). Protein Kinase R Contributes to Immunity against Specific Viruses by Regulating Interferon mRNA Integrity. Cell Host Microbe *7*, 354–361.

Stanley, S.A., Johndrow, J.E., Manzanillo, P., and Cox, J.S. (2007). The Type I IFN Response to Infection with Mycobacterium tuberculosis Requires ESX-1-Mediated Secretion and Contributes to Pathogenesis. J. Immunol. *178*, 3143–3152.

Wallis, R.S., and Hafner, R. (2015). Advancing host-directed therapy for tuberculosis. Nat. Rev. Immunol. *15*, 255–263.

Williams, B.R. (1999). PKR; a sentinel kinase for cellular stress. Oncogene *18*, 6112–6120.

Williams, B.R. (2001). Signal integration via PKR. Sci. STKE Signal Transduct. Knowl. Environ. *2001*, re2.

Wu, K., Koo, J., Jiang, X., Chen, R., Cohen, S.N., and Nathan, C. (2012). Improved control of tuberculosis and activation of macrophages in mice lacking protein kinase R. PloS One *7*, e30512.

Yang, Y.L., Reis, L.F., Pavlovic, J., Aguzzi, A., Schäfer, R., Kumar, A., Williams, B.R., Aguet, M., and Weissmann, C. (1995). Deficient signaling in mice devoid of double-stranded RNA-dependent protein kinase. EMBO J. *14*, 6095–6106.

Zamanian-Daryoush, M., Mogensen, T.H., DiDonato, J.A., and Williams, B.R. (2000). NF-kappaB activation by double-stranded-RNA-activated protein kinase (PKR) is mediated through NF-kappaB-inducing kinase and IkappaB kinase. Mol. Cell. Biol. *20*, 1278–1290.

Zumla, A., Rao, M., Wallis, R.S., Kaufmann, S.H.E., Rustomjee, R., Mwaba, P., Vilaplana, C., Yeboah-Manu, D., Chakaya, J., Ippolito, G., et al. (2016). Host-directed therapies for infectious diseases: current status, recent progress, and future prospects. Lancet Infect. Dis. *16*, e47-63.

CHAPTER 3

Characterization of mechanisms of small molecules in host-directed therapy of TB

CHAPTER 3

INTRODUCTION

Host-directed, immunomodulatory treatment of tuberculosis (TB) has shown promise in several studies that used different approaches such as cytokine supplementation (Condos et al., 1997), vitamin supplementation (Wallis and Zumla, 2016), DNA vaccination (Lowrie et al., 1999), heat-killed *Mycobacterium vaccae* (Johnson et al., 2000), therapeutic multi-stage vaccination to control reactivation (Aagaard et al., 2011) and targeted siRNA treatment (Rosas-Taraco et al., 2009) among others. Some of these approaches have been demonstrated to be effective against drug-resistant Mtb strains in murine models of TB (Bertholet et al., 2010; Okada et al., 2009) and in TB patients (Condos et al., 1997). In the recent years, host-directed small molecules have shown potential in reducing bacterial burden in various models of mycobacterial infection. Such inhibitors were directed against phosphodiesterase (PE) type four (Koo et al., 2011), ABL tyrosine kinase family (Napier et al., 2011, 2015), PE types three and five (Maiga et al., 2012), HMG-CoA reductase *i.e.* statins (Parihar et al., 2014), AMPK activators *i.e.* metformin (Singhal et al., 2014), and drugs augmenting prostaglandin E2 levels (Mayer-Barber et al., 2014),

In this chapter, we investigate the potential of small molecules C2062 and C85, identified in the screen described in Chapter 2, as agents for host-directed therapy (HDT) of TB and as tools to identify the pathways involved in enhanced activation of macrophages.

RESULTS

Characterization of actions of small molecules in uninfected macrophages

As described in Chapter 2, we screened over 150 inhibitors from the CGH library on bone marrow-derived macrophages (BMMs) in the presence of IFNγ for increases in production of RNI and TNFα and decrease in production of IL-10 compared to IFNγ alone (Fig. 1 chapter 2). Concentration-response curves for the two small molecules C85 and C2062 are shown in Figure 1. C85 produced nitrite and TNFα at 10 μM and 30 μM and reduced IL-10 as well at higher concentrations (Figure 1A; left, middle and right panels respectively). C2062 produced nitrite and TNFα 5 μM and 10 μM and lowered IL-10 at those concentrations (Figure 1B; left, middle and right panels respectively). It was toxic at 30 μM. To investigate further, we sought to determine whether these small molecules could enhance these mediators at a transcriptional level. To this end, we primed BMMs with IFNγ for 24 hr and treated with compounds for 6 hr at different concentrations prior to RNA isolation.C85 increased expression of *Nos2* by 170-fold compared to IFNγ alone. The highest expression of *Tnf* and lowest expression of *Il10* was observed at the highest concentration of 10 μM of C85 (Fig. 1C). C2062 also enhanced *Nos2* expression by 750-fold and *Tnf* expression by 6-fold compared to vehicle. In addition, C2062 abrogated *Il10* expression completely compared to vehicle (Fig. 1D). However, in both experiments, we observed that vehicle (DMSO) alone was reduced *Il10* gene expression. This could be attributed to DMSO having an effect on *Il10* transcription. However, compared to vehicle,

we did see a decrease in *Il10* gene expression at 10 μM for both compounds suggesting that this effect was compound-dependent and not just due to DMSO. It is to be noted that a rise in transcripts need not result from increased transcription. It could be due to reduced mRNA decay. A rise in protein levels could be due to increased transcription, decreased proteasomal degradation or increased cytokine secretion. Those studies were not performed in this dissertation work.

We wanted to further investigate whether these small molecules increased the production of other pro-inflammatory cytokines. We observed that C2062 and C85 increased production of IL-12p40 at 10 μM while the inactive control, C2753 did not. IL-12p40 has been implicated to be critical in control of Mtb (Méndez-Samperio, 2010). The continuous presence of IL-12 is required to maintain pulmonary Th1 immune response in chronic tuberculosis infection. In addition, it has been shown that in patients with Mendelian susceptibility to mycobacterial disease, the disease is caused as a result of IL-12B1 and IL-12p40 deficiency among several other factors (Filipe-Santos et al., 2006). Taken together, our data show that these small molecules can increase production of mediators important for TB control.

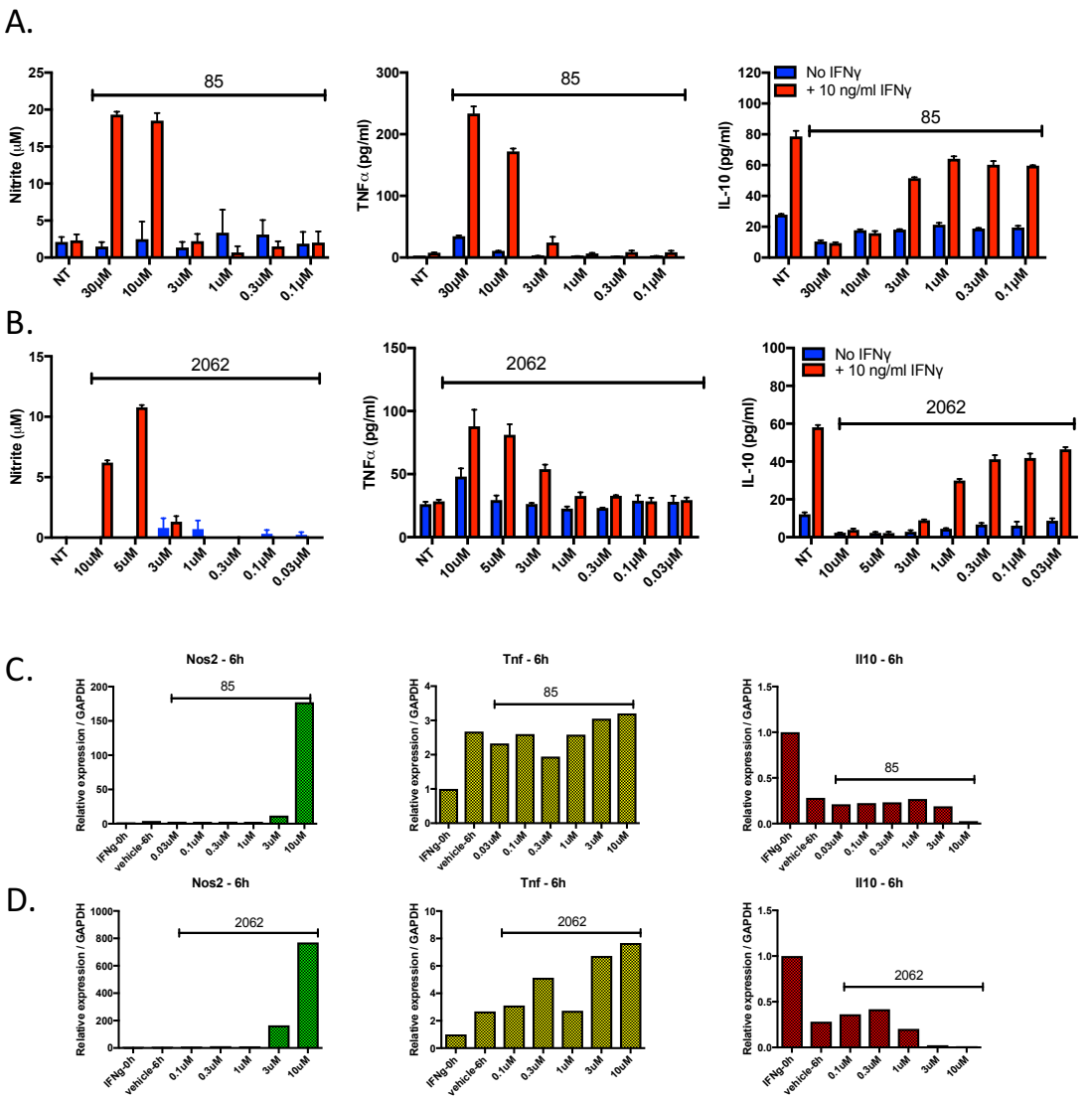

Fig. 1 C85 and C2062 enhance macrophage activation at the mRNA and protein product level. Concentration-response curve of C85 (A and C) and C2062 (B and D) and its impact on IL-10 reduction, nitrite and TNFα production at a protein level and transcriptional level. WT BMMs were primed with IFNγ (10 ng/ml) for 24 hr then treated with compounds for 48 hr. Results are means ± SD of triplicates in one experiment representative of two.

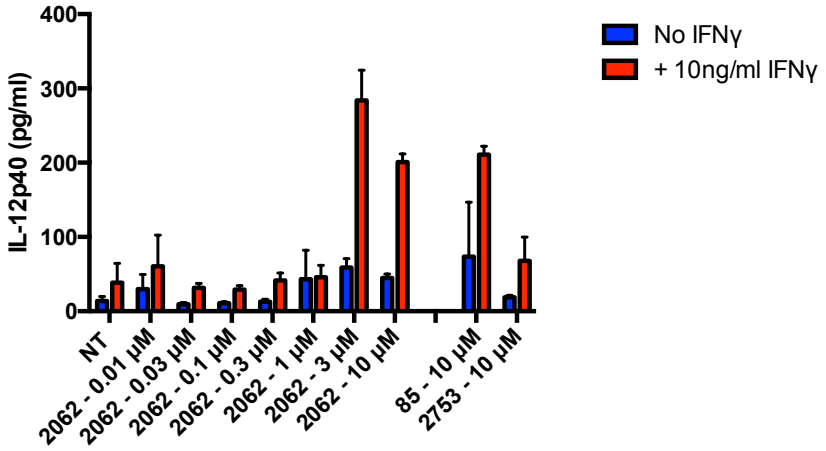

Fig. 2 C85 and C2062 increase production of IL-12 p40 in the presence of IFNγ. Results are means ± SEM of triplicates in one experiment representative of two independent experiments.

Experiments described above were conducted with IFNγ as the sole stimulus. We wanted to investigate whether small molecules can reduce IL-10 produced by other stimuli. We tested two stimuli - lipopolysaccharide (LPS) and heat-killed Mtb (HKMT). Both are known to be potent inducers of IL-10 (Barsig et al., 1995; Saraiva and O'Garra, 2010). We observed that after 24 hr stimulation with 10 ng/ml of LPS, macrophages produced massive amounts of IL-10, and the addition of 2062 5 µM reduced these levels (Fig. 3A). C2062 also reduced IL-10 produced by HKMT stimulation (Fig. 3B). IL-10 levels in the presence of IFNγ remained low (Fig. 3A and 3B), as IFNγ is known to antagonize the production of IL-10 (Hu et al., 2006; Saraiva and O'Garra, 2010). Therefore, C2062 was able to decrease IL-10 production in the presence of a TLR4 agonist (LPS) and a TLR2 agonist (HKMT), suggesting it was targeting a generic IL-10 induction pathway.

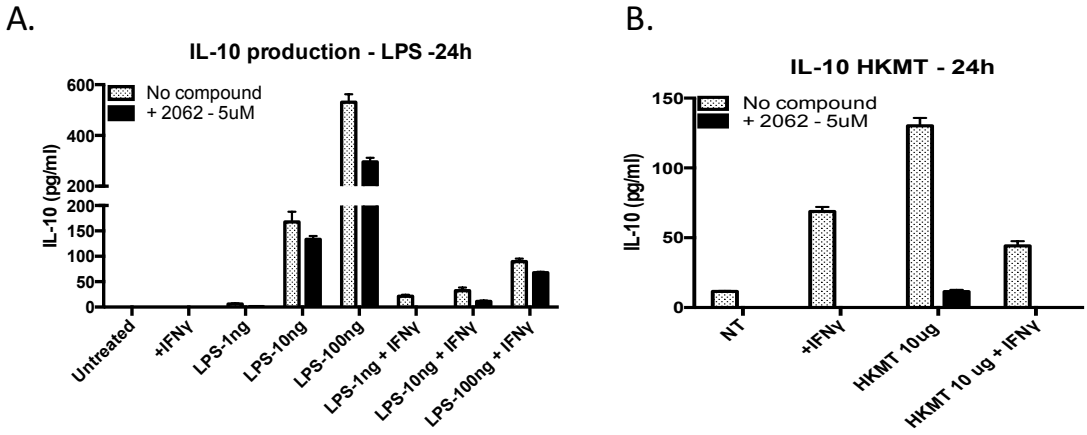

Figure 3. C2062 reduces IL-10 in response LPS and HKMT.
(A) BMMs treated with 1, 10 and 100 ng/ml of LPS for 24 hr +/- 5 μM C2062 added for 24 hr. IL-10 levels measured in the supernatants.
(B) IL-10 produced by BMMs when stimulated with HKMT for 24 hr +/- C2062.

IL-10 is known to antagonize TNFα production (Bogdan et al., 1991) in macrophages. Moreover, inhibition of IL-10 production has been shown to correlate with increased TNFα expression in human monocytes (Donnelly et al., 1995). We sought to investigate whether TNFα production was increasing in response to decreased IL-10 levels. We tested 3 compounds - C85, C2062 and an inactive control 2753 in a concentration - dependent manner in $IL10^{-/-}$ BMMs derived from IL-10 KO mice compared to WT mice (both on C57BL/6J background) (Fig. 4A). We observed that the WT and $IL10^{-/-}$ macrophages produced TNFα and nitrite to similar levels at 48 hours (Fig. 3B), suggesting that these effects were independent of IL-10 reduction. However, this experiment was performed only at one time-point – 48hr and it possible that these effects could be different at early or later time-

points. Hence, these results suggested that nitrite and TNFα elevation and IL-10 reduction are separate pathways.

Additional steps towards understanding the mechanism of C2062 and C85 in uninfected macrophages.

To further understand what pathways could be involved in these phenotypes, we performed RNA sequencing on RNA extracted from macrophages treated with these small molecules. We sent RNA isolated from macrophages treated at 3 time-points – 1 hr, 2 hr and 3 hr with C85 and C2062 at 10 μM which increased *Tnf* and *Nos2* (Fig. 5A and Fig. 5B) gene expression and reduced *I10* (Fig. 5C) expression. C2753 was used as an inactive control.

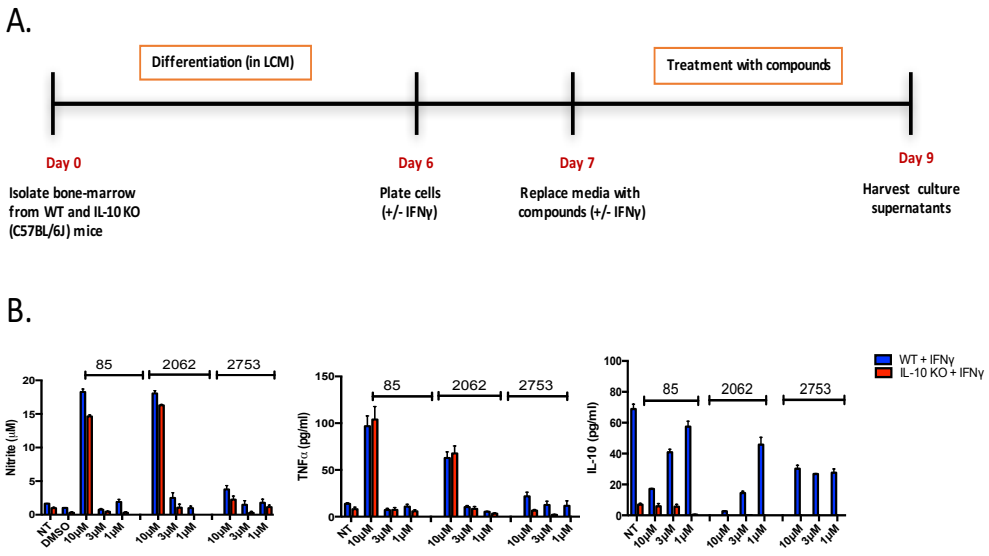

Figure 4. The increase in nitrite and TNFα is IL-10 independent.

A) Schematic representation of the experimental outline

B) Concentration-response curve of C85, C2062, and C2753 and its impact on nitrite and TNFα production by WT BMMs primed with IFNγ (10 ng/ml) for 24 hr then treated with compounds for 48 hr. Results are means ± SD of triplicates in one experiment representative of two

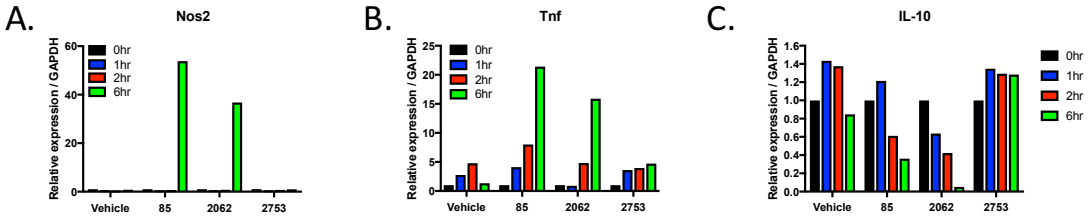

Fig. 5 Gene expression profile of samples treated with C85, C2062, and C2753 at 1, 2 and 6 hr and sent for RNA-sequencing.

A) Expression of *Nos2* gene
B) Expression of *Tnf* gene
C) Expression of *Il10* gene

Results are representative of four independent experiments.

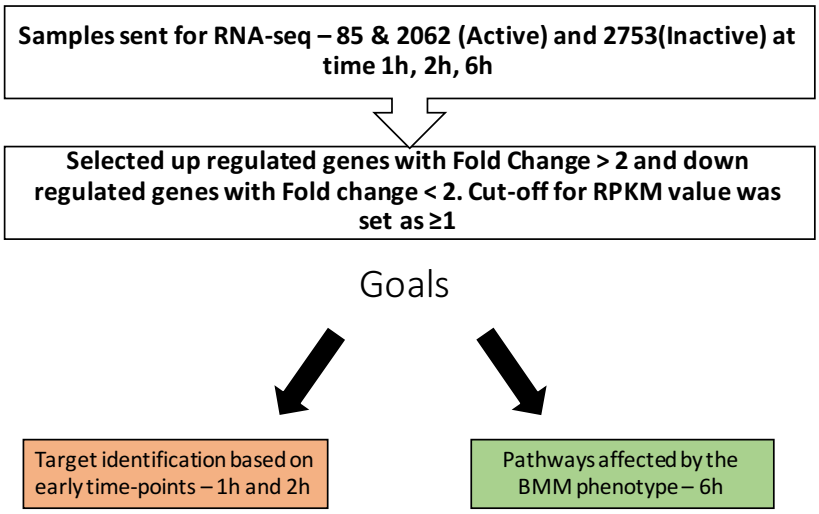

Figure 6. The methodology used for RNA-seq analysis An outline of RNA-seq analysis is shown as a schematic.

We hypothesized that at early time-points (1 hr and 2 hr), genes that overlap with increased expression between the C85 and C2062 but are not present in C2753 might be key candidates in the pathway being targeted. The premise is that, if the small molecules were inhibiting certain enzymes such as kinases, the cell would try to

compensate by upregulating them. We also hypothesized that at 6 hr time point, there would be an amplification of the effects caused by the small molecule treatment, such as secondary effects of changes in gene expression caused by the primary effects. Hence, the 6 hr time-point would be ideal to observe the changes in pathways being dysregulated. Supplementary Figure 1 and 2 give a list of the common genes upregulated and downregulated respectively between C85 and C2062. Supplementary Figure 3 shows the key pathways that were upregulated at 6 hr. We observed that many pro-inflammatory pathways common between C85 and C2062 were upregulated. As expected, C2753 did not have an effect on any of those pathways.

A.

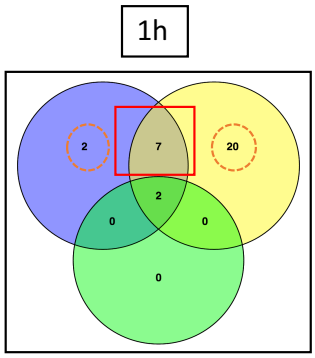

B.

Common genes upregulated at 1h in 2062 and 85
rhov
ppp1r15a
ddit3
osgin1
chac1
sik1
bhlhe40

C.

ID	Entrez Gene Name	Type(s)	85-1h	85-2h	2062-1h	2062-2h	2753-1h	2753-2h
Sik1	salt inducible kinase 1	kinase	2.26	4.98	5.94	8.87	1.49	1.90

Fig. 7 Salt-inducible kinase 1 is the only kinase upregulated by C85 and C2062 treatment at 1 hr.

(A) Venn diagram showing number of common genes upregulated by C85 and C2062 (highlighted in a red box)
(B) List showing names of genes upregulated (from A)
(C) Fold change values of Sik1 at indicated time-points compared to their respective vehicle control.

For the purpose of this chapter, we will highlight the genes that we picked for further study. As we had shown earlier that 85 (Chapter 2, Fig. 1A) and 2062 (data not shown), both inhibited PKR in an ATP-competitive manner, hence we thought the target of these small molecules could be a kinase. The only kinase which was upregulated in macrophages treated with C85 and C2062 at 1 hr, but not so in C2753, was salt-inducible kinase 1 (Sik1). Our data is also shown in a Venn diagram (Fig. 7A) along with the list of genes common between C85 and C2062 (Fig. 7B). Treatment with C85 and C2062, but not the inactive control compound C2753, upregulated expression of Sik1 when compared to vehicle, up to five-fold by 1 hr and nine-fold by 2 hr. These results indicated that Sik1 could be a potential target.

Table 1. NUAK1 and ARK5 (AMPK related kinase were inhibited by C85 and C2062 but not by C2753. All compounds were tested at 3 μM for kinase selectivity in assays performed by Life Technologies' SelectScreen® Profiling Service. The values are mean % activity remaining. Kinases are highlighted in red that were inhibited to the point that <20% activity remained.

Kinases hit	2062	85	2753
ABL1	18	80	
ABL1 G250E	12	70	
ABL1 Y253F	16	61	
ABL2 (mouse)	17	71	
ABL2 (mouse)	17	71	
BRAF V599E	12	87	
CSF1R (FMS)	10	20	23
EPHA1	13	91	
FLT3	9	49	
FLT3 D835Y	4	42	
FLT4 (VEGFR3)	11	78	
IKBKE (IKK epsilon)	9	46	
JAK2	10	58	
JAK2 JH1 JH2 V617F	13	68	
JAK3	11	69	
KDR (VEGFR2)	16	77	
LRRK2	5	28	17
LRRK2 G2019S	4	44	
MAP4K2 (GCK)	15	7	
MAP4K4 (HGK)	1	0	13
MINK1	12	6	20
MYLK2 (skMLCK)	2	63	
NEK1	10	44	
NUAK1 (ARK5)	6	18	32
PDGFRA D842V	15	85	
PDGFRA V561D	10	66	
PRKCN (PKD3)	6	118	
PRKD1 (PKC mu)	2	90	
PRKD2 (PKD2)	6	99	
TBK1	5	33	
TYK2	3	79	
SNF1LK2	7	72	

Among the other genes in Figure 7B- *rhov* encodes Rho family GTPases and is not expressed in humans; *ppp1r15a* encodes protein phosphatase 1 regulatory subunit 15A that recruits the phosphatase PP1 that dephosphorylates eIF2α; *ddit3* encodes DNA damage inducible transcript 3 which is a multifunctional transcription factor in ER stress response; *osgin1* encodes oxidative stress induced growth inhibitor 1 which is known to regulate cell growth and tumor formation; *chac1* encodes glutathione specific gamma glutamylcyclotransferase 1 which promotes neurogenesis in embryos and *bhlhe40* encodes a basic helix-loop-helix protein expressed in various tissues. As inhibiting any of these did not seem useful in the context of TB infection, and from our studies described in Chapter 2, we hypothesized that one of the targets could potentially be a kinase. Therefore, we decided to look into the literature to better understand the relationship between SIK1 and NUAK1. NUAK1 is a serine/threonine-protein kinase involved in various processes such a cell adhesion, cell proliferation, regulation of cell ploidy and senescence and tumor progression (Sun et al., 2013). We found that both were members of the same family – AMPK or 5' Adenosine Mono Phosphate-activated kinase family (Fig. 8). This family of kinases can be regulated by an upstream kinase known as liver kinase B1 (LKB1), which is also a tumor suppressor (Hardie and Alessi, 2013).

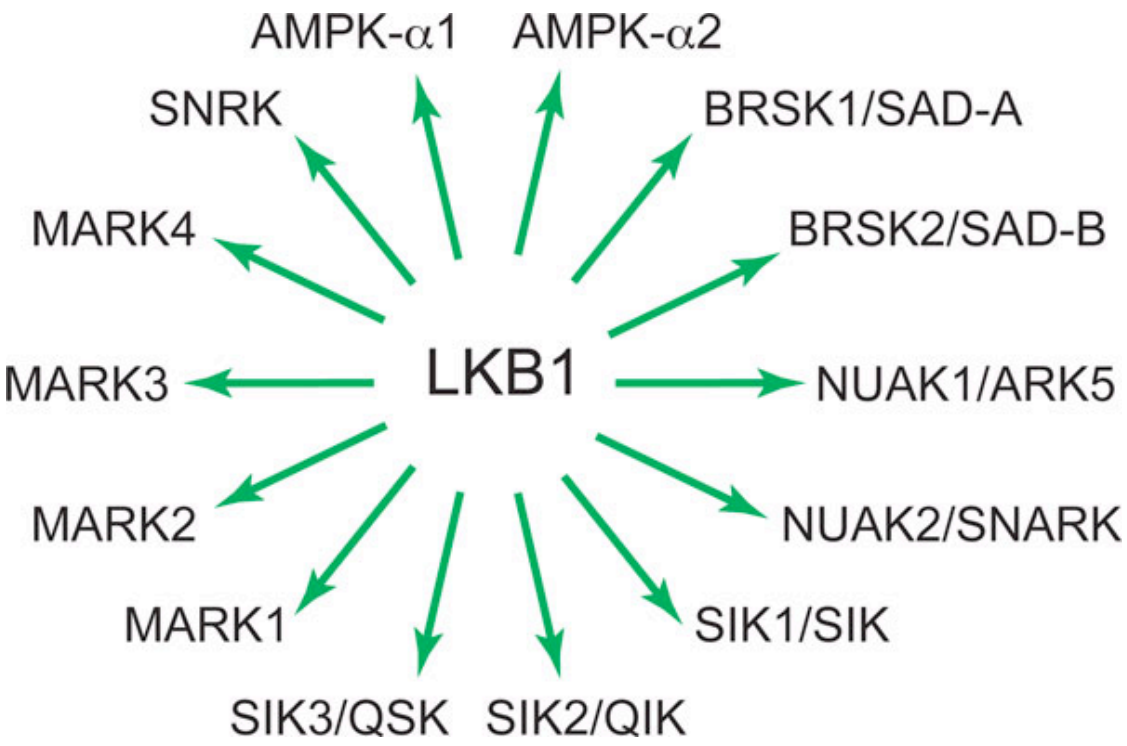

Fig. 8 Members of AMPK and AMPK related kinase family (ARK) Adapted from (Hardie and Alessi, 2013)

We sent our small molecules, C2062, and C2753, to be profiled against all kinases in the AMPK family at DiscoveRx Kinome Profiling Service. Surprisingly, we observed that C2062 inhibited both NUAK 1/2 and the master regulator – LKB1 (Fig. 9). This inhibition of the AMPK pathway suggested that if C2062 was inhibiting the master regulator LKB1, the downstream kinases would most likely also be inhibited.

Further literature research showed that BMMs from mice that had a myeloid-specific deletion of LKB1 produced more pro-inflammatory enzymes and cytokines in response to LPS, compared to their littermate WT controls. This was due to LKB1 inhibition of LPS-induced NF- κB activation in macrophages (Liu et al., 2015).

Additionally, AMPKα1 has been shown to be crucial for phagocytosis-induced macrophage skewing from a pro- to anti-inflammatory phenotype at the time of resolution of inflammation (Mounier et al., 2013). AMPK $\alpha^{-/-}$ macrophages were shown to be incapable of switching to an M2 (anti-inflammatory) phenotype from an M1 (pro-inflammatory phenotype).

These results indicated that C2062-mediated induction of nitrite and TNFα could be due to LKB1 inhibition. We investigated this further in the context of Mtb-infected macrophages (described in the subsequent section).

C85 and C2062, both produced large vacuoles in the presence of IFNγ (Fig. 10B and Fig. 10C) compared to untreated BMMs (Fig. 10A). Literature search and experiments conducted by Ruslana Bryk suggest that these inhibitors could be targeting PI3 kinases, specifically PIKfyve (a FYVE finger containing inositide kinase). PIKfyve inhibition is known to result in vacuolar phenotype in macrophages (Kim et al., 2014). We sought to investigate if inhibition of PIKfyve would also give the phenotypes of nitrite and TNFα elevation and IL-10 reduction. We tested two different inhibitors of PIKfyve that are currently available: YM201636 (IC50 = 33 nM), a widely used PIKfyve antagonist (Jefferies et al., 2008; Sbrissa et al., 2012) and MF4 (IC50 = 23 nM), a compound chemically related to YM201636, differing in an amino group on the pyrimidine ring (Kim et al., 2014). We also used an

Target	2062	2753
Gene Symbol	%Ctrl @ 3000nM	%Ctrl @ 3000nM
AMPK-alpha1	97	91
AMPK-alpha2	92	100
ARK5	8.9	89
BRSK1	100	90
BRSK2	100	94
LKB1	8.2	99
MARK1	97	92
MARK2	49	68
MARK3	100	100
MARK4	95	87
MELK	100	99
QSK	79	100
SIK	65	71
SIK2	37	68
SNARK	3.6	75
SNRK	84	92
TSSK1B	100	97

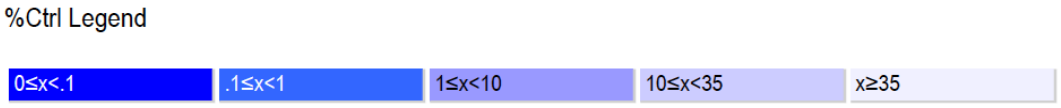

Fig. 9 Profiling of C2062 and C2753 against all kinases belonging to the AMPK family. Both compounds were tested at 3 μM for kinase selectivity in assays performed by DiscoveRx KINOMEscan Profiling Service. The values are mean % activity remaining, calculated by subtracting mean % inhibition from 100 %. Kinases that were inhibited to the point that <20% activity remained highlighted in a red box. *R. Bryk conceived the idea and sent out samples for profiling service.*

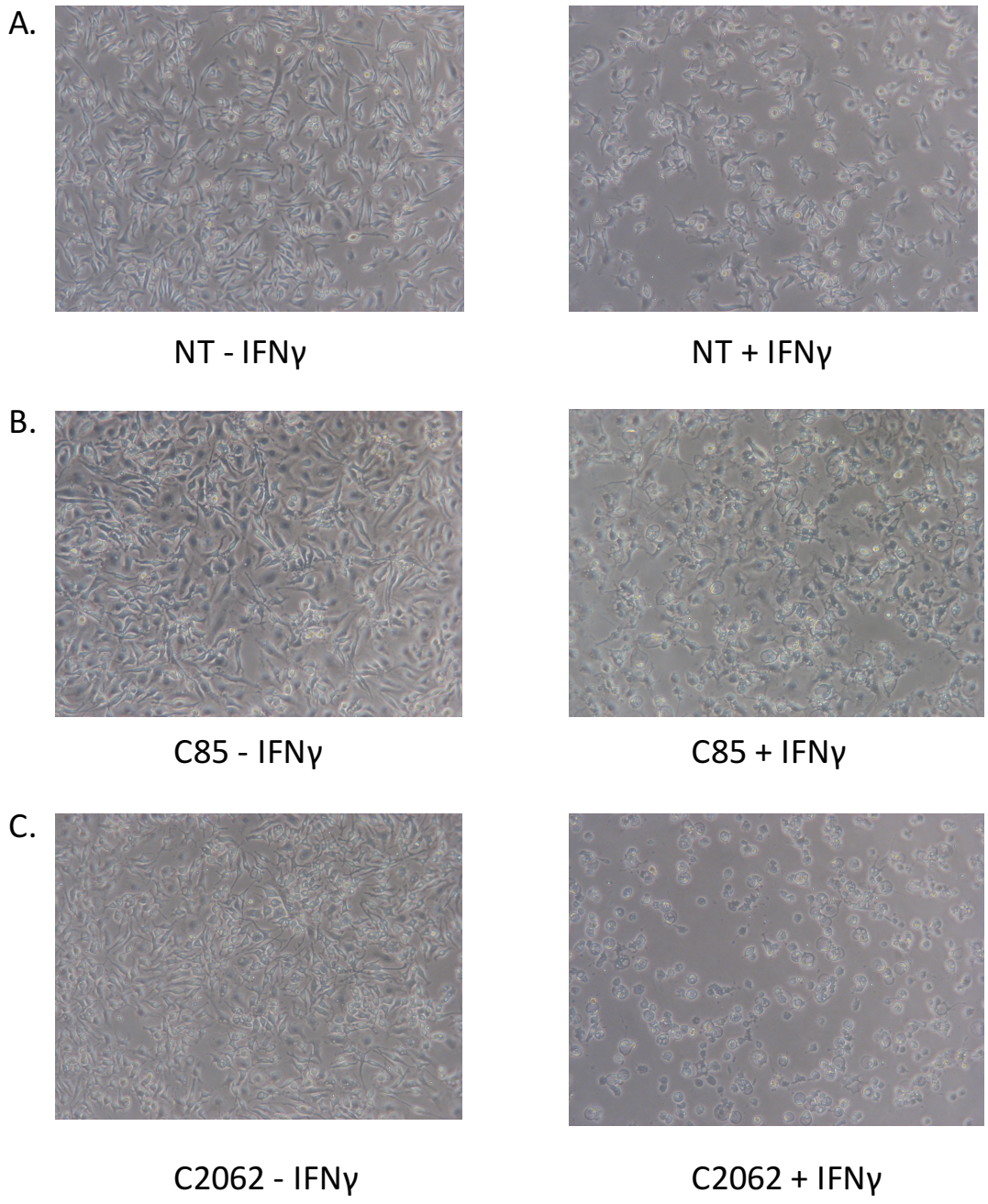

Fig. 10 C85 and C2062 produce vacuoles 24 hr post treatment.

(A) BMMs in absence or presence of IFNγ (left and right panels respectively). No compound treatment is abbreviated as NT.

(B) BMMs treated with C85 (10 μM) in absence or presence of IFNγ (left and right panels respectively)

(C) BMMs treated with C2062 (5 μM) in absence or presence of IFNγ (left and right panels respectively). All images have been taken at a magnification of 20X.

inactive congener of MF4 called MF2 as an inactive control. We observed that both MF4 (Fig. 11A) and YM201636 (Fig. 11B) increased nitrite and TNFα and reduced IL-10 in the presence of IFNγ at 3 μM and 10 μM. MF2, the inactive control did not do so. These effects were enhanced when combined with 1 μM C2062 treatment (Reported by R. Bryk, data not shown).

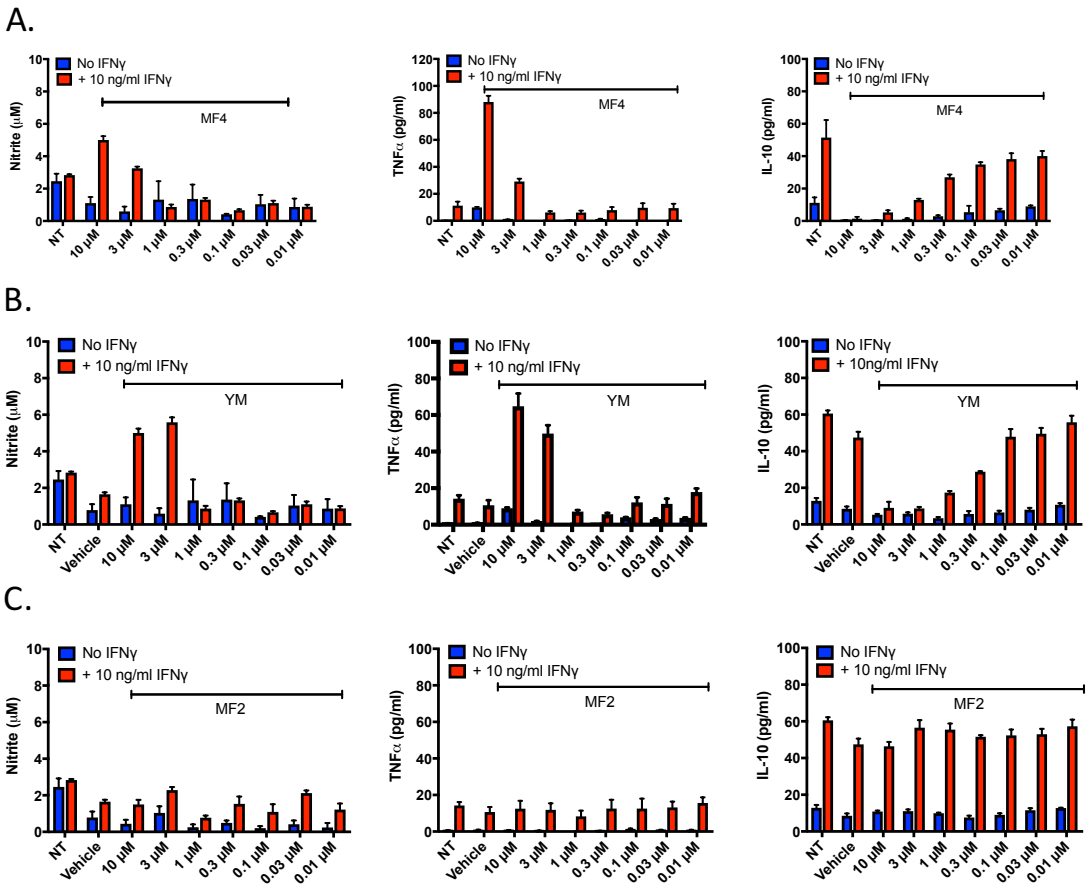

Fig. 11 MF4 and YM201636 enhance macrophage activation. Concentration-response curve of MF4 (A) and YM201636 (B) and the inactive congener of MF4 – MF2 (C) and its impact on nitrite and TNFα production and IL-10 reduction. WT BMMs were primed with IFNγ (10 ng/ml) for 24 hr then treated with compounds for 48 hr. Results are means ± SEM of triplicates in one experiment.

These results prompted us to test C2062 in a DiscoveRx kinase binding assay against PIKfyve along with a congener (considered to be a control because it did not produce the three phenotypes when tested at 10 μM). Their dissociation constants' (Kd) were reported to be 260 nM and 1400 nM, respectively.

Since our phenotypes are only observed at concentrations far above the Kd's for PIKfyve, we suspect that the desired phenotypes result from a combination of PIKfyve inhibition and less potent inhibition of some other target(s) common to the inhibitors, MF4 and YM201636, even though the core chemophore of C2062 is different from that of MF4 and YM201636. We believe that PIKfyve inhibition is necessary but not sufficient to attain BMM phenotypes. We tested C2062 at 1 μM, a concentration at which no vacuoles or other phenotypes are observed, in combination with MF4 (1 μM), a PIKfyve inhibitor producing vacuoles but no other phenotypes at 1 μM. We observed BMM phenotypes with 2062/MF4 co-treatment. This suggests that when C2062 is used alone, it inhibits other targets at lower concentrations. However, it takes higher concentrations for C2062 to inhibit PIKfyve and trigger manifestation of the phenotypes. Taken together, these results suggest that there are targets and/or signaling pathways inhibited in common by MF4, YM203616, and C2062, but a different concentration is required by the above mentioned small molecules to selectively inhibit PIKfyve vs the other target(s).

Having characterized these small molecules in uninfected macrophages, we next sought to study the effects of C2062 in Mtb-

infected macrophages and to further study if the enhanced activation of macrophages with C2062 would lead to reduced Mtb burden if used in combination with known antibiotics.

Characterization of actions of small molecules in Mtb-infected macrophages

We next wanted to study the effect of our small molecules in the context of Mtb infection. First, we infected BMMs primed with IFNγ (10 ng/ml) for 24 hr and then infected them with Mtb strain H37Rv for 4 hr. We treated the infected macrophages with the small molecules and monitored for the bacterial burden on days 3 and 5 post-treatment (Fig. 13). We tested C2062 alone and in combination with two antibiotics – rifampicin (Rif) and isoniazid (INH). We also tested MRT67307 (MRT), which is an inhibitor of LKB1, and therefore inhibits the AMPK pathway. As mentioned previously, we had observed that MRT-mediated inhibition of LKB1 leads to a pro-inflammatory phenotype. We wanted to test this in the context of Mtb infection. We also tested metformin, which is known to activate the AMPK pathway.

We observed that MRT alone slightly reduced Mtb burden, and MRT + rif seemed to hasten the reduction in bacterial burden compared to rif alone. Metformin did not reduce CFU burden alone, nor did it improve the reduction as seen with rif (Fig.13 A and B). This is contrary to what has been reported (Singhal et al., 2014). MRT seemed to enhance the control of Mtb in presence of IFNγ (Fig. 13B). C2062 seemed to reduce bacterial burden slightly more when treated in combination

with rif (13. C and D) and isoniazid (13 E and F) suggesting that it would be an ideal candidate for HDT.

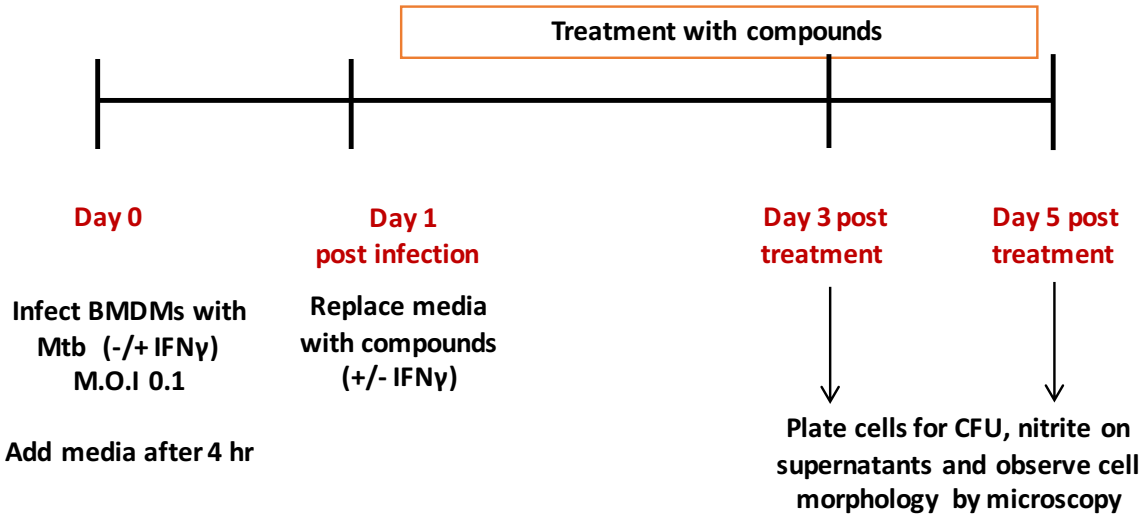

Fig. 12 Schematic representation of the experimental outline

We observed cell morphology and in Mtb-infected macrophages, MRT did not form vacuoles (Fig. 14 C and D) unlike C2062 (Fig. 14 B and E). Cells were alive up to day 5 post compound treatment, suggesting that the compounds were not toxic in the presence of rif. The presence of vacuoles indicate that the compound is not metabolized.

Fig. 13 Impact of small molecules enhancing macrophage activation on the bacterial burden in conjunction with antibiotics. The impact of MRT and metformin on Mtb burden in macrophages without (A) and with IFN γ (B) in conjunction with rif. The impact of C2062 and rif on Mtb burden in macrophages in the absence (C) and in the presence of IFNγ (D). Impact of C2062 and isoniazid on Mtb burden in macrophages in absence (E) and in the presence of IFN γ (F). Results in A – D are means ± SEM of triplicates in one experiment representative of two independent experiments.

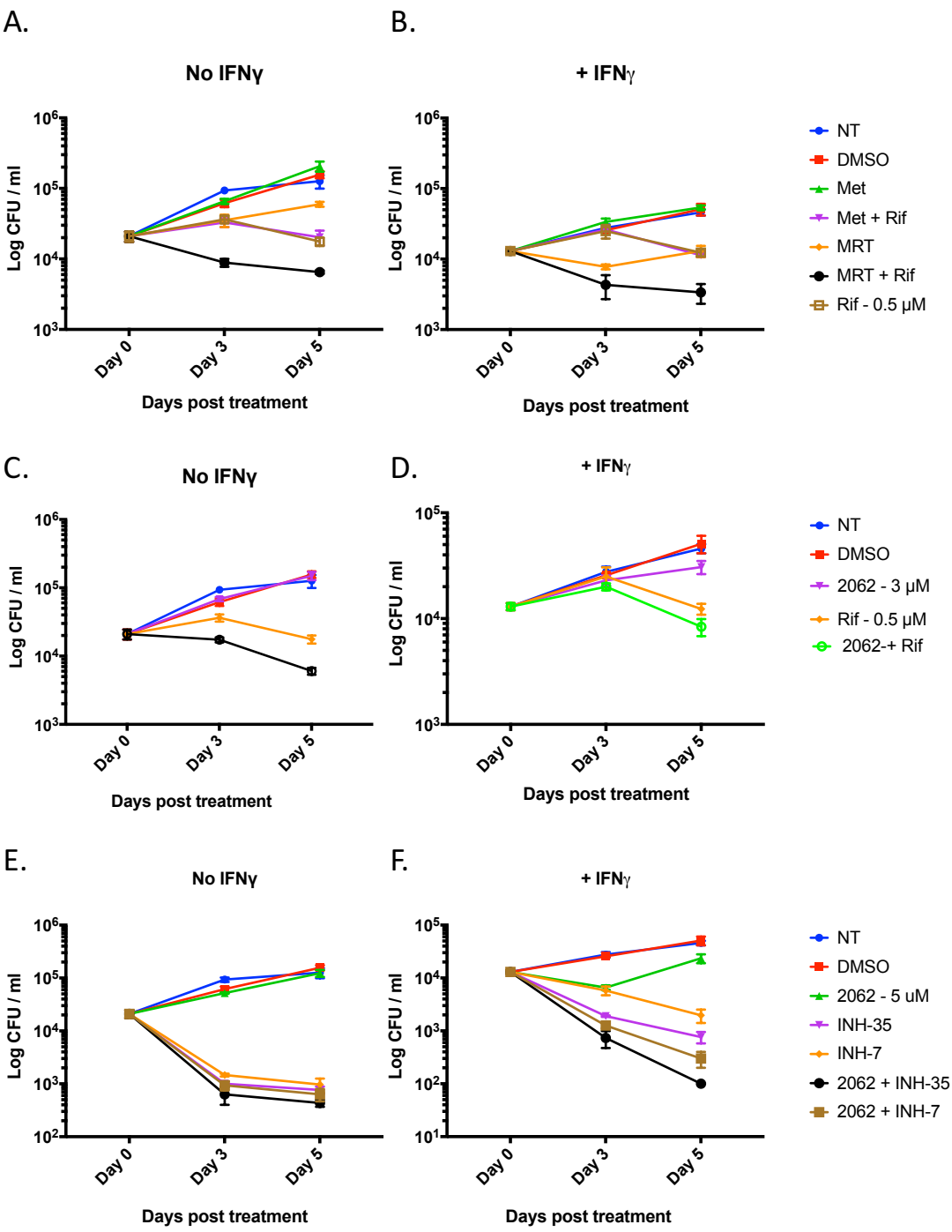
A.
No IFNγ
Log CFU / ml
Days post treatment
Day 0
Day 3
Day 5
B.
+ IFNγ
NT
DMSO
Met
Met + Rif
MRT
MRT + Rif
Rif - 0.5 µM
C.
No IFNγ
D.
+ IFNγ
2062 - 3 µM
Rif - 0.5 µM
2062-+ Rif
E.
No IFNγ
F.
+ IFNγ
2062 - 5 uM
INH-35
INH-7
2062 + INH-35
2062 + INH-7

We also observed that MRT greatly increased nitrite production (Fig. 15) in Mtb-infected macrophages compared to C2062 alone on days 3 and 5 post-treatment. This could be the reason why it led to better control of Mtb as observed in Fig. 14 A and B.

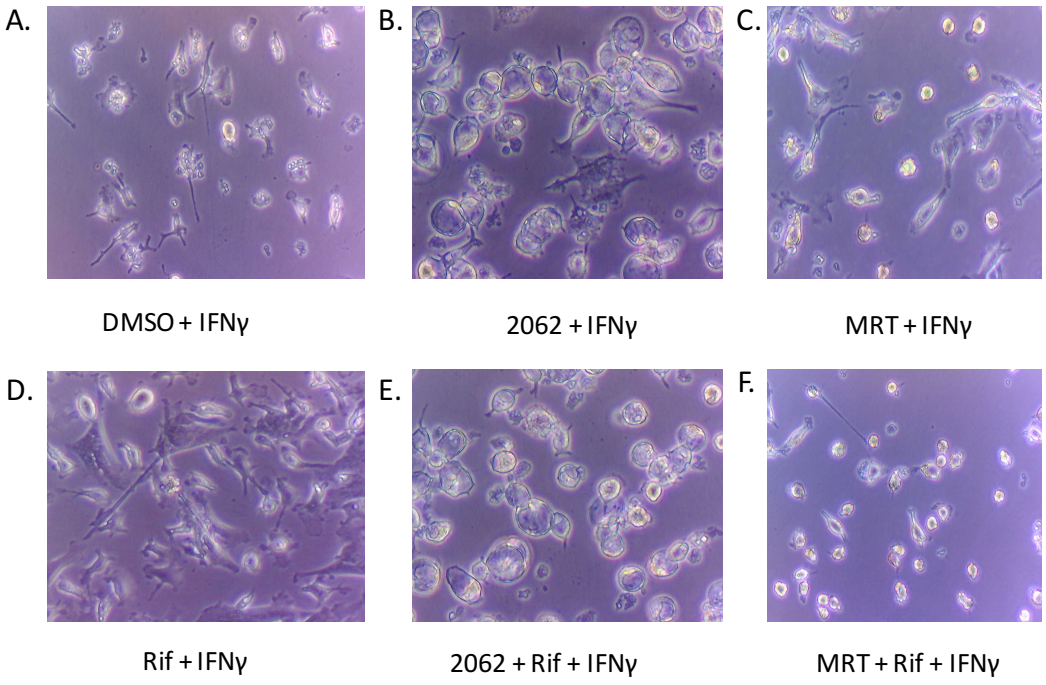

Fig. 14 Images of cell morphology of Mtb-infected macrophages day 5 post treatment. Images taken at 20X maginification.

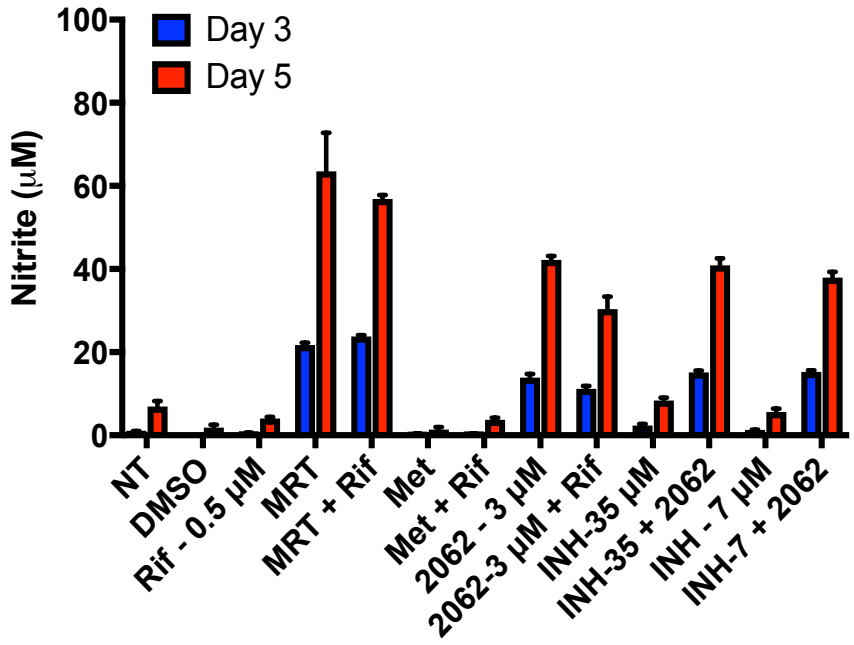

Fig. 15 MRT and C2062 greatly enhance nitrite production in IFNγ treated BMMs day 3 and day 5 post treatment in Mtb-infected macrophages. Results are means ± SEM of triplicates in one experiment representative of two independent experiments.

We repeated the co-treatment experiment of 5 μM C2062 along with 0.5 μM Rif at three different time-points and observed a statistically significant increase in reduction of Mtb burden when C2062 was used in combination with rif compared to rif alone. (Fig. 16). To rule out the effects of C2062 on Mtb, we performed Minimal Inhibitory concentration assays against Mtb in replicating conditions and observed that C2062 had no effect on Mtb, suggesting that it was reducing Mtb burden due to its effects on macrophage activation.

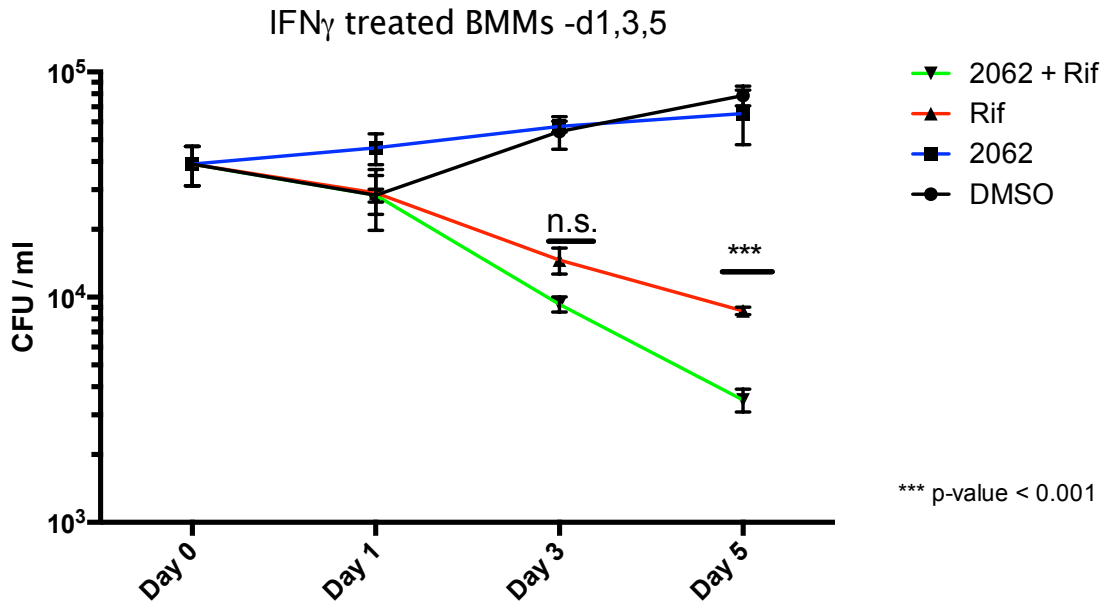

Fig. 16 C2062 reduces bacterial burden in combination with rif compared to rif alone in IFNγ treated macrophages. Results are means ± SEM of triplicates in one experiment representative of three independent experiments.

Taken together, our data show that C2062 is a potential candidate for HDT in the context of Mtb infection *in vitro.* We next decided to investigate this further in a mouse model of Mtb infection.

Characterization of C2062 in Mtb-infected mice

Based on the screen described in Chapter 2 (Fig. 2), we identified five inhibitors (C2071, C2004, C55, C2062, C2011) that enhanced macrophage activation *i.e.* increased nitrite and TNFα production while reducing IL-10 (Fig 17). These five inhibitors showed good pharmacokinetic properties when administered to mice (Performed by our collaborators at CGH and University of Cape Town).

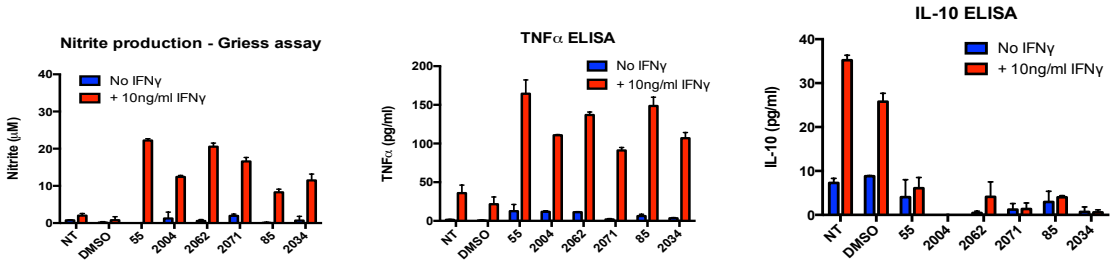

Fig 17. Small molecules that enhance macrophage activation *in vitro*. The impact of lead inhibitors on nitrite and TNFα production and IL-10 reduction in WT BMMs primed with IFNγ (10ng/ml) for 24 hr and then treated with indicated compound for 48 hr. (Left; middle and right panels respectively). Results are mean ± SEM representative of one of two experiments, each performed in triplicate.

We tested C55, C2011, C2062, C2071, and C2004 in a mouse model of Mtb infection (Fig. 18A). Two compounds, namely C2011 and C2062 lowered mean CFU burden by 0.5 log10 (Fig. 18B). Individual mice treated with C2011 or 2C062 had a multi-log reduction in bacterial burden in the lung (Fig. 18C). C2011 lowered mean CFU burden by 2.5 log10 mice in spleen and two mice treated with C2011 and one mouse treated with C2062 had no detectable CFU burden in spleen (Fig. 18D). C2071 was dosed at 30 mg / kg (mpk). C2004 and C55 had insoluble deposits of the compound in the peritoneum. C2011 treatment in mice elevated nitrate + nitrite in lungs (Fig. 18E). No elevation of nitrate + nitrite was seen in the serum of mice treated with C2011 and C2062 (data not shown). However, both compounds elevated TNFα levels in lung homogenates (Fig. 18E). There was no exacerbation of inflammatory pathology in the lungs, as evident from H&E stained sections of the lung (Fig. 18G)

Figure 18. C2011 and C2062 reduce bacterial burden *in vivo* in a mouse model of Mtb infection and do not exacerbate inflammatory pathology in lung.

A. Experimental design of the infection and compound treatment. N=5 per group
B. C2062 and C2011 reduce bacterial burden day 56 post infection
C. CFU burden in the lung and
D. CFU burden in the spleen of individual mice on day 56 post-infection. Data represented as Mean with n=5 mice per group. * indicates no CFU recovered in spleens of 2 mice treated with C2011 and 1 mouse treated with C2062
E. Nitrate + nitrite levels in lung homogenates
F. Levels of TNFα in lung homogenates
G. Histopathology of lungs with H&E staining of Vehicle (top panel) and C2062 (bottom panel) treated mice.

All results are represented as mean in one experiment. *X.Jiang performed the infection and compound treatment. S.Mundhra and R. Bryk analyzed and graphed the data.*

Day 0
ect with
Mtb

Day 1
Harvest
lung

Day 14
Harvest
lung

Day 29
Harvest Lung and
Spleen

Day 57
Harvest Lung
and Spleen

C.

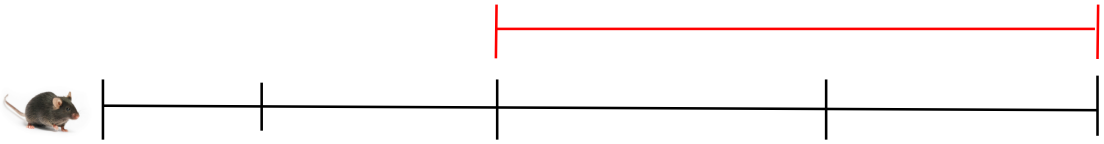

1 14 21
56

D.

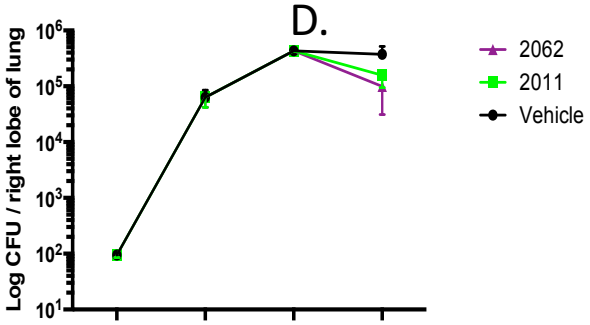

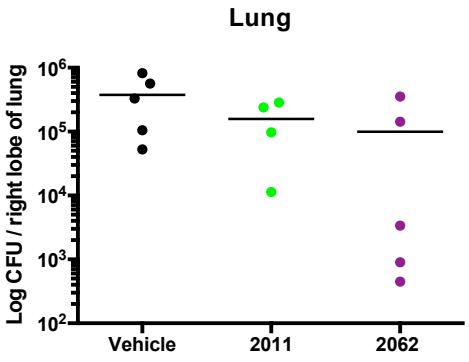

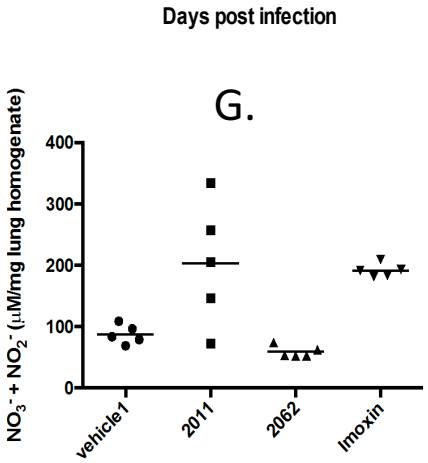

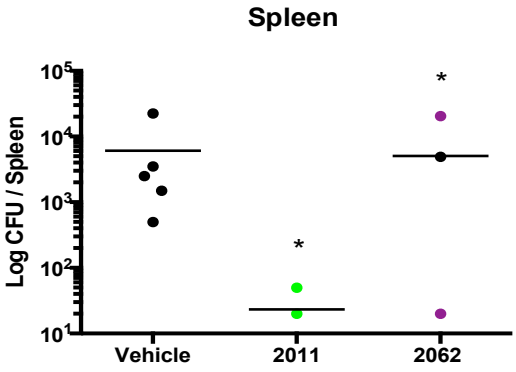

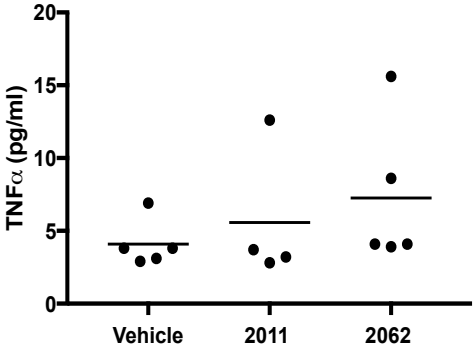

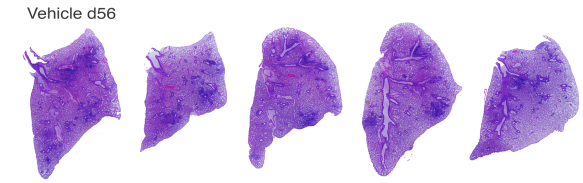

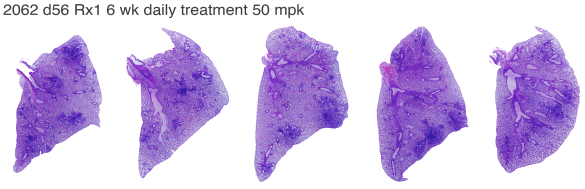

C2062 reduced Mtb burden by 0.5 log10, which is the usual reduction reported by groups studying HDT (Napier et al., 2011; Singhal et al., 2014). Since C2062 inhibited fewer kinases than C2011 in a kinase selectivity panel conducted at Celgene, we decided to repeat the mouse infection experiment with C2062 (Fig. 19A). In the repeat experiment, the mean CFU burden in the lung of 2062-treated mice on day 56 post-infection was lower compared to vehicle control group (Fig. 19B) and all five mice showed reduced bacterial burden in spleen (Fig. 19C) compared to vehicle control group. In this experiment, we wanted to study the impact of C2062 on immune cell types *in vivo*. We observed that C2062-treated mice had an increase in the percentage of neutrophils (Fig. 19D) in lung draining lymph nodes as marked by $Ly6C^{hi}Ly6G^{hi}$ cells when gated on $CD11b^{+}$ $CD45^{+}$ cells. C2062-treated mice also showed an increase in the percentage of iNOS producing myeloid cells as marked by iNOS+Cd11b+ cell population (Fig. 20E) and an increase in the percentage of TNFα producing myeloid cells as marked by TNFα+CD11b+ cell population (Fig. 19F) in lung draining lymph nodes. This increase directly correlated with a decrease in CFU burden. The mice in the C2062 treated group that had higher percentage of neutrophils (Fig. 19G), iNOS producing myeloid cells (Fig. 19H) or TNFα producing myeloid cells (Fig. 19I) had reduced CFU burden compared to their counterparts. These results suggest that the phenotypes of enhanced macrophage activation correlate with improved clearance of Mtb. Similar trends were observed in broncho-alveolar lavage fluid (BALF), though statistically insignificant (Fig. 20 A,B,C). Hence, C2062 was shown to have a pharmacodynamic effect.

Figure 19. C2062 reduces bacterial burden *in vivo* in a mouse model of Mtb infection and this reduction directly correlates with increases in neutrophils, TNFα+ and iNOS+ myeloid cells. Experimental design of the infection and compound treatment. CFU burden in lung and (C) CFU burden in spleen of individual mice on day 56 post-infection. Data represented as Mean with n=5 mice per group. (D) Percentage of neutrophils (E) Percentage of myeloid cells producing iNOS and (F) Percentage of myeloid cells producing TNFα in Vehicle and C2062 treated mice. Representative FACS plots (middle panels) and quantification (far right panels). Correlation between CFU burden in 2062 treated mice and (G) Percentage of neutrophils (H) Percentage of iNOS+ myeloid cells and (I) Percentage of TNFα+ myeloid cells. Results in B are represented as Mean with n=5 mice per group. Results in D, E and F are Mean ± SEM. *X.Jiang and S. Mundhra performed the infection. X. Jiang treated mice with the compound. S.Mundhra analyzed and graphed the data.*

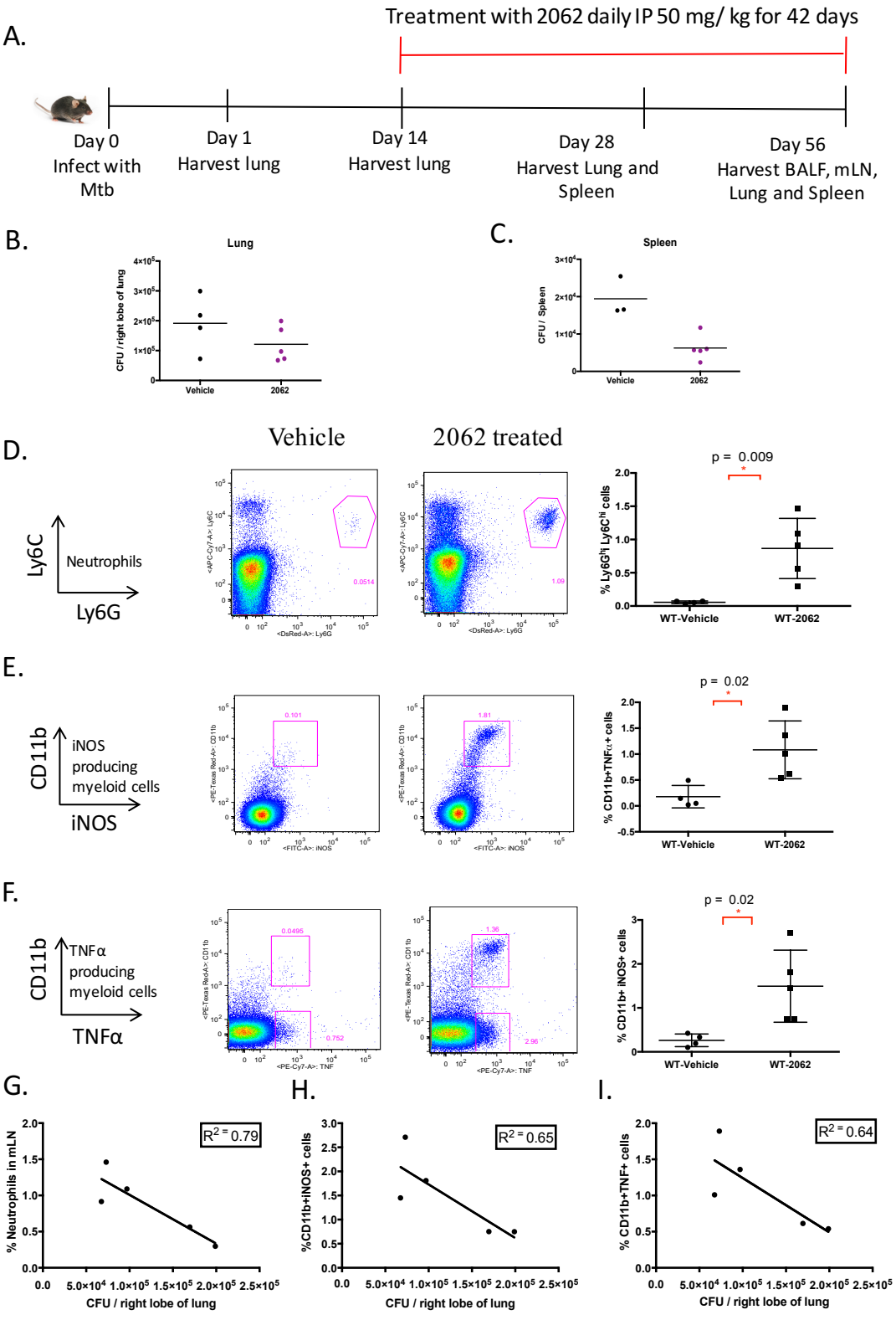
A.
Treatment with 2062 daily IP 50 mg/ kg for 42 days
Day 0
Infect with
Mtb
Day 1
Harvest lung
Day 14
Harvest lung
Day 28
Harvest Lung and
Spleen
Day 56
Harvest BALF, mLN,
Lung and Spleen
B.
Lung
CFU / right lobe of lung
Vehicle
2062
C.
Spleen
CFU / Spleen
Vehicle
2062
D.
Vehicle
2062 treated
Ly6C
Neutrophils
Ly6G
p = 0.009
% Ly6G^hi Ly6C^hi cells
WT-Vehicle
WT-2062
E.
CD11b
iNOS
producing
myeloid cells
iNOS
p = 0.02
% CD11b+TNFα+ cells
WT-Vehicle
WT-2062
F.
CD11b
TNFα
producing
myeloid cells
TNFα
p = 0.02
% CD11b+ iNOS+ cells
WT-Vehicle
WT-2062
G.
R² = 0.79
% Neutrophils in mLN
CFU / right lobe of lung
H.
R² = 0.65
%CD11b+iNOS+ cells
CFU / right lobe of lung
I.
R² = 0.64
% CD11b+TNF+ cells
CFU / right lobe of lung

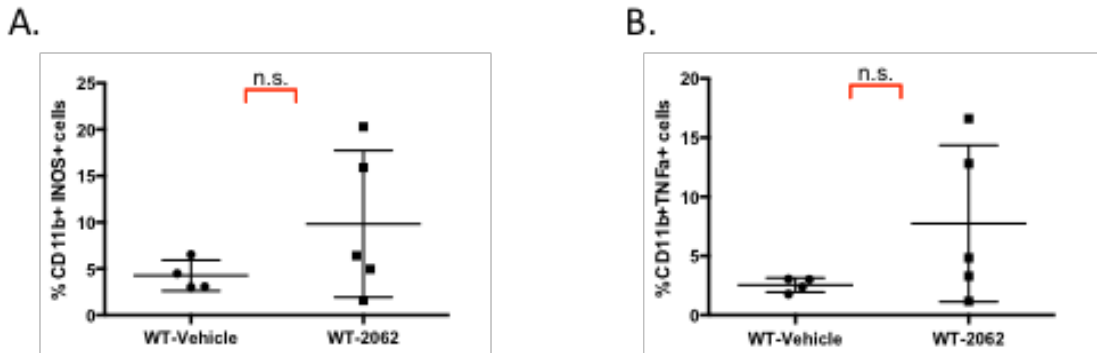

Figure 20. The impact of 2062 treatment on cell types *in vivo* in BALF. (A) iNOS+ myeloid cells and (B) TNFa+ myeloid cells. n=4 in vehicle treated and n-5 mice in 2062-treated group. All results are represented as mean +-SEM in one experiment.

Despite an increase in pro-inflammatory mediators, C2062 did not exacerbate immunopathology in the lung. H&E stained sections of lung were evaluated by a pathologist in a blinded manner (Sebastien Monette at MSKCC Laboratory of Comparative Pathology). The inflammation score was similar between the two groups of mice (Fig. 21A). Histopathology images of lung sections from representative mice of the vehicle and C2062-treated groups are shown (Fig. 21B). We also observed a significant increase in pro-inflammatory cytokines such as IL-12p70 (Fig. 21C), IFNγ (Fig. 21D) and IL-6 (Fig. 21E) in lung homogenates from C2062-treated mice. We also observed a slight reduction in IL-10 (Fig. 21F) although this was not statistically significant. These results demonstrate, again, the pharmacodynamic effects of C2062.

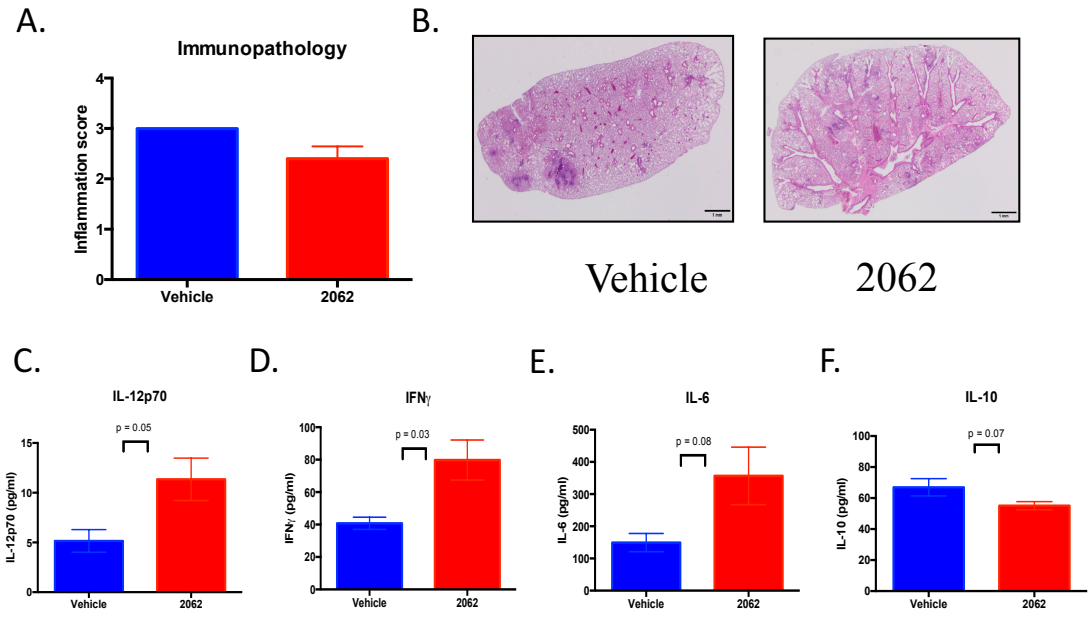

Figure 21. C2062 increases pro-inflammatory cytokines in the lung without exacerbating immunopathology.
(A). Inflammation score on histopathology of lungs from Vehicle and C2062 treated mice. Score based on extent (size and no. of foci) of inflammatory lesions: 0 = No lesions; 1= Minimal inflammation; 2 = Mild inflammation; 3 = Moderate inflammation; 4 = Marked inflammation. (B) Representative images of histopathology of lungs with H&E staining of Vehicle and C2062 treated mice.
Levels of (C) IL-12p70, (D) IFNγ, (E) IL-6 and (F) IL-10 in lung homogenates from Vehicle and C2062 treated mice, d56 post infection. n=4 in vehicle treated and n-5 mice in 2062-treated group. All results are represented as mean +-SEM in one experiment.

Figure 22. C2062 in combination with rif reduces bacterial burden *in vivo* in a mouse model of Mtb infection. (A) Experimental design of the infection and compound treatment. (B) CFU burden in the lung and (C) CFU burden in the spleen of individual mice on day 66 post-infection. Data represented as mean with n=5 mice per group. (D) Percentage of myeloid cells producing iNOS in lung draining lymph nodes (E) Percentage of myeloid cells producing TNFα in lung draining lymph nodes (F) Percentage of neutrophils in lung draining lymph nodes. (G) Percentage of myeloid cells producing iNOS in the lung (H) Percentage of myeloid cells producing TNFα in the lung (I) Percentage of neutrophils in the lung.

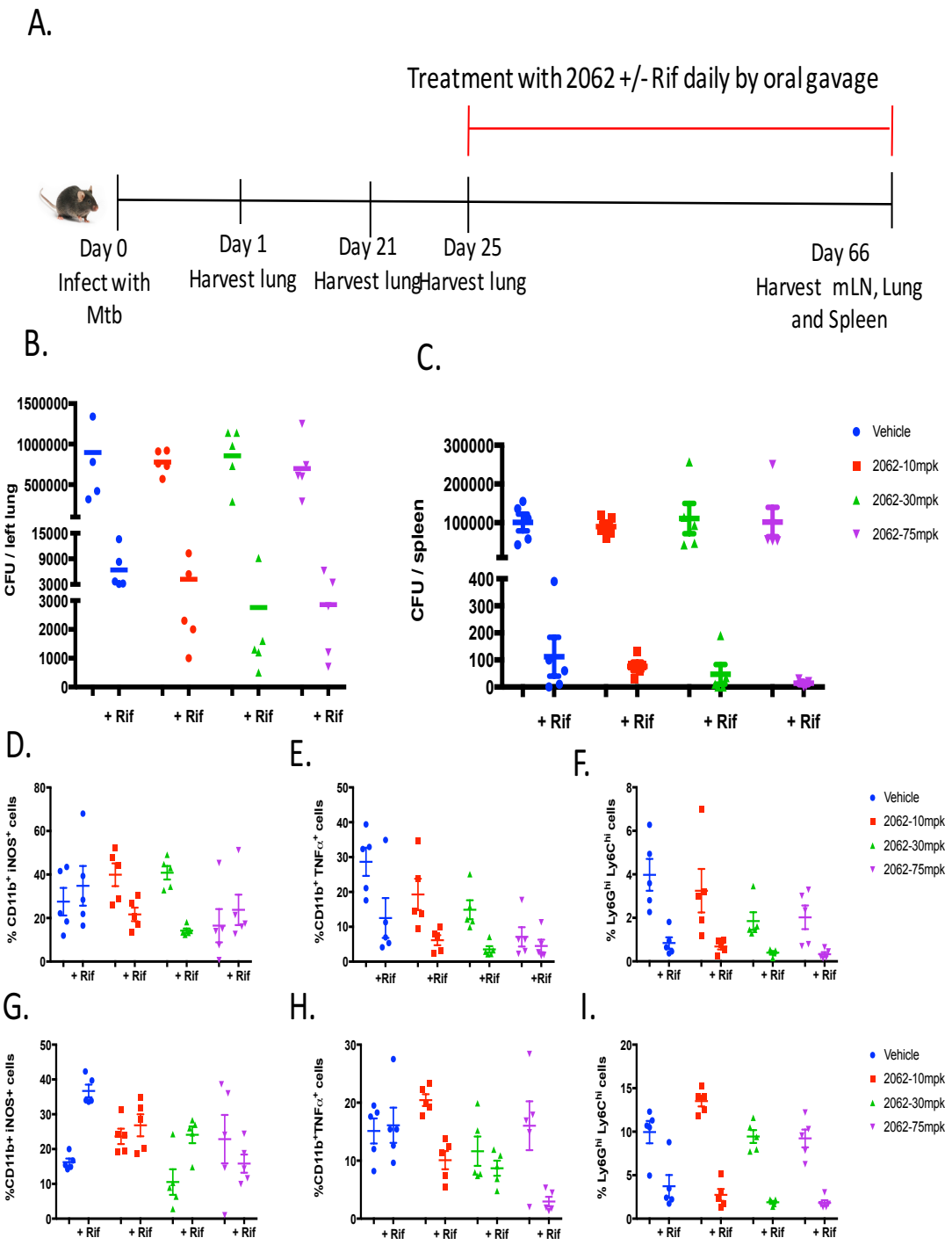
A.
Treatment with 2062 +/- Rif daily by oral gavage
Day 0
Infect with Mtb
Day 1
Harvest lung
Day 21
Harvest lung
Day 25
Harvest lung
Day 66
Harvest mLN, Lung and Spleen
B.
CFU / left lung
+ Rif
C.
CFU / spleen
Vehicle
2062-10mpk
2062-30mpk
2062-75mpk
D.
% CD11b+ iNOS+ cells
E.
%CD11b+ TNFα+ cells
F.
% Ly6Ghi Ly6Chi cells
G.
%CD11b+ iNOS+ cells
H.
%CD11b+TNFα+ cells
I.
% Ly6Ghi Ly6Chi cells

Since C2062 showed efficacy *in vivo* in reducing bacterial burden, we decided to test it in conjunction with rifampicin (rif), a well-known antibiotic against Mtb, for proof of concept of HDT as an adjunctive treatment for TB. As rif is administered orally, CGH changed the formulation of C2062 to be given by oral gavage. We selected 3 doses for administration ± Rif (10 mg/kg): 10 mg/kg, 30 mg/kg and 75 mg/kg. The time-points for harvest are indicated in Fig. 22A. We observed 3/5 mice in 2062-10 mg/kg group, 4/5 mice in 2062-30 mg/kg group and 2/5 mice in 2062-75 mg/kg group reduce bacterial burden in conjunction with rif, compared to rif alone. However, we did not see any decrease in C2062 alone groups (all three doses) compared to the vehicle group (Fig. 22B). All rif treated groups had reduced bacterial burden in the spleen to similar amounts (Fig. 22C).

We observed a slight increase in the percentage of iNOS+ myeloid cells in lung draining lymph nodes (Fig. 22D) in 2062-10 mpk and 2062-30 mpk groups but not so in the lung (Fig. 22G). We observed a slight increase in the percentage of TNF α+ myeloid cells (Fig. 22H) and the percentage of neutrophils in lung of 2062-10 mpk group. The variability in the percentage of immune cell populations could be attributed to the differences in exposure of the compounds in mice when administered by oral gavage as compared to intraperitoneal (as in the previous experiment). We are currently investigating this and are in the process of repeating it.

DISCUSSION

We have shown that the phenotypes of enhanced macrophage activation – namely an increase in nitrite and TNFα, accompanied a reduction in IL-10 does lead to improved clearance of Mtb, both *in vitro* in BMMs and *in vivo* in mice. We believe that these pathways are critical for the control of Mtb as shown by the direct correlation between the reduction in bacterial burden and an increase in the percentage of neutrophils and CD11b+ iNOS+ TNFα+ cells in lung draining lymph nodes and bronchoalveolar lavage fluid. As mentioned in Chapter 1, neutrophils can play a dual role in Mtb infection and in our model system, they seemed to playing a beneficial role.

Although we are not sure of the exact target of C2062, we do know that it does inhibit LKB1, a master regulator of AMPK pathway. It will be interesting to infect BMMs from myeloid-specific knockout mice of LKB1 or challenge those mice with Mtb infection. We would speculate that, due to the extreme pro-inflammatory phenotype, the bacterial burden would be reduced. However, these mice are known to have severe lung damage, when challenged with LPS, due to increase in pro-inflammatory mediators (Liu et al., 2015). Hence, targeting LKB1 alone in the context of TB will not be feasible, as Mtb infection causes liquefaction of lungs in patients. The AMPK complex coordinates glucose metabolism with fatty acid oxidation to regulate energy availability (Xiao et al., 2011). In macrophages, AMPKα1 is predominantly expressed, and AMPKα2 is negligible (Kumase et al., 2016). The role of AMPK in myeloid lineage, mainly during pathogen

specific immune responses are not well characterized. It has been proposed that myeloid-derived AMPK contributes toward the IL-4 driven pathway that promotes M2 polarization and as loss of AMPKα1 in myeloid cell exacerbated lung tissue injury in the context of hookworm infection (Nieves et al., 2016). AMPKα1 has been shown to be crucial for phagocytosis-induced macrophage skewing from a pro- to anti-inflammatory phenotype during resolution of inflammation in the context of skeletal muscle regeneration, as AMPKα1 deficiency led to a decrease in macrophage phagocytic activity (Mounier et al., 2013). Hence, developing an AMPKα1 specific inhibitor would not be beneficial in the context of Mtb infection. Moreover, AMPK activators such as Metformin have been implicated as an HDT agent for TB (Singhal et al., 2014)

In addition, targeting PIKfyve alone also would be futile as PIKfyve inhibition is known to reduce the degradative capacity of phagosomes. PIKfyve, likely through phosphatidylinositol-3,5-bisphosphate synthesis, plays a critical role in endolysosomal and phagosome maturation in macrophages. As endolysosomal and phagosome maturation are key steps in the clearance of Mtb (Weiss and Schaible, 2015), we speculate that inhibiting PIKfyve would lead to an increase in bacterial burden. This increase in bacterial burden was observed in Mtb-infected BMMs when treated with MF4, a selective Pikfyve inhibitor, (Supplementary Fig. 5) and Dr. Maximiliano Gutierrez observed the same increase upon knocking down PIKfyve in macrophage cell lines and infecting with Mtb (personal communication).

C2062 is targeting a pathway that can increase pro-inflammatory mediators while reducing IL-10, without exacerbating immunopathology in the lung. Even though we do not know the exact target of C2062, we have identified and proven that these pathways are critical for the control of TB. Dr. Ruslana Bryk is carrying out experiments on the mechanism of action of C2062, and those studies will be reported elsewhere.

We observed that C2062 by itself reduced bacterial burden by 0.5 $\log_{10}$ in lungs of Mtb-infected mice twice. However, in our combination experiment with C2062 and rif, C2062 had no effect on its own unlike the two previous experiments, but modestly augmented the robust impact of rif. We speculate that the key difference between the experiments may be attributed to delay in the start of treatment in the combination experiment, day 25 as opposed to day 14 in the previous experiments. We observed that IL-10 was high in myeloid cells isolated from lung draining lymph nodes in Mtb-infected mice on day 21, and IL-10 was below the limit of detection in myeloid cells in lung draining lymph nodes of Mtb-infected mice on day 42. This may have shrunken the window of opportunity for C2062 to act as HDT since one of the key features of C2062 is to lower IL-10 production. IL-10 has been shown to block phagosome maturation in Mtb-infected human macrophages (O'Leary et al., 2011). Thus, lowering IL-10 early in the infection might lead to improved clearance of Mtb. We are planning to repeat the combination experiment as described in Fig. 23, starting the treatment of compounds on day 14 post infection.

In summary, we have identified candidates for HDT of TB, and also identified pathways whose inhibition could be critical for control of Mtb. However, the mechanism of action of these small molecules remains yet to be elucidated.

METHODS

Macrophage culture, Mtb infection in mice, kinase selectivity assay and measurements of cytokines and RNI

These protocols are described in detail in Chapter 2.

Macrophage infection

H37Rv strain was from R. North (Trudeau Institute). Macrophages were seeded in 48-well plates at a density of 2.0 × 10^5 cells per well with or without 10 ng/ml IFNγ (Roche) for 24 hrs. The macrophages were infected at an M.O.I of 0.1 of Mtb from early log phase cultures (O.D 0.6 – 0.8). 4 hr after infection, monolayers were washed twice with pre-warmed PBS to remove extracellular bacteria. Fresh complete medium was added to all wells. Next day, the media in wells was completely replaced with new media (10% LCM) with and without IFNγ (as primed before) and small molecules at desired concentrations. At day 1, 3 and 5 post-treatment of compounds, monolayers were lysed with 0.5% Triton X-100 by incubating at 37°C for 10 mins. Serial dilutions were plated on agar plates (Middlebrook 7H11, 10% OADC enrichment; Difco). CFUs were evaluated after 21 days at 37°C. All assays were done with three wells per condition in two independent experiments.

RNA isolation and real-time qPCR

Total RNA isolation from BMM was performed using Qiagen RNAeasy Kit) and DNase digestion using Qiagen kit as per manufacturer's protocol. cDNA was made using Quanta Bioscience qScript cDNA synthesis kit (#95049). PerfecTa qPCR FastMix, UNG from Quanta Biosciences was used as Mix (#95076). Real-time quantitative PCR was performed using validated TaqMan Gene Expression primer and probe sets (Life Technologies) according to the manufacturer's instructions. Following primer and probe sets were used:
Tnf (Mm00443258_m1), Nos2 (Mm00440502_m1), Il10 (Mm01288386_m1) and Gapdh (Mm99999915_g1). qRT-PCR reactions were carried out using the ABI PRISM 7700 Sequence System (Applied Biosystems). mRNA expression was calculated using the $2-\Delta Ct$ method using GAPDH as the internal reference control.

RNA-seq

BMM from three C57BL/6J mice were treated with DMSO, C85, C2062 and C2753 (all at 10 μM) for 1 hr, 2 hr, and 6 hr, and RNA was isolated using Qiagen RNA-easy kit. Quality control of RNA and libraries was performed using the BioAnalyzer 2100. Pair-end sequencing with 40-50 million reads prepared and sequenced using Illumina Hi-Seq platform was performed at the Weill Cornell Genomics Core Facility. The RNA-seq data was analyzed by Weill Cornell Genomics Core Facility using DE-seq algorithm. Genes differentially expressed (~2fold) at FDR 10% and $p<0.05$ were clustered for further analysis.

Cytokine and nitrate/ nitrite measurements in lung homogenates and serum

Lungs were homogenized in PBS containing Complete Mini, EDTA-free protease inhibitor (Roche Applied Science) and the debris-free supernatant was collected for cytokine measurement and stored at -80 °C until further use. Secreted cytokines lung homogenates were measured by magnetic bead-based assays (Affymetrix) according to the manufacturers' instructions. Data were acquired and analyzed using the Luminex automated system at Rockefeller University with the assistance of Dr. Juana Gonzalez. Nitrate/Nitrite Assay Kit by Cayman Biochemicals was used to measure nitrate/nitrite concentrations as per the kit protocol.

Antibodies and Flow Cytometry

Flow cytometric analyses of single cell suspension of cells from lung draining lymph nodes, lungs, and bronchoalveolar lavage was done on LSR-II (BD Immunocytometry Systems), and data analysis was performed using FlowJo software (Tree Star version 9.9).

Antibody List	Format	Dilution	Isotype	Clone	Company	Catalog No.
iNOS (NOS Type 2)	FITC	1/200			BD Pharmingen	610331
CD4 (L3T4)	PerCP-Cy5.5	1/500	Rat IgG2a, κ	RM4-5	Tonbo Bioscience	65-0042-U100
CD8a, Ly-2	PerCP-Cy5.5	1/500	Rat IgG2a, κ	53-6.7	Tonbo Bioscience	65-0081-U025
CD45R (B220)	PerCP-Cy5.5	1/500	Rat IgG2a, κ	RA3-6B2	eBioscience	45-0452-82
NK-1.1	PerCP-Cy5.5	1/250	IgG2a		BioLegend	108728
CD11c (Integrin αX, p1	APC	1/500	Ar Ham IgG	N418	eBioscience	17-0114-82
CD45(LCA, Ly-5)	AlexaFluor 700	1/500	IgG2b, κ	30-F11	eBioscience	56-0451-82
Ly-6C	APC-eFluor 780	1/1000	Rat IgG2c, κ	HK1.4	eBioscience	47-5932-82
F4|80	Brilliant Violet 605		Rat IgG2a, k	BM8	BioLegend	123133
CD11b	PE-eFluor610	1/1500	Rat IgG2b, κ	M1/70	eBioscience	61-0112-82
TNFα	PE-Cy7		IgG1	MP6-XT22	BD Pharmingen™	557644
Ghost Dye™	Violet 510	1/1000			Tonbo	13-0870-T100

Ingenuity Pathway Analysis (IPA)

Ingenuity Knowledge Base (Ingenuity System, Redwood City, CA) was used to identify common pathways in the data set generated from RNA-seq at 6 hr time-point on macrophages treated with C85, C2062, and C2753.

Statistics

Results shown are mean values ± SEM unless otherwise stated. Student's unpaired two-tailed t-test was used for comparisons involving two groups. Differences between groups were considered significant when $p \leq 0.05$. All statistical analyses were performed using GraphPad Prism 7.0 software (La Jolla, CA).

Contributions

R. Bryk conceived ideas as mentioned in the text. Tuo Zhang analyzed the RNA-seq data. X. Jiang administered the compounds in mice in all four experiments. J. Roberts performed the MIC assays. J. Roberts assisted with CFU assays for Mtb-infected macrophages and S. Mundhra analyzed and graphed the data. Femurs from IL-$10^{-/-}$ mice were a generous gift from Dr. Randy Longman (Weill Cornell Medicine).

REFERENCES

Aagaard, C., Hoang, T., Dietrich, J., Cardona, P.-J., Izzo, A., Dolganov, G., Schoolnik, G.K., Cassidy, J.P., Billeskov, R., and Andersen, P. (2011). A multistage tuberculosis vaccine that confers efficient protection before and after exposure. Nat. Med. *17*, 189–194.

Barsig, J., Küsters, S., Vogt, K., Volk, H.D., Tiegs, G., and Wendel, A. (1995). Lipopolysaccharide-induced interleukin-10 in mice: role of endogenous tumor necrosis factor-alpha. Eur. J. Immunol. *25*, 2888–2893.

Bertholet, S., Ireton, G.C., Ordway, D.J., Windish, H.P., Pine, S.O., Kahn, M., Phan, T., Orme, I.M., Vedvick, T.S., Baldwin, S.L., et al. (2010). A defined tuberculosis vaccine candidate boosts BCG and protects against multidrug-resistant Mycobacterium tuberculosis. Sci. Transl. Med. *2*, 53ra74.

Bogdan, C., Vodovotz, Y., and Nathan, C. (1991). Macrophage deactivation by interleukin 10. J. Exp. Med. *174*, 1549–1555.

Condos, R., Rom, W.N., and Schluger, N.W. (1997). Treatment of multidrug-resistant pulmonary tuberculosis with interferon-gamma via aerosol. Lancet Lond. Engl. *349*, 1513–1515.

Donnelly, R.P., Freeman, S.L., and Hayes, M.P. (1995). Inhibition of IL-10 expression by IFN-gamma up-regulates transcription of TNF-alpha in human monocytes. J. Immunol. *155*, 1420–1427.

Filipe-Santos, O., Bustamante, J., Chapgier, A., Vogt, G., de Beaucoudrey, L., Feinberg, J., Jouanguy, E., Boisson-Dupuis, S., Fieschi, C., Picard, C., et al. (2006). Inborn errors of IL-12/23- and IFN-gamma-mediated immunity: molecular, cellular, and clinical features. Semin. Immunol. *18*, 347–361.

Hardie, D.G., and Alessi, D.R. (2013). LKB1 and AMPK and the cancer-metabolism link - ten years after. BMC Biol. *11*, 36.

Hu, X., Paik, P.K., Chen, J., Yarilina, A., Kockeritz, L., Lu, T.T., Woodgett, J.R., and Ivashkiv, L.B. (2006). IFN-γ Suppresses IL-10 Production and Synergizes with TLR2 by Regulating GSK3 and CREB/AP-1 Proteins. Immunity *24*, 563–574.

Jefferies, H.B.J., Cooke, F.T., Jat, P., Boucheron, C., Koizumi, T., Hayakawa, M., Kaizawa, H., Ohishi, T., Workman, P., Waterfield, M.D., et al. (2008). A selective PIKfyve inhibitor blocks PtdIns(3,5)P(2)

production and disrupts endomembrane transport and retroviral budding. EMBO Rep. *9*, 164–170.

Johnson, J.L., Kamya, R.M., Okwera, A., Loughlin, A.M., Nyole, S., Hom, D.L., Wallis, R.S., Hirsch, C.S., Wolski, K., Foulds, J., et al. (2000). Randomized controlled trial of Mycobacterium vaccae immunotherapy in non-human immunodeficiency virus-infected Ugandan adults with newly diagnosed pulmonary tuberculosis. J. Infect. Dis. *181*, 1304–1312.

Kim, G.H.E., Dayam, R.M., Prashar, A., Terebiznik, M., and Botelho, R.J. (2014). PIKfyve Inhibition Interferes with Phagosome and Endosome Maturation in Macrophages. Traffic *15*, 1143–1163.

Koo, M.-S., Manca, C., Yang, G., O'Brien, P., Sung, N., Tsenova, L., Subbian, S., Fallows, D., Muller, G., Ehrt, S., et al. (2011). Phosphodiesterase 4 inhibition reduces innate immunity and improves isoniazid clearance of Mycobacterium tuberculosis in the lungs of infected mice. PloS One *6*, e17091.

Kumase, F., Takeuchi, K., Morizane, Y., Suzuki, J., Matsumoto, H., Kataoka, K., Al-Moujahed, A., Maidana, D.E., Miller, J.W., and Vavvas, D.G. (2016). AMPK-Activated Protein Kinase Suppresses Ccr2 Expression by Inhibiting the NF-κB Pathway in RAW264.7 Macrophages. PLoS ONE *11*.

Liu, Z., Zhang, W., Zhang, M., Zhu, H., Moriasi, C., and Zou, M.-H. (2015). Liver Kinase B1 Suppresses Lipopolysaccharide-induced Nuclear Factor κB (NF-κB) Activation in Macrophages. J. Biol. Chem. *290*, 2312–2320.

Lowrie, D.B., Tascon, R.E., Bonato, V.L., Lima, V.M., Faccioli, L.H., Stavropoulos, E., Colston, M.J., Hewinson, R.G., Moelling, K., and Silva, C.L. (1999). Therapy of tuberculosis in mice by DNA vaccination. Nature *400*, 269–271.

Maiga, M., Agarwal, N., Ammerman, N.C., Gupta, R., Guo, H., Maiga, M.C., Lun, S., and Bishai, W.R. (2012). Successful Shortening of Tuberculosis Treatment Using Adjuvant Host-Directed Therapy with FDA-Approved Phosphodiesterase Inhibitors in the Mouse Model. PLOS ONE *7*, e30749.

Mayer-Barber, K.D., Andrade, B.B., Oland, S.D., Amaral, E.P., Barber, D.L., Gonzales, J., Derrick, S.C., Shi, R., Kumar, N.P., Wei, W., et al. (2014). Host-directed therapy of tuberculosis based on interleukin-1 and type I interferon crosstalk. Nature *511*, 99–103.

Méndez-Samperio, P. (2010). Role of interleukin-12 family cytokines in the cellular response to mycobacterial disease. Int. J. Infect. Dis. *14*, e366–e371.

Mounier, R., Théret, M., Arnold, L., Cuvellier, S., Bultot, L., Göransson, O., Sanz, N., Ferry, A., Sakamoto, K., Foretz, M., et al. (2013). AMPKα1 regulates macrophage skewing at the time of resolution of inflammation during skeletal muscle regeneration. Cell Metab. *18*, 251–264.

Napier, R.J., Rafi, W., Cheruvu, M., Powell, K.R., Zaunbrecher, M.A., Bornmann, W., Salgame, P., Shinnick, T.M., and Kalman, D. (2011). Imatinib-sensitive tyrosine kinases regulate mycobacterial pathogenesis and represent therapeutic targets against tuberculosis. Cell Host Microbe *10*, 475–485.

Napier, R.J., Norris, B.A., Swimm, A., Giver, C.R., Harris, W.A.C., Laval, J., Napier, B.A., Patel, G., Crump, R., Peng, Z., et al. (2015). Low Doses of Imatinib Induce Myelopoiesis and Enhance Host Anti-microbial Immunity. PLOS Pathog. *11*, e1004770.

Nieves, W., Hung, L.-Y., Oniskey, T.K., Boon, L., Foretz, M., Viollet, B., and Herbert, D.R. (2016). Myeloid-Restricted AMPKα1 Promotes Host Immunity and Protects against IL-12/23p40-Dependent Lung Injury during Hookworm Infection. J. Immunol. Baltim. Md 1950 *196*, 4632–4640.

Okada, M., Kita, Y., Nakajima, T., Kanamaru, N., Hashimoto, S., Nagasawa, T., Kaneda, Y., Yoshida, S., Nishida, Y., Nakatani, H., et al. (2009). Novel prophylactic and therapeutic vaccine against tuberculosis. Vaccine *27*, 3267–3270.

O'Leary, S., O'Sullivan, M.P., and Keane, J. (2011). IL-10 Blocks Phagosome Maturation in Mycobacterium tuberculosis–Infected Human Macrophages. Am. J. Respir. Cell Mol. Biol. *45*, 172–180.

Parihar, S.P., Guler, R., Khutlang, R., Lang, D.M., Hurdayal, R., Mhlanga, M.M., Suzuki, H., Marais, A.D., and Brombacher, F. (2014). Statin therapy reduces the mycobacterium tuberculosis burden in human macrophages and in mice by enhancing autophagy and phagosome maturation. J. Infect. Dis. *209*, 754–763.

Rosas-Taraco, A.G., Higgins, D.M., Sánchez-Campillo, J., Lee, E.J., Orme, I.M., and González-Juarrero, M. (2009). Intrapulmonary delivery of XCL1-targeting small interfering RNA in mice chronically

infected with Mycobacterium tuberculosis. Am. J. Respir. Cell Mol. Biol. *41*, 136–145.

Saraiva, M., and O'Garra, A. (2010). The regulation of IL-10 production by immune cells. Nat. Rev. Immunol. *10*, 170–181.

Sbrissa, D., Ikonomov, O.C., Filios, C., Delvecchio, K., and Shisheva, A. (2012). Functional dissociation between PIKfyve-synthesized PtdIns5P and PtdIns(3,5)P2 by means of the PIKfyve inhibitor YM201636. Am. J. Physiol. Cell Physiol. *303*, C436-446.

Singhal, A., Jie, L., Kumar, P., Hong, G.S., Leow, M.K.-S., Paleja, B., Tsenova, L., Kurepina, N., Chen, J., Zolezzi, F., et al. (2014). Metformin as adjunct antituberculosis therapy. Sci. Transl. Med. *6*, 263ra159-263ra159.

Sun, X., Gao, L., Chien, H.-Y., Li, W.-C., and Zhao, J. (2013). The regulation and function of the NUAK family. J. Mol. Endocrinol. *51*, R15-22.

Wallis, R.S., and Zumla, A. (2016). Vitamin D as Adjunctive Host-Directed Therapy in Tuberculosis: A Systematic Review. Open Forum Infect. Dis. *3*.

Weiss, G., and Schaible, U.E. (2015). Macrophage defense mechanisms against intracellular bacteria. Immunol. Rev. *264*, 182–203.

Xiao, B., Sanders, M.J., Underwood, E., Heath, R., Mayer, F.V., Carmena, D., Jing, C., Walker, P.A., Eccleston, J.F., Haire, L.F., et al. (2011). Structure of mammalian AMPK and its regulation by ADP. Nature *472*, 230–233.

CHAPTER 4

CONCLUSIONS

CONCLUSIONS

Increasing emergence of drug-resistant *Mycobacterium tuberculosis* (Mtb), the causative agent of tuberculosis (TB), led to interest in developing adjunctive therapies targeting host molecules to avoid pathogen resistance. An ideal candidate for host-directed therapy (HDT) would be a host enzyme whose temporary, partial inhibition is selectively detrimental for Mtb pathogenesis but not so for the host, and augments host immunity without exacerbating immunopathology. It was shown that mice deficient in protein kinase R (PKR) on 129S1/SvImJ background were partially protected from Mtb infection, in part due to reduction in interferon gamma (IFNγ) - induced macrophage expression of interleukin 10 (IL-10) (Wu et al., 2012). The authors of this study concluded that the absence of PKR led to "super-activation of macrophages," as indicated by an increase in the IFNγ–induced production of reactive nitrogen intermediates (RNI) and pro-inflammatory cytokine tumor necrosis factor alpha (TNFα) and decrease in anti-inflammatory cytokine IL-10 (Wu et al., 2012).

Since PKR-deficiency led to improved control of TB, we collaborated with Celgene Global Health (CGH) to develop non-toxic small molecules targeting PKR that are bioavailable for HDT of TB *in vivo*. Among the small molecules we screened, we selected those which enhanced release of RNI and TNFα while reducing IL-10. For this purpose, we used IFNγ –primed bone marrow derived macrophages (BMM) from wild-type (WT) C57BL/6J mice. In a mouse model of Mtb

infection, one such small molecule - C2062 reduced Mtb-burden in lungs by 0.5 $\log_{10}$ without exacerbating immunopathology in lung. This decrease in bacterial burden in lungs correlated with increase in neutrophils and $CD11b^{+}$ $TNF\alpha^{+}$ $iNOS^{+}$ cells in lung draining lymph nodes and bronchoalveolar lavage fluid, and pro-inflammatory cytokine levels in lung homogenates. This suggested that these molecules are modulating important immune signaling pathways that lead to improved Mtb control *in vivo.* In combination with rifampicin (rif), a known antibiotic active against Mtb, C2062 reduced bacterial burden by 0.5 $\log_{10}$ in Mtb-infected BMMs compared to rif alone. Furthermore, C2062 modestly augmented the robust effects of rif in a mouse model of Mtb infection.

However, the small molecules – C2062 and C85 had similar effects on IFNγ – primed BMMs WT and PKR-deficient C57BL/6J mice excluding PKR as the its sole target. Furthermore, WT and PKR-deficient mice with a shared C57BL/6J background, had similar Mtb burden in lungs and spleen, ruling out the relevance of PKR in TB. Even though we identified that the earlier phenotypes observed in the Wu study (Wu et al., 2012) were mouse strain-specific and PKR-independent, nonetheless it led to the identification of novel PKR inhibitors with great selectivity.

We have identified that small molecule-mediated enhancement of macrophage activation can be used as agents for HDT, to help the immune system control TB in conjunction with anti-mycobacterials.

Future directions and perspectives:

This study demonstrates that PKR is not the ideal target for HDT of TB. The knowledge that PKR is not required for host control of TB in mice helps the scientific community and the pharmaceutical industry, to avoid investing further in discovery of PKR inhibitors in the context of TB treatment. In addition, the PKR inhibitors identified in our screen (chapter 2) may have value for pathological conditions other than TB. For instance, they may be used for other diseases such as insulin resistance, neurodegeneration and cancer where PKR inhibition has shown to be beneficial (Mouton-Liger et al., 2015; Nakamura et al., 2014; Pataer et al., 2009).

Moreover, this study highlights the importance and cautions the investigators of using strain-matched backgrounds in studies prior to making any scientific conclusions. The microbiome has been implicated in many disease settings (Cho and Blaser, 2012; Shreiner et al., 2015), however, the importance of co-housed littermate controls has just started to gain recognition. Herein, we used co-housed genetically-matched strains to account for the differences in microbiota.

In this study, we made the serendipitous discovery that macrophages from 129S1/SvImJ mice are more activated than macrophages of C57BL/6J mice upon IFNγ treatment. This information could also be useful in urging the scientific community to be cautious while interpreting results in mouse models of various diseases where phenotypes are IFNγ-dependent. In the earlier days, targeted mutagenesis in mice was mostly performed by using

embryonic stem cells from 129-derived mice, and C57BL/6J as recipient strains. It has been predicted though comparative genomics that nearly all 129-derived genetically modified congenic mice are affected by multiple inactivating passenger mutations which influence the phenotypic outcome, despite intensive backcrossing (Vanden Berghe et al., 2015). The authors of this study showed that there are indels and SNPs that result in aberrant or alternative amino acid sequences in 1,084 genes in the 129-strain genome. Hence, there is a highly underestimated issue of false-positive results using genetically modified lines. These confounding results could be one of the reasons leading to variable translatability of the results of mouse studies to humans.

Additionally, macrophages from 129S1/SvImJ mice, when treated with IFNγ result in similar phenotypes, as what we would expect from knocking out of knocking down the target in macrophages from C57BL/6J mice treated with IFNγ and our compound. Therefore, the phenotypes are manifested in activated 129S1/SvImJ macrophages without the compound, and the compound has no further effect. The latter macrophages could potentially be useful in identification of a candidate target. We could have potential targets in B6 background and look for a diminution of the function of that candidate target in 129S1/SvImJ genome to confirm the target.

A caveat of our study is that mice on C57BL/6J background are not the best model of TB, since they do not form human-like granulomas. In addition, most mice strains seem to be unable to decrease bacterial burden and ultimately die of TB (Apt and Kramnik,

2009). Macaques are better compared to mice, as they can model granuloma structure and differential clinical outcomes of human infection and disease. However, they are also expensive to maintain and not suitable for preliminary studies.

The RNA-seq data obtained on macrophages treated with C85 and C2062 remains a largely unmined bed of useful information. The results of this screen lend itself well to candidate approaches for understanding macrophage activation. This is especially true for pathways hit in context of treatment with both candidate molecules – C85 and C2062.

Loss of function screens may also be carried out for identification of the target(s) of the compound that gives the three phenotypes of increase in nitrite and TNFα production and IL-10 reduction. However, this type of screen does have certain limitations – (1) the phenotypes could be a result of inhibition of multiple targets and hence a library of single-gene loss of function mutants may not contain any clones that would result in the phenotype, (2) loss of function screens can result in lethality if the candidate gene is essential for survival.

Although the use of antibiotics is well established for the treatment of TB, due to the long duration of current TB therapy, it is expensive and difficult for patients to adhere to treatment. Hence, the need for an HDT agent is warranted. Preliminary experiments have suggested that C2062 in combination with rif results in marginally decreased CFU burden. We are currently starting a repeat experiment with a reduced dose of rif and earlier start of treatment of compounds

– day 14 instead of day 28 as performed previously (Chapter 3). If future studies can identify the physiologically relevant target of C2062, it will facilitate the development of more selective inhibitors against that target and lead to potential new therapeutic avenues for HDT against Mtb. Furthermore, small molecules enhancing macrophage activation could also find potential use in the context of other diseases where macrophages play a key role in clearance of pathogen such as *Leishmania* and *Listeria* (Bogdan and Röllinghoff, 1998; Pamer, 2004; Thi et al., 2012).

Although more work is needed to elucidate how C2062 acts mechanistically, we have identified a direct correlation between the actions of C2062 (increase in percentage of neutrophils and iNOS+ TNFα+ myeloid cells) and reduction in bacterial burden. Hence, these phenotypes do have physiological relevance and do lead to improved TB control. This work may aid in the development of more therapeutic strategies to develop the small molecules targeting these pathways. My colleague, R. Bryk is carrying out research to understand mechanism of C2062 and those results will be reported elsewhere.

It is not known why diabetes increases the risk of TB. It has been shown that inhibiting PKR improves glucose homeostasis in obese diabetic mice (Nakamura et al., 2014). Perhaps in a dual disease model of diabetes and TB, treatment with C2062, which enhances macrophage activation and inhibits PKR (IC50 = 0.88 μM as reported by R. Bryk), might prove to be beneficial.

The prime motivation for our work is the breadth and depth of human suffering caused by TB around the world. Of the other major

diseases, worldwide, many affect primarily older individuals (cancer, cardiovascular diseases) or young children (diarrheal diseases). TB, especially in the world of growing HIV prevalence and co-infection, affects primarily working-age adults. Thus, TB is devastating socio-economically and pathologically. Poor communities, those most affected by the HIV and TB epidemics, are particularly vulnerable to losing members of their workforce. From a human perspective, the loss is much more difficult to calculate. TB is both the cause and a consequence of poverty. It is inextricably linked to those in under-served and under-resourced communities of the world. Accordingly, there is an immediate and urgent need to reduce the cost and duration of TB treatment. Our efforts aimed at developing a novel adjunctive method to target TB necessarily fall within this global context. Here, we made a small attempt towards developing a potential new therapy against TB and understanding the biology behind it. Many promising potential host-directed therapeutics are already being explored in clinical trials (as described in Chapter 1). At the same time, we must also continue the development of antibiotics against Mtb, since drug resistance is a constant battle for all novel drugs. Efforts need to be made on all levels to translate our current understanding of TB in order to create effective treatments, preventions, and programs for its eradication. With the development of novel and effective adjunctive therapy, more effective vaccines and quicker-acting anti-mycobacterials —the goal of TB eradication will be ever closer.

REFERENCES

Apt, A., and Kramnik, I. (2009). Man and mouse TB: contradictions and solutions. Tuberc. Edinb. Scotl. *89*, 195–198.

Bogdan, C., and Röllinghoff, M. (1998). The immune response to Leishmania: mechanisms of parasite control and evasion. Int. J. Parasitol. *28*, 121–134.

Cho, I., and Blaser, M.J. (2012). The Human Microbiome: at the interface of health and disease. Nat. Rev. Genet. *13*, 260–270.

Mouton-Liger, F., Rebillat, A.-S., Gourmaud, S., Paquet, C., Leguen, A., Dumurgier, J., Bernadelli, P., Taupin, V., Pradier, L., Rooney, T., et al. (2015). PKR downregulation prevents neurodegeneration and β-amyloid production in a thiamine-deficient model. Cell Death Dis. *6*, e1594.

Nakamura, T., Arduini, A., Baccaro, B., Furuhashi, M., and Hotamisligil, G.S. (2014). Small-molecule inhibitors of PKR improve glucose homeostasis in obese diabetic mice. Diabetes *63*, 526–534.

Pamer, E.G. (2004). Immune responses to Listeria monocytogenes. Nat. Rev. Immunol. *4*, 812–823.

Pataer, A., Swisher, S.G., Roth, J.A., Logothetis, C.J., and Corn, P. (2009). Inhibition of RNA-dependent protein kinase (PKR) leads to cancer cell death and increases chemosensitivity. Cancer Biol. Ther. *8*, 245–252.

Shreiner, A.B., Kao, J.Y., and Young, V.B. (2015). The gut microbiome in health and in disease. Curr. Opin. Gastroenterol. *31*, 69–75.

Thi, E.P., Lambertz, U., and Reiner, N.E. (2012). Sleeping with the Enemy: How Intracellular Pathogens Cope with a Macrophage Lifestyle. PLoS Pathog. *8*.

Vanden Berghe, T., Hulpiau, P., Martens, L., Vandenbroucke, R.E., Van Wonterghem, E., Perry, S.W., Bruggeman, I., Divert, T., Choi, S.M., Vuylsteke, M., et al. (2015). Passenger Mutations Confound Interpretation of All Genetically Modified Congenic Mice. Immunity *43*, 200–209.

Wu, K., Koo, J., Jiang, X., Chen, R., Cohen, S.N., and Nathan, C. (2012). Improved control of tuberculosis and activation of macrophages in mice lacking protein kinase R. PloS One *7*, e30512.

APPENDIX 1

Supplementary Table 1.
Data obtained by searching for 'Ifngr1' and 'Ifngr2' in mouse strain 129S1SvImJ from
http://www.sanger.ac.uk/sanger/Mouse_SnpViewer/rel-1505.
The data-base uses mouse strain C57BL/6J GRCm38 assembly as a reference. All SNP/ indels and structural variant types were included in the search.

List of SNPs						
Chr	Position	Gene	dbSNP	C57Bl/6J	129S1_SvImJ	Consequence
10	19592175	Ifngr1	rs13467527	T	C*	synonymous_variant nmd_transcript_variant
10	19592443	Ifngr1	rs29336579	A	G*	intron_variant nmd_transcript_variant
10	19592450	Ifngr1	rs29359700	A	T*	intron_variant nmd_transcript_variant
10	19592459	Ifngr1	rs29326407	C	T*	intron_variant nmd_transcript_variant
10	19592655	Ifngr1	rs6307185	A	G*	intron_variant nmd_transcript_variant
10	19592660	Ifngr1	rs6307192	A	G*	intron_variant nmd_transcript_variant
10	19592707	Ifngr1	rs3681091	C	G*	intron_variant nmd_transcript_variant
10	19593773	Ifngr1	rs29372567	A	G*	intron_variant nmd_transcript_variant
10	19594032	Ifngr1	rs233513847	C	T*	intron_variant nmd_transcript_variant
10	19595816	Ifngr1	rs579458786	G	A*	intron_variant nmd_transcript_variant
10	19595858	Ifngr1	rs4137440	G	T*	intron_variant nmd_transcript_variant
10	19596087	Ifngr1	rs254189437	T	C*	intron_variant nmd_transcript_variant
10	19596137	Ifngr1	rs266214047	A	C*	intron_variant nmd_transcript_variant
10	19596216	Ifngr1	rs229060147	C	G*	intron_variant nmd_transcript_variant
10	19596224	Ifngr1	rs243297678	A	G*	intron_variant nmd_transcript_variant
10	19596247	Ifngr1	rs212570699	A	G*	intron_variant nmd_transcript_variant
10	19596335	Ifngr1	rs231296450	G	T*	intron_variant nmd_transcript_variant
10	19596343	Ifngr1	rs255829360	T	C*	intron_variant nmd_transcript_variant
10	19596381	Ifngr1	rs243554315	G	A*	intron_variant nmd_transcript_variant
10	19598124	Ifngr1	rs29315942	T	G*	intron_variant nmd_transcript_variant downstream_gene_variant
10	19598146	Ifngr1	rs226986894	C	T*	intron_variant nmd_transcript_variant downstream_gene_variant
10	19598171	Ifngr1	rs230183849	T	C*	intron_variant nmd_transcript_variant downstream_gene_variant
10	19598174	Ifngr1	rs249047138	A	G*	intron_variant nmd_transcript_variant downstream_gene_variant
10	19598219	Ifngr1	-	A	a/c*	intron_variant nmd_transcript_variant downstream_gene_variant
10	19598553	Ifngr1	rs51633668	T	A*	intron_variant nmd_transcript_variant downstream_gene_variant
10	19598662	Ifngr1	rs48059797	C	T*	intron_variant nmd_transcript_variant downstream_gene_variant
10	19598725	Ifngr1	rs51862239	C	T*	intron_variant nmd_transcript_variant downstream_gene_variant
10	19598855	Ifngr1	rs29377033	A	G*	intron_variant nmd_transcript_variant downstream_gene_variant
10	19598942	Ifngr1	rs224452593	C	G*	intron_variant nmd_transcript_variant downstream_gene_variant
10	19599043	Ifngr1	rs244512522	T	C*	missense_variant intron_variant nmd_transcript_variant downstream_gene_variant
10	19600149	Ifngr1	rs29347154	A	G*	intron_variant nmd_transcript_variant downstream_gene_variant
10	19600402	Ifngr1	rs251194780	A	G*	intron_variant nmd_transcript_variant downstream_gene_variant
10	19600562	Ifngr1	rs215768634	C	G*	intron_variant nmd_transcript_variant downstream_gene_variant
10	19600850	Ifngr1	rs238697052	T	A*	intron_variant nmd_transcript_variant downstream_gene_variant
10	19601201	Ifngr1	rs49603673	T	C*	intron_variant nmd_transcript_variant upstream_gene_variant downstream_gene_variant
10	19601502	Ifngr1	rs46637409	T	C*	intron_variant nmd_transcript_variant upstream_gene_variant downstream_gene_variant
10	19602080	Ifngr1	rs46104437	T	A*	intron_variant nmd_transcript_variant upstream_gene_variant downstream_gene_variant
10	19602364	Ifngr1	rs29320505	G	T*	intron_variant nmd_transcript_variant upstream_gene_variant downstream_gene_variant
10	19602459	Ifngr1	rs29359910	A	G*	intron_variant nmd_transcript_variant upstream_gene_variant downstream_gene_variant
10	19602599	Ifngr1	rs29331763	C	T*	intron_variant nmd_transcript_variant upstream_gene_variant downstream_gene_variant
10	19603365	Ifngr1	rs3702815	C	G*	intron_variant nmd_transcript_variant upstream_gene_variant downstream_gene_variant
10	19603572	Ifngr1	rs29327973	A	G*	intron_variant nmd_transcript_variant upstream_gene_variant downstream_gene_variant
10	19603711	Ifngr1	rs29316518	T	C*	intron_variant nmd_transcript_variant upstream_gene_variant downstream_gene_variant
10	19604014	Ifngr1	rs29323906	A	G*	intron_variant upstream_gene_variant downstream_gene_variant
10	19604695	Ifngr1	rs29324397	T	G*	intron_variant upstream_gene_variant downstream_gene_variant
10	19605570	Ifngr1	rs29346781	A	G*	intron_variant upstream_gene_variant downstream_gene_variant
10	19606638	Ifngr1	rs3691292	G	A*	intron_variant downstream_gene_variant
10	19609070	Ifngr1	rs29323743	C	T	intron_variant
List of Insertions / deletions						
Chr	Position	Gene	dbSNP	C57Bl/6J	129S1_SvImJ	Consequence
10	19592031	Ifngr1	rs228443125	AAGGCC	A*	5_prime_utr_variant nmd_transcript_variant upstream_gene_variant
10	19592502	Ifngr1	rs214343522	ATTTG	A*	intron_variant nmd_transcript_variant
10	19594311	Ifngr1	rs237129992	CA	C*	intron_variant nmd_transcript_variant
10	19595818	Ifngr1	rs236400721	AT	A*	intron_variant nmd_transcript_variant
10	19595833	Ifngr1	-	AATT	A*	intron_variant nmd_transcript_variant
10	19596387	Ifngr1	rs220919952	C	CA*	intron_variant nmd_transcript_variant
10	19596675	Ifngr1	rs262116476	A	AC*	intron_variant nmd_transcript_variant
10	19601519	Ifngr1	-	AGTGTGTGTG	AGTGT*	intron_variant nmd_transcript_variant upstream_gene_variant downstream_gene_variant
10	19603212	Ifngr1	4638730;rs23706	TAGATAGAT	C*	intron_variant nmd_transcript_variant upstream_gene_variant downstream_gene_variant
10	19608805	Ifngr1	-	ACACACACA	acacacac/tacaca	intron_variant
10	19608892	Ifngr1	-	TAC	TACAC	intron_variant
List of Structural variants						
Chr	Gene	Start	End	129S1_SvImJ		
10	Ifngr1	19604249	19604251	**insertion**		
List of SNPs						
Chr	Position	Gene	dbSNP	C57Bl/6J	129S1_SvImJ	Consequence
16	91547997	Ifngr2	rs4219190	T	A*	intron_variant nmd_transcript_variant
16	91548147	Ifngr2	rs4219191	A	T*	intron_variant nmd_transcript_variant
List of Insertions / deletions						
Chr	Position	Gene	dbSNP	C57Bl/6J	129S1_SvImJ	Consequence
16	91547987	Ifngr2	rs244865141	G	GT*	intron_variant nmd_transcript_variant
16	91554882	Ifngr2	rs262242221	A	AATTCAGT*	intron_variant nmd_transcript_variant

Supplementary Table 2.
Using Ensemble's Variant Predictor software, the following lists were generated with the biotypes mentioned. IMPACT: LOW = Assumed to be harmless. IMPACT: MODIFIER = Usually non-coding variants or variants affecting non-coding genes, where predictions are difficult or there is no evidence of impact.

Variant effect predictor results for list of SNPs							
#Uploaded_variation	Location	Allele	Consequence	IMPACT	SYMBOL	Feature_type	BIOTYPE
rs13467527	10:19592175-19592175	C	synonymous_variant	LOW	Ifngr1	Transcript	protein_coding
rs13467527	10:19592175-19592175	C	non_coding_transcript_exon_variant	MODIFIER	Ifngr1	Transcript	retained_intron
rs13467527	10:19592175-19592175	C	synonymous_variant,NMD_transcript_variant	LOW	Ifngr1	Transcript	nonsense_mediated_decay
rs13467527	10:19592175-19592175	C	non_coding_transcript_exon_variant	MODIFIER	Ifngr1	Transcript	processed_transcript
rs13467527	10:19592175-19592175	C	non_coding_transcript_exon_variant	MODIFIER	Ifngr1	Transcript	processed_transcript
rs13467527	10:19592175-19592175	C	regulatory_region_variant	MODIFIER	-	RegulatoryFeature	promoter
rs29336579	10:19592443-19592443	G	intron_variant	MODIFIER	Ifngr1	Transcript	protein_coding
rs29336579	10:19592443-19592443	G	intron_variant,non_coding_transcript_variant	MODIFIER	Ifngr1	Transcript	retained_intron
rs29336579	10:19592443-19592443	G	intron_variant,NMD_transcript_variant	MODIFIER	Ifngr1	Transcript	nonsense_mediated_decay
rs29336579	10:19592443-19592443	G	intron_variant,non_coding_transcript_variant	MODIFIER	Ifngr1	Transcript	processed_transcript
rs29336579	10:19592443-19592443	G	intron_variant,non_coding_transcript_variant	MODIFIER	Ifngr1	Transcript	processed_transcript
rs29336579	10:19592443-19592443	G	regulatory_region_variant	MODIFIER	-	RegulatoryFeature	promoter
rs29359700	10:19592450-19592450	G	intron_variant	MODIFIER	Ifngr1	Transcript	protein_coding
rs29359700	10:19592450-19592450	T	intron_variant	MODIFIER	Ifngr1	Transcript	protein_coding
rs29359700	10:19592450-19592450	G	intron_variant,non_coding_transcript_variant	MODIFIER	Ifngr1	Transcript	retained_intron
rs29359700	10:19592450-19592450	T	intron_variant,non_coding_transcript_variant	MODIFIER	Ifngr1	Transcript	retained_intron
rs29359700	10:19592450-19592450	G	intron_variant,NMD_transcript_variant	MODIFIER	Ifngr1	Transcript	nonsense_mediated_decay
rs29359700	10:19592450-19592450	T	intron_variant,NMD_transcript_variant	MODIFIER	Ifngr1	Transcript	nonsense_mediated_decay
rs29359700	10:19592450-19592450	G	intron_variant,non_coding_transcript_variant	MODIFIER	Ifngr1	Transcript	processed_transcript
rs29359700	10:19592450-19592450	T	intron_variant,non_coding_transcript_variant	MODIFIER	Ifngr1	Transcript	processed_transcript
rs29359700	10:19592450-19592450	G	intron_variant,non_coding_transcript_variant	MODIFIER	Ifngr1	Transcript	processed_transcript
rs29359700	10:19592450-19592450	T	intron_variant,non_coding_transcript_variant	MODIFIER	Ifngr1	Transcript	processed_transcript
rs29359700	10:19592450-19592450	G	regulatory_region_variant	MODIFIER	-	RegulatoryFeature	promoter
rs29359700	10:19592450-19592450	T	regulatory_region_variant	MODIFIER	-	RegulatoryFeature	promoter
rs29326407	10:19592459-19592459	T	intron_variant	MODIFIER	Ifngr1	Transcript	protein_coding
rs29326407	10:19592459-19592459	T	intron_variant,non_coding_transcript_variant	MODIFIER	Ifngr1	Transcript	retained_intron
rs29326407	10:19592459-19592459	T	intron_variant,NMD_transcript_variant	MODIFIER	Ifngr1	Transcript	nonsense_mediated_decay
rs29326407	10:19592459-19592459	T	intron_variant,non_coding_transcript_variant	MODIFIER	Ifngr1	Transcript	processed_transcript
rs29326407	10:19592459-19592459	T	intron_variant,non_coding_transcript_variant	MODIFIER	Ifngr1	Transcript	processed_transcript
rs29326407	10:19592459-19592459	T	regulatory_region_variant	MODIFIER	-	RegulatoryFeature	promoter
rs6307185	10:19592655-19592655	G	intron_variant	MODIFIER	Ifngr1	Transcript	protein_coding
rs6307185	10:19592655-19592655	G	intron_variant,non_coding_transcript_variant	MODIFIER	Ifngr1	Transcript	retained_intron
rs6307185	10:19592655-19592655	G	intron_variant,NMD_transcript_variant	MODIFIER	Ifngr1	Transcript	nonsense_mediated_decay
rs6307185	10:19592655-19592655	G	intron_variant,non_coding_transcript_variant	MODIFIER	Ifngr1	Transcript	processed_transcript
rs6307185	10:19592655-19592655	G	intron_variant,non_coding_transcript_variant	MODIFIER	Ifngr1	Transcript	processed_transcript
rs6307185	10:19592655-19592655	G	regulatory_region_variant	MODIFIER	-	RegulatoryFeature	promoter
rs6307192	10:19592660-19592660	G	intron_variant	MODIFIER	Ifngr1	Transcript	protein_coding
rs6307192	10:19592660-19592660	G	intron_variant,non_coding_transcript_variant	MODIFIER	Ifngr1	Transcript	retained_intron
rs6307192	10:19592660-19592660	G	intron_variant,NMD_transcript_variant	MODIFIER	Ifngr1	Transcript	nonsense_mediated_decay
rs6307192	10:19592660-19592660	G	intron_variant,non_coding_transcript_variant	MODIFIER	Ifngr1	Transcript	processed_transcript
rs6307192	10:19592660-19592660	G	intron_variant,non_coding_transcript_variant	MODIFIER	Ifngr1	Transcript	processed_transcript
rs6307192	10:19592660-19592660	G	regulatory_region_variant	MODIFIER	-	RegulatoryFeature	promoter
rs3681091	10:19592707-19592707	G	intron_variant	MODIFIER	Ifngr1	Transcript	protein_coding
rs3681091	10:19592707-19592707	G	intron_variant,non_coding_transcript_variant	MODIFIER	Ifngr1	Transcript	retained_intron
rs3681091	10:19592707-19592707	G	intron_variant,NMD_transcript_variant	MODIFIER	Ifngr1	Transcript	nonsense_mediated_decay
rs3681091	10:19592707-19592707	G	intron_variant,non_coding_transcript_variant	MODIFIER	Ifngr1	Transcript	processed_transcript
rs3681091	10:19592707-19592707	G	intron_variant,non_coding_transcript_variant	MODIFIER	Ifngr1	Transcript	processed_transcript
rs3681091	10:19592707-19592707	G	regulatory_region_variant	MODIFIER	-	RegulatoryFeature	promoter
rs29372567	10:19593773-19593773	G	intron_variant	MODIFIER	Ifngr1	Transcript	protein_coding
rs29372567	10:19593773-19593773	G	intron_variant,non_coding_transcript_variant	MODIFIER	Ifngr1	Transcript	retained_intron
rs29372567	10:19593773-19593773	G	intron_variant,NMD_transcript_variant	MODIFIER	Ifngr1	Transcript	nonsense_mediated_decay
rs29372567	10:19593773-19593773	G	intron_variant,non_coding_transcript_variant	MODIFIER	Ifngr1	Transcript	processed_transcript
rs29372567	10:19593773-19593773	G	intron_variant,non_coding_transcript_variant	MODIFIER	Ifngr1	Transcript	processed_transcript
rs29372567	10:19593773-19593773	G	regulatory_region_variant	MODIFIER	-	RegulatoryFeature	promoter
rs233513847	10:19594032-19594032	T	intron_variant	MODIFIER	Ifngr1	Transcript	protein_coding
rs233513847	10:19594032-19594032	T	intron_variant,non_coding_transcript_variant	MODIFIER	Ifngr1	Transcript	retained_intron
rs233513847	10:19594032-19594032	T	intron_variant,NMD_transcript_variant	MODIFIER	Ifngr1	Transcript	nonsense_mediated_decay
rs233513847	10:19594032-19594032	T	intron_variant,non_coding_transcript_variant	MODIFIER	Ifngr1	Transcript	processed_transcript
rs233513847	10:19594032-19594032	T	intron_variant,non_coding_transcript_variant	MODIFIER	Ifngr1	Transcript	processed_transcript
rs233513847	10:19594032-19594032	T	regulatory_region_variant	MODIFIER	-	RegulatoryFeature	promoter
rs579458786	10:19595816-19595816	A	intron_variant	MODIFIER	Ifngr1	Transcript	protein_coding
rs579458786	10:19595816-19595816	A	intron_variant,non_coding_transcript_variant	MODIFIER	Ifngr1	Transcript	retained_intron
rs579458786	10:19595816-19595816	A	intron_variant,NMD_transcript_variant	MODIFIER	Ifngr1	Transcript	nonsense_mediated_decay
rs579458786	10:19595816-19595816	A	intron_variant,non_coding_transcript_variant	MODIFIER	Ifngr1	Transcript	processed_transcript
rs579458786	10:19595816-19595816	A	intron_variant,non_coding_transcript_variant	MODIFIER	Ifngr1	Transcript	processed_transcript
rs4137440	10:19595858-19595858	T	intron_variant	MODIFIER	Ifngr1	Transcript	protein_coding
rs4137440	10:19595858-19595858	T	intron_variant,non_coding_transcript_variant	MODIFIER	Ifngr1	Transcript	retained_intron
rs4137440	10:19595858-19595858	T	intron_variant,NMD_transcript_variant	MODIFIER	Ifngr1	Transcript	nonsense_mediated_decay
rs4137440	10:19595858-19595858	T	intron_variant,non_coding_transcript_variant	MODIFIER	Ifngr1	Transcript	processed_transcript
rs4137440	10:19595858-19595858	T	intron_variant,non_coding_transcript_variant	MODIFIER	Ifngr1	Transcript	processed_transcript
rs254189437	10:19596087-19596087	C	intron_variant	MODIFIER	Ifngr1	Transcript	protein_coding
rs254189437	10:19596087-19596087	C	intron_variant,non_coding_transcript_variant	MODIFIER	Ifngr1	Transcript	retained_intron
rs254189437	10:19596087-19596087	C	intron_variant,NMD_transcript_variant	MODIFIER	Ifngr1	Transcript	nonsense_mediated_decay
rs254189437	10:19596087-19596087	C	intron_variant,non_coding_transcript_variant	MODIFIER	Ifngr1	Transcript	processed_transcript
rs254189437	10:19596087-19596087	C	intron_variant,non_coding_transcript_variant	MODIFIER	Ifngr1	Transcript	processed_transcript
rs254189437	10:19596087-19596087	C	regulatory_region_variant	MODIFIER	-	RegulatoryFeature	promoter_flanking_region
rs266214047	10:19596137-19596137	C	intron_variant	MODIFIER	Ifngr1	Transcript	protein_coding
rs266214047	10:19596137-19596137	C	intron_variant,non_coding_transcript_variant	MODIFIER	Ifngr1	Transcript	retained_intron
rs266214047	10:19596137-19596137	C	intron_variant,NMD_transcript_variant	MODIFIER	Ifngr1	Transcript	nonsense_mediated_decay
rs266214047	10:19596137-19596137	C	intron_variant,non_coding_transcript_variant	MODIFIER	Ifngr1	Transcript	processed_transcript
rs266214047	10:19596137-19596137	C	intron_variant,non_coding_transcript_variant	MODIFIER	Ifngr1	Transcript	processed_transcript
rs266214047	10:19596137-19596137	C	regulatory_region_variant	MODIFIER	-	RegulatoryFeature	promoter_flanking_region
rs229060147	10:19596216-19596216	G	intron_variant	MODIFIER	Ifngr1	Transcript	protein_coding
rs229060147	10:19596216-19596216	G	intron_variant,non_coding_transcript_variant	MODIFIER	Ifngr1	Transcript	retained_intron
rs229060147	10:19596216-19596216	G	intron_variant,NMD_transcript_variant	MODIFIER	Ifngr1	Transcript	nonsense_mediated_decay
rs229060147	10:19596216-19596216	G	intron_variant,non_coding_transcript_variant	MODIFIER	Ifngr1	Transcript	processed_transcript
rs229060147	10:19596216-19596216	G	intron_variant,non_coding_transcript_variant	MODIFIER	Ifngr1	Transcript	processed_transcript
rs229060147	10:19596216-19596216	G	regulatory_region_variant	MODIFIER	-	RegulatoryFeature	promoter_flanking_region
rs243297678	10:19596224-19596224	G	intron_variant	MODIFIER	Ifngr1	Transcript	protein_coding
rs243297678	10:19596224-19596224	G	intron_variant,non_coding_transcript_variant	MODIFIER	Ifngr1	Transcript	retained_intron
rs243297678	10:19596224-19596224	G	intron_variant,NMD_transcript_variant	MODIFIER	Ifngr1	Transcript	nonsense_mediated_decay
rs243297678	10:19596224-19596224	G	intron_variant,non_coding_transcript_variant	MODIFIER	Ifngr1	Transcript	processed_transcript
rs243297678	10:19596224-19596224	G	intron_variant,non_coding_transcript_variant	MODIFIER	Ifngr1	Transcript	processed_transcript
rs243297678	10:19596224-19596224	G	regulatory_region_variant	MODIFIER	-	RegulatoryFeature	promoter_flanking_region
rs212570699	10:19596247-19596247	G	intron_variant	MODIFIER	Ifngr1	Transcript	protein_coding
rs212570699	10:19596247-19596247	G	intron_variant,non_coding_transcript_variant	MODIFIER	Ifngr1	Transcript	retained_intron
rs212570699	10:19596247-19596247	G	intron_variant,NMD_transcript_variant	MODIFIER	Ifngr1	Transcript	nonsense_mediated_decay
rs212570699	10:19596247-19596247	G	intron_variant,non_coding_transcript_variant	MODIFIER	Ifngr1	Transcript	processed_transcript

Supplementary Table 2 (Contd.)

Variant effect predictor results for list of SNPs							
#Uploaded_variation	Location	Allele	Consequence	IMPACT	SYMBOL	Feature_type	BIOTYPE
rs212570699	10:19596247-19596247	G	intron_variant,non_coding_transcript_variant	MODIFIER	Ifngr1	Transcript	processed_transcript
rs212570699	10:19596247-19596247	G	regulatory_region_variant	MODIFIER	-	RegulatoryFeature	promoter_flanking_region
rs231296450	10:19596335-19596335	T	intron_variant	MODIFIER	Ifngr1	Transcript	protein_coding
rs231296450	10:19596335-19596335	T	intron_variant,non_coding_transcript_variant	MODIFIER	Ifngr1	Transcript	retained_intron
rs231296450	10:19596335-19596335	T	intron_variant,NMD_transcript_variant	MODIFIER	Ifngr1	Transcript	nonsense_mediated_decay
rs231296450	10:19596335-19596335	T	intron_variant,non_coding_transcript_variant	MODIFIER	Ifngr1	Transcript	processed_transcript
rs231296450	10:19596335-19596335	T	intron_variant,non_coding_transcript_variant	MODIFIER	Ifngr1	Transcript	processed_transcript
rs231296450	10:19596335-19596335	T	regulatory_region_variant	MODIFIER	-	RegulatoryFeature	promoter_flanking_region
rs255829360	10:19596343-19596343	C	intron_variant	MODIFIER	Ifngr1	Transcript	protein_coding
rs255829360	10:19596343-19596343	C	intron_variant,non_coding_transcript_variant	MODIFIER	Ifngr1	Transcript	retained_intron
rs255829360	10:19596343-19596343	C	intron_variant,NMD_transcript_variant	MODIFIER	Ifngr1	Transcript	nonsense_mediated_decay
rs255829360	10:19596343-19596343	C	intron_variant,non_coding_transcript_variant	MODIFIER	Ifngr1	Transcript	processed_transcript
rs255829360	10:19596343-19596343	C	intron_variant,non_coding_transcript_variant	MODIFIER	Ifngr1	Transcript	processed_transcript
rs255829360	10:19596343-19596343	C	regulatory_region_variant	MODIFIER	-	RegulatoryFeature	promoter_flanking_region
rs243554315	10:19596381-19596381	A	intron_variant	MODIFIER	Ifngr1	Transcript	protein_coding
rs243554315	10:19596381-19596381	A	intron_variant,non_coding_transcript_variant	MODIFIER	Ifngr1	Transcript	retained_intron
rs243554315	10:19596381-19596381	A	intron_variant,NMD_transcript_variant	MODIFIER	Ifngr1	Transcript	nonsense_mediated_decay
rs243554315	10:19596381-19596381	A	intron_variant,non_coding_transcript_variant	MODIFIER	Ifngr1	Transcript	processed_transcript
rs243554315	10:19596381-19596381	A	intron_variant,non_coding_transcript_variant	MODIFIER	Ifngr1	Transcript	processed_transcript
rs243554315	10:19596381-19596381	A	regulatory_region_variant	MODIFIER	-	RegulatoryFeature	promoter_flanking_region
rs29315942	10:19598124-19598124	C	intron_variant	MODIFIER	Ifngr1	Transcript	protein_coding
rs29315942	10:19598124-19598124	G	intron_variant	MODIFIER	Ifngr1	Transcript	protein_coding
rs29315942	10:19598124-19598124	C	downstream_gene_variant	MODIFIER	Ifngr1	Transcript	retained_intron
rs29315942	10:19598124-19598124	G	downstream_gene_variant	MODIFIER	Ifngr1	Transcript	retained_intron
rs29315942	10:19598124-19598124	C	intron_variant,NMD_transcript_variant	MODIFIER	Ifngr1	Transcript	nonsense_mediated_decay
rs29315942	10:19598124-19598124	G	intron_variant,NMD_transcript_variant	MODIFIER	Ifngr1	Transcript	nonsense_mediated_decay
rs29315942	10:19598124-19598124	C	intron_variant,non_coding_transcript_variant	MODIFIER	Ifngr1	Transcript	processed_transcript
rs29315942	10:19598124-19598124	G	intron_variant,non_coding_transcript_variant	MODIFIER	Ifngr1	Transcript	processed_transcript
rs29315942	10:19598124-19598124	C	intron_variant,non_coding_transcript_variant	MODIFIER	Ifngr1	Transcript	processed_transcript
rs29315942	10:19598124-19598124	G	intron_variant,non_coding_transcript_variant	MODIFIER	Ifngr1	Transcript	processed_transcript
rs29315942	10:19598124-19598124	C	regulatory_region_variant	MODIFIER	-	RegulatoryFeature	promoter_flanking_region
rs29315942	10:19598124-19598124	G	regulatory_region_variant	MODIFIER	-	RegulatoryFeature	promoter_flanking_region
rs226986894	10:19598146-19598146	T	intron_variant	MODIFIER	Ifngr1	Transcript	protein_coding
rs226986894	10:19598146-19598146	T	downstream_gene_variant	MODIFIER	Ifngr1	Transcript	retained_intron
rs226986894	10:19598146-19598146	T	intron_variant,NMD_transcript_variant	MODIFIER	Ifngr1	Transcript	nonsense_mediated_decay
rs226986894	10:19598146-19598146	T	intron_variant,non_coding_transcript_variant	MODIFIER	Ifngr1	Transcript	processed_transcript
rs226986894	10:19598146-19598146	T	intron_variant,non_coding_transcript_variant	MODIFIER	Ifngr1	Transcript	processed_transcript
rs226986894	10:19598146-19598146	T	regulatory_region_variant	MODIFIER	-	RegulatoryFeature	promoter_flanking_region
rs230183849	10:19598171-19598171	C	intron_variant	MODIFIER	Ifngr1	Transcript	protein_coding
rs230183849	10:19598171-19598171	C	downstream_gene_variant	MODIFIER	Ifngr1	Transcript	retained_intron
rs230183849	10:19598171-19598171	C	intron_variant,NMD_transcript_variant	MODIFIER	Ifngr1	Transcript	nonsense_mediated_decay
rs230183849	10:19598171-19598171	C	intron_variant,non_coding_transcript_variant	MODIFIER	Ifngr1	Transcript	processed_transcript
rs230183849	10:19598171-19598171	C	intron_variant,non_coding_transcript_variant	MODIFIER	Ifngr1	Transcript	processed_transcript
rs230183849	10:19598171-19598171	C	regulatory_region_variant	MODIFIER	-	RegulatoryFeature	promoter_flanking_region
rs249047138	10:19598174-19598174	G	intron_variant	MODIFIER	Ifngr1	Transcript	protein_coding
rs249047138	10:19598174-19598174	G	downstream_gene_variant	MODIFIER	Ifngr1	Transcript	retained_intron
rs249047138	10:19598174-19598174	G	intron_variant,NMD_transcript_variant	MODIFIER	Ifngr1	Transcript	nonsense_mediated_decay
rs249047138	10:19598174-19598174	G	intron_variant,non_coding_transcript_variant	MODIFIER	Ifngr1	Transcript	processed_transcript
rs249047138	10:19598174-19598174	G	intron_variant,non_coding_transcript_variant	MODIFIER	Ifngr1	Transcript	processed_transcript
rs249047138	10:19598174-19598174	G	regulatory_region_variant	MODIFIER	-	RegulatoryFeature	promoter_flanking_region
rs51633668	10:19598553-19598553	A	intron_variant	MODIFIER	Ifngr1	Transcript	protein_coding
rs51633668	10:19598553-19598553	G	intron_variant	MODIFIER	Ifngr1	Transcript	protein_coding
rs51633668	10:19598553-19598553	A	downstream_gene_variant	MODIFIER	Ifngr1	Transcript	retained_intron
rs51633668	10:19598553-19598553	G	downstream_gene_variant	MODIFIER	Ifngr1	Transcript	retained_intron
rs51633668	10:19598553-19598553	A	intron_variant,NMD_transcript_variant	MODIFIER	Ifngr1	Transcript	nonsense_mediated_decay
rs51633668	10:19598553-19598553	G	intron_variant,NMD_transcript_variant	MODIFIER	Ifngr1	Transcript	nonsense_mediated_decay
rs51633668	10:19598553-19598553	A	intron_variant,non_coding_transcript_variant	MODIFIER	Ifngr1	Transcript	processed_transcript
rs51633668	10:19598553-19598553	G	intron_variant,non_coding_transcript_variant	MODIFIER	Ifngr1	Transcript	processed_transcript
rs51633668	10:19598553-19598553	A	intron_variant,non_coding_transcript_variant	MODIFIER	Ifngr1	Transcript	processed_transcript
rs51633668	10:19598553-19598553	G	intron_variant,non_coding_transcript_variant	MODIFIER	Ifngr1	Transcript	processed_transcript
rs51633668	10:19598553-19598553	A	regulatory_region_variant	MODIFIER	-	RegulatoryFeature	promoter_flanking_region
rs51633668	10:19598553-19598553	G	regulatory_region_variant	MODIFIER	-	RegulatoryFeature	promoter_flanking_region
rs48059797	10:19598662-19598662	T	intron_variant	MODIFIER	Ifngr1	Transcript	protein_coding
rs48059797	10:19598662-19598662	T	downstream_gene_variant	MODIFIER	Ifngr1	Transcript	retained_intron
rs48059797	10:19598662-19598662	T	intron_variant,NMD_transcript_variant	MODIFIER	Ifngr1	Transcript	nonsense_mediated_decay
rs48059797	10:19598662-19598662	T	intron_variant,non_coding_transcript_variant	MODIFIER	Ifngr1	Transcript	processed_transcript
rs48059797	10:19598662-19598662	T	intron_variant,non_coding_transcript_variant	MODIFIER	Ifngr1	Transcript	processed_transcript
rs48059797	10:19598662-19598662	T	regulatory_region_variant	MODIFIER	-	RegulatoryFeature	promoter_flanking_region
rs51862239	10:19598725-19598725	T	intron_variant	MODIFIER	Ifngr1	Transcript	protein_coding
rs51862239	10:19598725-19598725	T	downstream_gene_variant	MODIFIER	Ifngr1	Transcript	retained_intron
rs51862239	10:19598725-19598725	T	intron_variant,NMD_transcript_variant	MODIFIER	Ifngr1	Transcript	nonsense_mediated_decay
rs51862239	10:19598725-19598725	T	intron_variant,non_coding_transcript_variant	MODIFIER	Ifngr1	Transcript	processed_transcript
rs51862239	10:19598725-19598725	T	intron_variant,non_coding_transcript_variant	MODIFIER	Ifngr1	Transcript	processed_transcript
rs51862239	10:19598725-19598725	T	regulatory_region_variant	MODIFIER	-	RegulatoryFeature	promoter_flanking_region
rs29377033	10:19598855-19598855	G	intron_variant	MODIFIER	Ifngr1	Transcript	protein_coding
rs29377033	10:19598855-19598855	G	downstream_gene_variant	MODIFIER	Ifngr1	Transcript	retained_intron
rs29377033	10:19598855-19598855	G	intron_variant,NMD_transcript_variant	MODIFIER	Ifngr1	Transcript	nonsense_mediated_decay
rs29377033	10:19598855-19598855	G	intron_variant,non_coding_transcript_variant	MODIFIER	Ifngr1	Transcript	processed_transcript
rs29377033	10:19598855-19598855	G	intron_variant,non_coding_transcript_variant	MODIFIER	Ifngr1	Transcript	processed_transcript
rs29377033	10:19598855-19598855	G	regulatory_region_variant	MODIFIER	-	RegulatoryFeature	promoter_flanking_region
rs224452593	10:19598942-19598942	G	intron_variant	MODIFIER	Ifngr1	Transcript	protein_coding
rs224452593	10:19598942-19598942	G	downstream_gene_variant	MODIFIER	Ifngr1	Transcript	retained_intron
rs224452593	10:19598942-19598942	G	intron_variant,NMD_transcript_variant	MODIFIER	Ifngr1	Transcript	nonsense_mediated_decay
rs224452593	10:19598942-19598942	G	intron_variant,non_coding_transcript_variant	MODIFIER	Ifngr1	Transcript	processed_transcript
rs224452593	10:19598942-19598942	G	intron_variant,non_coding_transcript_variant	MODIFIER	Ifngr1	Transcript	processed_transcript
rs224452593	10:19598942-19598942	G	regulatory_region_variant	MODIFIER	-	RegulatoryFeature	promoter_flanking_region
rs244512522	10:19599043-19599043	C	intron_variant	MODIFIER	Ifngr1	Transcript	protein_coding
rs244512522	10:19599043-19599043	C	downstream_gene_variant	MODIFIER	Ifngr1	Transcript	retained_intron
rs244512522	10:19599043-19599043	C	intron_variant,NMD_transcript_variant	MODIFIER	Ifngr1	Transcript	nonsense_mediated_decay
rs244512522	10:19599043-19599043	C	non_coding_transcript_exon_variant	MODIFIER	Ifngr1	Transcript	processed_transcript
rs244512522	10:19599043-19599043	C	intron_variant,non_coding_transcript_variant	MODIFIER	Ifngr1	Transcript	processed_transcript
rs244512522	10:19599043-19599043	C	regulatory_region_variant	MODIFIER	-	RegulatoryFeature	promoter_flanking_region
rs29347154	10:19600149-19600149	G	intron_variant	MODIFIER	Ifngr1	Transcript	protein_coding
rs29347154	10:19600149-19600149	G	downstream_gene_variant	MODIFIER	Ifngr1	Transcript	retained_intron
rs29347154	10:19600149-19600149	G	intron_variant,NMD_transcript_variant	MODIFIER	Ifngr1	Transcript	nonsense_mediated_decay
rs29347154	10:19600149-19600149	G	intron_variant,non_coding_transcript_variant	MODIFIER	Ifngr1	Transcript	processed_transcript
rs29347154	10:19600149-19600149	G	intron_variant,non_coding_transcript_variant	MODIFIER	Ifngr1	Transcript	processed_transcript
rs251194780	10:19600402-19600402	G	intron_variant	MODIFIER	Ifngr1	Transcript	protein_coding

Supplementary Table 2 (Contd.)

Variant effect predictor results for list of SNPs							
#Uploaded_variation	Location	Allele	Consequence	IMPACT	SYMBOL	Feature_type	BIOTYPE
rs251194780	10:19600402-19600402	G	downstream_gene_variant	MODIFIER	Ifngr1	Transcript	retained_intron
rs251194780	10:19600402-19600402	G	intron_variant,NMD_transcript_variant	MODIFIER	Ifngr1	Transcript	nonsense_mediated_decay
rs251194780	10:19600402-19600402	G	intron_variant,non_coding_transcript_variant	MODIFIER	Ifngr1	Transcript	processed_transcript
rs251194780	10:19600402-19600402	G	intron_variant,non_coding_transcript_variant	MODIFIER	Ifngr1	Transcript	processed_transcript
rs215768634	10:19600562-19600562	A	intron_variant	MODIFIER	Ifngr1	Transcript	protein_coding
rs215768634	10:19600562-19600562	G	intron_variant	MODIFIER	Ifngr1	Transcript	protein_coding
rs215768634	10:19600562-19600562	A	downstream_gene_variant	MODIFIER	Ifngr1	Transcript	retained_intron
rs215768634	10:19600562-19600562	G	downstream_gene_variant	MODIFIER	Ifngr1	Transcript	retained_intron
rs215768634	10:19600562-19600562	A	intron_variant,NMD_transcript_variant	MODIFIER	Ifngr1	Transcript	nonsense_mediated_decay
rs215768634	10:19600562-19600562	G	intron_variant,NMD_transcript_variant	MODIFIER	Ifngr1	Transcript	nonsense_mediated_decay
rs215768634	10:19600562-19600562	A	intron_variant,non_coding_transcript_variant	MODIFIER	Ifngr1	Transcript	processed_transcript
rs215768634	10:19600562-19600562	G	intron_variant,non_coding_transcript_variant	MODIFIER	Ifngr1	Transcript	processed_transcript
rs215768634	10:19600562-19600562	A	intron_variant,non_coding_transcript_variant	MODIFIER	Ifngr1	Transcript	processed_transcript
rs215768634	10:19600562-19600562	G	intron_variant,non_coding_transcript_variant	MODIFIER	Ifngr1	Transcript	processed_transcript
rs238697052	10:19600850-19600850	A	intron_variant	MODIFIER	Ifngr1	Transcript	protein_coding
rs238697052	10:19600850-19600850	A	downstream_gene_variant	MODIFIER	Ifngr1	Transcript	retained_intron
rs238697052	10:19600850-19600850	A	intron_variant,NMD_transcript_variant	MODIFIER	Ifngr1	Transcript	nonsense_mediated_decay
rs238697052	10:19600850-19600850	A	intron_variant,non_coding_transcript_variant	MODIFIER	Ifngr1	Transcript	processed_transcript
rs238697052	10:19600850-19600850	A	intron_variant,non_coding_transcript_variant	MODIFIER	Ifngr1	Transcript	processed_transcript
rs49603673	10:19601201-19601201	C	intron_variant	MODIFIER	Ifngr1	Transcript	protein_coding
rs49603673	10:19601201-19601201	C	downstream_gene_variant	MODIFIER	Ifngr1	Transcript	retained_intron
rs49603673	10:19601201-19601201	C	intron_variant,NMD_transcript_variant	MODIFIER	Ifngr1	Transcript	nonsense_mediated_decay
rs49603673	10:19601201-19601201	C	upstream_gene_variant	MODIFIER	Ifngr1	Transcript	retained_intron
rs49603673	10:19601201-19601201	C	intron_variant,non_coding_transcript_variant	MODIFIER	Ifngr1	Transcript	processed_transcript
rs49603673	10:19601201-19601201	C	intron_variant,non_coding_transcript_variant	MODIFIER	Ifngr1	Transcript	processed_transcript
rs46637409	10:19601502-19601502	C	intron_variant	MODIFIER	Ifngr1	Transcript	protein_coding
rs46637409	10:19601502-19601502	C	downstream_gene_variant	MODIFIER	Ifngr1	Transcript	retained_intron
rs46637409	10:19601502-19601502	C	intron_variant,NMD_transcript_variant	MODIFIER	Ifngr1	Transcript	nonsense_mediated_decay
rs46637409	10:19601502-19601502	C	upstream_gene_variant	MODIFIER	Ifngr1	Transcript	retained_intron
rs46637409	10:19601502-19601502	C	downstream_gene_variant	MODIFIER	Ifngr1	Transcript	processed_transcript
rs46637409	10:19601502-19601502	C	intron_variant,non_coding_transcript_variant	MODIFIER	Ifngr1	Transcript	processed_transcript
rs46637409	10:19601502-19601502	C	regulatory_region_variant	MODIFIER	-	RegulatoryFeature	CTCF_binding_site
rs46637409	10:19601502-19601502	C	regulatory_region_variant	MODIFIER	-	RegulatoryFeature	promoter_flanking_region
rs46104437	10:19602080-19602080	A	intron_variant	MODIFIER	Ifngr1	Transcript	protein_coding
rs46104437	10:19602080-19602080	A	downstream_gene_variant	MODIFIER	Ifngr1	Transcript	retained_intron
rs46104437	10:19602080-19602080	A	intron_variant,NMD_transcript_variant	MODIFIER	Ifngr1	Transcript	nonsense_mediated_decay
rs46104437	10:19602080-19602080	A	upstream_gene_variant	MODIFIER	Ifngr1	Transcript	retained_intron
rs46104437	10:19602080-19602080	A	downstream_gene_variant	MODIFIER	Ifngr1	Transcript	processed_transcript
rs46104437	10:19602080-19602080	A	intron_variant,non_coding_transcript_variant	MODIFIER	Ifngr1	Transcript	processed_transcript
rs29320505	10:19602364-19602364	T	intron_variant	MODIFIER	Ifngr1	Transcript	protein_coding
rs29320505	10:19602364-19602364	T	downstream_gene_variant	MODIFIER	Ifngr1	Transcript	retained_intron
rs29320505	10:19602364-19602364	T	intron_variant,NMD_transcript_variant	MODIFIER	Ifngr1	Transcript	nonsense_mediated_decay
rs29320505	10:19602364-19602364	T	upstream_gene_variant	MODIFIER	Ifngr1	Transcript	retained_intron
rs29320505	10:19602364-19602364	T	downstream_gene_variant	MODIFIER	Ifngr1	Transcript	processed_transcript
rs29320505	10:19602364-19602364	T	intron_variant,non_coding_transcript_variant	MODIFIER	Ifngr1	Transcript	processed_transcript
rs29359910	10:19602459-19602459	G	intron_variant	MODIFIER	Ifngr1	Transcript	protein_coding
rs29359910	10:19602459-19602459	G	downstream_gene_variant	MODIFIER	Ifngr1	Transcript	retained_intron
rs29359910	10:19602459-19602459	G	intron_variant,NMD_transcript_variant	MODIFIER	Ifngr1	Transcript	nonsense_mediated_decay
rs29359910	10:19602459-19602459	G	upstream_gene_variant	MODIFIER	Ifngr1	Transcript	retained_intron
rs29359910	10:19602459-19602459	G	downstream_gene_variant	MODIFIER	Ifngr1	Transcript	processed_transcript
rs29359910	10:19602459-19602459	G	intron_variant,non_coding_transcript_variant	MODIFIER	Ifngr1	Transcript	processed_transcript
rs29331763	10:19602599-19602599	T	intron_variant	MODIFIER	Ifngr1	Transcript	protein_coding
rs29331763	10:19602599-19602599	T	downstream_gene_variant	MODIFIER	Ifngr1	Transcript	retained_intron
rs29331763	10:19602599-19602599	T	intron_variant,NMD_transcript_variant	MODIFIER	Ifngr1	Transcript	nonsense_mediated_decay
rs29331763	10:19602599-19602599	T	upstream_gene_variant	MODIFIER	Ifngr1	Transcript	retained_intron
rs29331763	10:19602599-19602599	T	downstream_gene_variant	MODIFIER	Ifngr1	Transcript	processed_transcript
rs29331763	10:19602599-19602599	T	intron_variant,non_coding_transcript_variant	MODIFIER	Ifngr1	Transcript	processed_transcript
rs3702815	10:19603365-19603365	G	intron_variant	MODIFIER	Ifngr1	Transcript	protein_coding
rs3702815	10:19603365-19603365	G	intron_variant,NMD_transcript_variant	MODIFIER	Ifngr1	Transcript	nonsense_mediated_decay
rs3702815	10:19603365-19603365	G	upstream_gene_variant	MODIFIER	Ifngr1	Transcript	retained_intron
rs3702815	10:19603365-19603365	G	downstream_gene_variant	MODIFIER	Ifngr1	Transcript	processed_transcript
rs3702815	10:19603365-19603365	G	intron_variant,non_coding_transcript_variant	MODIFIER	Ifngr1	Transcript	processed_transcript
rs3702815	10:19603365-19603365	G	regulatory_region_variant	MODIFIER	-	RegulatoryFeature	open_chromatin_region
rs29327973	10:19603572-19603572	G	intron_variant	MODIFIER	Ifngr1	Transcript	protein_coding
rs29327973	10:19603572-19603572	G	intron_variant,NMD_transcript_variant	MODIFIER	Ifngr1	Transcript	nonsense_mediated_decay
rs29327973	10:19603572-19603572	G	upstream_gene_variant	MODIFIER	Ifngr1	Transcript	retained_intron
rs29327973	10:19603572-19603572	G	downstream_gene_variant	MODIFIER	Ifngr1	Transcript	processed_transcript
rs29327973	10:19603572-19603572	G	intron_variant,non_coding_transcript_variant	MODIFIER	Ifngr1	Transcript	processed_transcript
rs29316518	10:19603711-19603711	C	intron_variant	MODIFIER	Ifngr1	Transcript	protein_coding
rs29316518	10:19603711-19603711	C	intron_variant,NMD_transcript_variant	MODIFIER	Ifngr1	Transcript	nonsense_mediated_decay
rs29316518	10:19603711-19603711	C	upstream_gene_variant	MODIFIER	Ifngr1	Transcript	retained_intron
rs29316518	10:19603711-19603711	C	downstream_gene_variant	MODIFIER	Ifngr1	Transcript	processed_transcript
rs29316518	10:19603711-19603711	C	intron_variant,non_coding_transcript_variant	MODIFIER	Ifngr1	Transcript	processed_transcript
rs29323906	10:19604014-19604014	G	intron_variant	MODIFIER	Ifngr1	Transcript	protein_coding
rs29323906	10:19604014-19604014	G	downstream_gene_variant	MODIFIER	Ifngr1	Transcript	nonsense_mediated_decay
rs29323906	10:19604014-19604014	G	upstream_gene_variant	MODIFIER	Ifngr1	Transcript	retained_intron
rs29323906	10:19604014-19604014	G	downstream_gene_variant	MODIFIER	Ifngr1	Transcript	processed_transcript
rs29323906	10:19604014-19604014	G	downstream_gene_variant	MODIFIER	Ifngr1	Transcript	processed_transcript
rs29324397	10:19604695-19604695	G	intron_variant	MODIFIER	Ifngr1	Transcript	protein_coding
rs29324397	10:19604695-19604695	G	downstream_gene_variant	MODIFIER	Ifngr1	Transcript	nonsense_mediated_decay
rs29324397	10:19604695-19604695	G	upstream_gene_variant	MODIFIER	Ifngr1	Transcript	retained_intron
rs29324397	10:19604695-19604695	G	downstream_gene_variant	MODIFIER	Ifngr1	Transcript	processed_transcript
rs29324397	10:19604695-19604695	G	downstream_gene_variant	MODIFIER	Ifngr1	Transcript	processed_transcript
rs29346781	10:19605570-19605570	G	intron_variant	MODIFIER	Ifngr1	Transcript	protein_coding
rs29346781	10:19605570-19605570	G	downstream_gene_variant	MODIFIER	Ifngr1	Transcript	nonsense_mediated_decay
rs29346781	10:19605570-19605570	G	upstream_gene_variant	MODIFIER	Ifngr1	Transcript	retained_intron
rs29346781	10:19605570-19605570	G	downstream_gene_variant	MODIFIER	Ifngr1	Transcript	processed_transcript
rs29346781	10:19605570-19605570	G	downstream_gene_variant	MODIFIER	Ifngr1	Transcript	processed_transcript
rs3691292	10:19606638-19606638	A	intron_variant	MODIFIER	Ifngr1	Transcript	protein_coding
rs3691292	10:19606638-19606638	A	downstream_gene_variant	MODIFIER	Ifngr1	Transcript	nonsense_mediated_decay
rs3691292	10:19606638-19606638	A	intron_variant,non_coding_transcript_variant	MODIFIER	Ifngr1	Transcript	retained_intron
rs3691292	10:19606638-19606638	A	downstream_gene_variant	MODIFIER	Ifngr1	Transcript	processed_transcript
rs29323743	10:19609070-19609070	T	intron_variant	MODIFIER	Ifngr1	Transcript	protein_coding
rs29323743	10:19609070-19609070	T	intron_variant,non_coding_transcript_variant	MODIFIER	Ifngr1	Transcript	retained_intron

Supplementary Table 2 (Contd.)

Variant effect predictor results for list of insertions/deletions							
#Uploaded_variation	Location	Allele	Consequence	IMPACT	SYMBOL	Feature_type	BIOTYPE
rs228443125	10:19592031-19592036	-	5_prime_UTR_variant	MODIFIER	Ifngr1	Transcript	protein_coding
rs228443125	10:19592031-19592036	-	non_coding_transcript_exon_variant	MODIFIER	Ifngr1	Transcript	retained_intron
rs228443125	10:19592031-19592036	-	5_prime_UTR_variant,NMD_transcript_variant	MODIFIER	Ifngr1	Transcript	nonsense_mediated_decay
rs228443125	10:19592031-19592036	-	upstream_gene_variant	MODIFIER	Ifngr1	Transcript	processed_transcript
rs228443125	10:19592031-19592036	-	upstream_gene_variant	MODIFIER	Ifngr1	Transcript	processed_transcript
rs228443125	10:19592031-19592036	-	regulatory_region_variant	MODIFIER	-	RegulatoryFeature	promoter
rs214343522	10:19592502-19592506	-	intron_variant	MODIFIER	Ifngr1	Transcript	protein_coding
rs214343522	10:19592502-19592506	-	intron_variant,non_coding_transcript_variant	MODIFIER	Ifngr1	Transcript	retained_intron
rs214343522	10:19592502-19592506	-	intron_variant,NMD_transcript_variant	MODIFIER	Ifngr1	Transcript	nonsense_mediated_decay
rs214343522	10:19592502-19592506	-	intron_variant,non_coding_transcript_variant	MODIFIER	Ifngr1	Transcript	processed_transcript
rs214343522	10:19592502-19592506	-	intron_variant,non_coding_transcript_variant	MODIFIER	Ifngr1	Transcript	processed_transcript
rs214343522	10:19592502-19592506	-	regulatory_region_variant	MODIFIER	-	RegulatoryFeature	promoter
rs237129992	10:19594311-19594312	-	intron_variant	MODIFIER	Ifngr1	Transcript	protein_coding
rs237129992	10:19594311-19594312	-	intron_variant,non_coding_transcript_variant	MODIFIER	Ifngr1	Transcript	retained_intron
rs237129992	10:19594311-19594312	-	intron_variant,NMD_transcript_variant	MODIFIER	Ifngr1	Transcript	nonsense_mediated_decay
rs237129992	10:19594311-19594312	-	intron_variant,non_coding_transcript_variant	MODIFIER	Ifngr1	Transcript	processed_transcript
rs237129992	10:19594311-19594312	-	intron_variant,non_coding_transcript_variant	MODIFIER	Ifngr1	Transcript	processed_transcript
rs237129992	10:19594311-19594312	-	regulatory_region_variant	MODIFIER	-	RegulatoryFeature	promoter
rs236400721	10:19595818-19595819	-	intron_variant	MODIFIER	Ifngr1	Transcript	protein_coding
rs236400721	10:19595818-19595819	-	intron_variant,non_coding_transcript_variant	MODIFIER	Ifngr1	Transcript	retained_intron
rs236400721	10:19595818-19595819	-	intron_variant,NMD_transcript_variant	MODIFIER	Ifngr1	Transcript	nonsense_mediated_decay
rs236400721	10:19595818-19595819	-	intron_variant,non_coding_transcript_variant	MODIFIER	Ifngr1	Transcript	processed_transcript
rs236400721	10:19595818-19595819	-	intron_variant,non_coding_transcript_variant	MODIFIER	Ifngr1	Transcript	processed_transcript
rs220919952	10:19596387-19596387	A	intron_variant	MODIFIER	Ifngr1	Transcript	protein_coding
rs220919952	10:19596387-19596387	A	intron_variant,non_coding_transcript_variant	MODIFIER	Ifngr1	Transcript	retained_intron
rs220919952	10:19596387-19596387	A	intron_variant,NMD_transcript_variant	MODIFIER	Ifngr1	Transcript	nonsense_mediated_decay
rs220919952	10:19596387-19596387	A	intron_variant,non_coding_transcript_variant	MODIFIER	Ifngr1	Transcript	processed_transcript
rs220919952	10:19596387-19596387	A	intron_variant,non_coding_transcript_variant	MODIFIER	Ifngr1	Transcript	processed_transcript
rs220919952	10:19596387-19596387	A	regulatory_region_variant	MODIFIER	-	RegulatoryFeature	promoter_flanking_region
rs262116476	10:19596675-19596675	C	intron_variant	MODIFIER	Ifngr1	Transcript	protein_coding
rs262116476	10:19596675-19596675	C	intron_variant,non_coding_transcript_variant	MODIFIER	Ifngr1	Transcript	retained_intron
rs262116476	10:19596675-19596675	C	intron_variant,NMD_transcript_variant	MODIFIER	Ifngr1	Transcript	nonsense_mediated_decay
rs262116476	10:19596675-19596675	C	intron_variant,non_coding_transcript_variant	MODIFIER	Ifngr1	Transcript	processed_transcript
rs262116476	10:19596675-19596675	C	intron_variant,non_coding_transcript_variant	MODIFIER	Ifngr1	Transcript	processed_transcript
rs262116476	10:19596675-19596675	C	regulatory_region_variant	MODIFIER	-	RegulatoryFeature	promoter_flanking_region
rs237068480	10:19603212-19603232	-	intron_variant	MODIFIER	Ifngr1	Transcript	protein_coding
rs237068480	10:19603212-19603232	-	intron_variant,NMD_transcript_variant	MODIFIER	Ifngr1	Transcript	nonsense_mediated_decay
rs237068480	10:19603212-19603232	-	upstream_gene_variant	MODIFIER	Ifngr1	Transcript	retained_intron
rs237068480	10:19603212-19603232	-	downstream_gene_variant	MODIFIER	Ifngr1	Transcript	processed_transcript
rs237068480	10:19603212-19603232	-	intron_variant,non_coding_transcript_variant	MODIFIER	Ifngr1	Transcript	processed_transcript
rs254638730	10:19603212-19603212	GATAGATAGA	intron_variant	MODIFIER	Ifngr1	Transcript	protein_coding
rs254638730	10:19603212-19603212	GATAGATAGA	intron_variant,NMD_transcript_variant	MODIFIER	Ifngr1	Transcript	nonsense_mediated_decay
rs254638730	10:19603212-19603212	GATAGATAGA	upstream_gene_variant	MODIFIER	Ifngr1	Transcript	retained_intron
rs254638730	10:19603212-19603212	GATAGATAGA	downstream_gene_variant	MODIFIER	Ifngr1	Transcript	processed_transcript
rs254638730	10:19603212-19603212	GATAGATAGA	intron_variant,non_coding_transcript_variant	MODIFIER	Ifngr1	Transcript	processed_transcript
Variant effect predictor results for list of SNPs							
#Uploaded_variation	Location	Allele	Consequence	IMPACT	SYMBOL	Feature_type	BIOTYPE
rs4219190	16:91547987-91547987	A	intron_variant	MODIFIER	Ifngr2	Transcript	protein_coding
rs4219190	16:91547987-91547987	A	intron_variant,NMD_transcript_variant	MODIFIER	Ifngr2	Transcript	nonsense_mediated_decay
rs4219190	16:91547987-91547987	A	regulatory_region_variant	MODIFIER	-	RegulatoryFeature	promoter
rs4219191	16:91554882-91554882	T	intron_variant	MODIFIER	Ifngr2	Transcript	protein_coding
rs4219191	16:91554882-91554882	T	intron_variant,NMD_transcript_variant	MODIFIER	Ifngr2	Transcript	nonsense_mediated_decay
rs4219191	16:91554882-91554882	T	regulatory_region_variant	MODIFIER	-	RegulatoryFeature	promoter
Variant effect predictor results for list of insertions/deletions							
#Uploaded_variation	Location	Allele	Consequence	IMPACT	SYMBOL	Feature_type	BIOTYPE
rs244865141	16:91547997-91547997	T	intron_variant	MODIFIER	Ifngr2	Transcript	protein_coding
rs244865141	16:91547997-91547997	T	intron_variant,NMD_transcript_variant	MODIFIER	Ifngr2	Transcript	nonsense_mediated_decay
rs244865141	16:91547997-91547997	T	regulatory_region_variant	MODIFIER	-	RegulatoryFeature	promoter
rs262242221	16:91548147-91548147	ATTCAGT	intron_variant	MODIFIER	Ifngr2	Transcript	protein_coding
rs262242221	16:91548147-91548147	ATTCAGT	intron_variant,NMD_transcript_variant	MODIFIER	Ifngr2	Transcript	nonsense_mediated_decay
rs262242221	16:91548147-91548147	ATTCAGT	regulatory_region_variant	MODIFIER	-	RegulatoryFeature	promoter_flanking_region

APPENDIX 2

A.

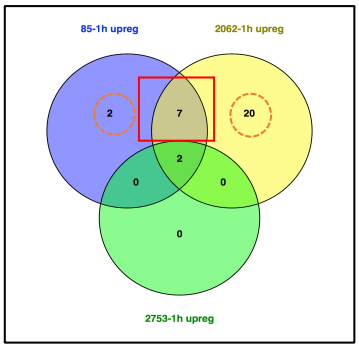

Common genes upregulated in 2062 and 85-1h			
rhov	ppp1r15a	ddit3	osgin1
chac1	sik1	bhlhe40	

B.

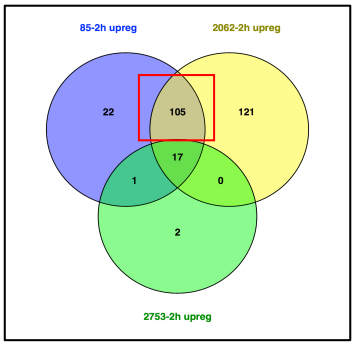

Common genes upregulated in 2062-2h and 85-2h						
Sorbs3	Aatk	E230016M11Rik	Maff	Gpr137b	Eya1	2310022A10Rik
Tha1	Hyal2	Ercc6	Gadd45b	Mafk	Irak2	Cd28
Spdl1	Wdr91	Fzd5	H2-K2	Nat6	Clk4	4930404N11Rik
Mfsd12	3110062M04Rik	Sdc1	Ankrd33b	Klhl21	Tmem140	Gm16515
Sgk1	Dirc2	Rusc2	Cd300a	Lonrf1	Samd8	Dvl2
Ppap2b	Nceh1	Gadd45a	Cdt1	Gpr162	Gas2l3	Nr1d1
P2ry2	Engase	Mnt	Zfand2a	Depdc7	Hilpda	Osm
Tbc1d2	2310044G17Rik	Atp6v0d2	Pfkfb3	Tmem251	N4bp2l1	Sik1
Snx30	Dedd2	Cebpb	Tmem86a	Xrcc6bp1	Ddit3	Gatsl3
Slc30a1	Tns1	Slc6a8				

Supplementary Fig. 1. Common genes upregulated by C85 and C2062 at 1 hr (A) and 2 hr (B) post treatment.

A.

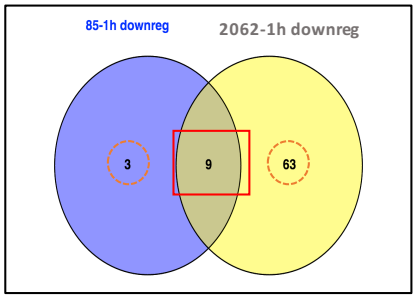

Common genes downregulated in 2062-1h and 85-1h				
Ier2	Fos	Ptger4	Egr1	Adrb2
Nfkbiz	Phlda1	Ch25h	Myc	

B.

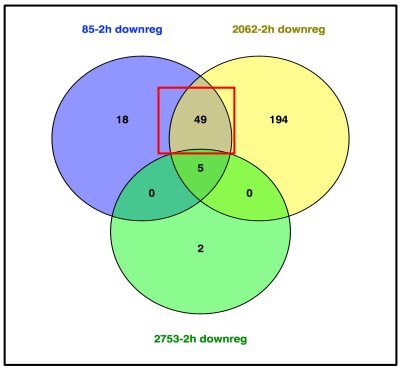

Common genes downregulated in 2062-2h and 85-2h									
I830077J02Rik	Hmga2-ps1	I830012O16Rik	Rnf34	Sc4mol	S1pr2	Phlda1	Ch25h	Filip1l	Pcdh7
Map3k9	Ccnd2	Nanos1	Sema4c	Slc25a25	Slco4a1	Gpr65	Fam72a	Rbm12	Cx3cr1
Gpr84	Hhex	Myc	Lpar6	Dusp16	Adora3	Cdc42ep3	Ell2	Zfp217	Zfc3h1
Nfxl1	Otud1	St3gal6	Rgs2	Gm8979	AA414768	Dusp10	Klf2	Tnip3	Sesn1
Mat2a	Fos	Gcnt1	Igsf9	Gm4841	Serpinb9	Rab39	Spred1	Ifi205	

Supplementary Fig. 2. Common genes downregulated by C85 and C2062 at 1 hr (A) and 2 hr (B) post treatment.

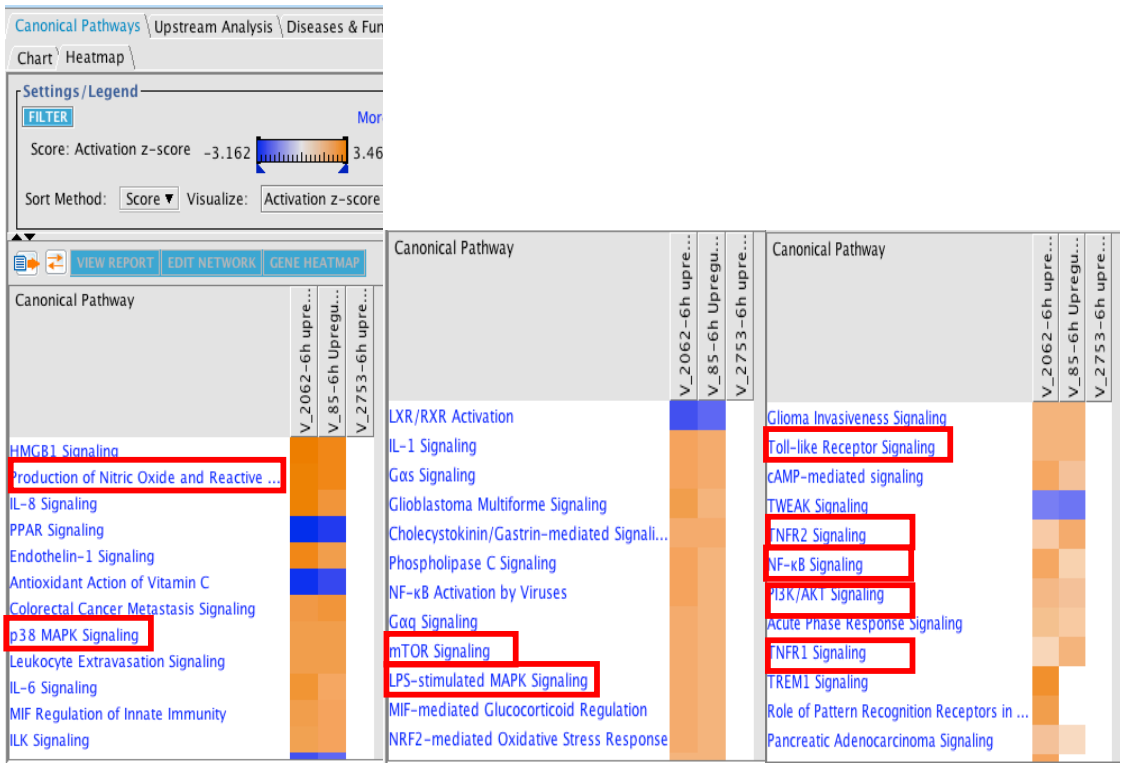

Supplementary Fig 3. Comparison analysis between 85, 2062 and 2753 at 6h showing some of the top significant upregulated pathways.

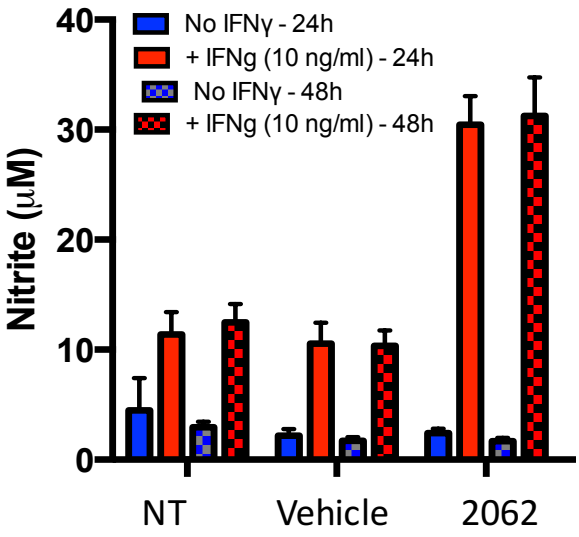

Supplementary Fig. 4. C2062 increases nitrite levels in a murine alveolar macrophage cell line.

We next wanted to investigate if the phenotypes we observed were applicable to other macrophages or not. My colleague, Ruslana Bryk, observed the same phenotypes in RAW264 murine macrophage cell line (data not shown). I tested C2062 on MHS, a murine alveolar macrophage cell line and observed that it did elevate nitrite levels in that cell line as well.

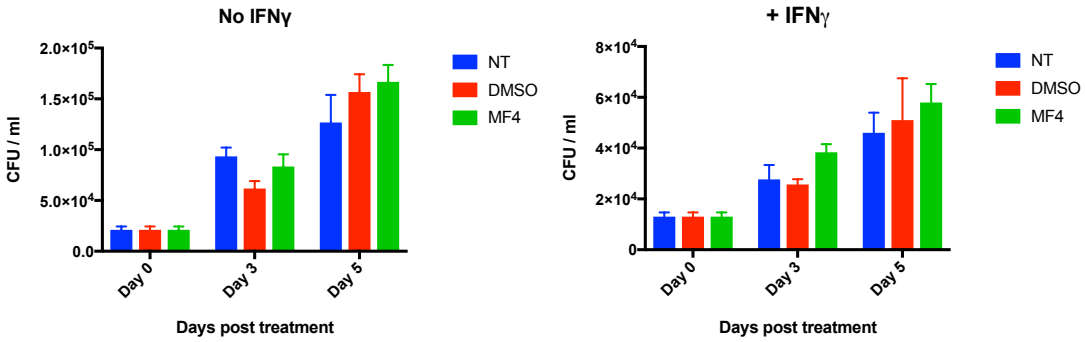

Supplementary Fig. 5. Similar Mtb burden in vehicle and MF4 treated macrophages.